



HAL
open science

Radio resources management for Terahertz nanonetworks

Lina Aliouat

► **To cite this version:**

Lina Aliouat. Radio resources management for Terahertz nanonetworks. Networking and Internet Architecture [cs.NI]. Université Bourgogne Franche-Comté, 2020. English. NNT : 2020UBFCD033 . tel-03324808

HAL Id: tel-03324808

<https://theses.hal.science/tel-03324808>

Submitted on 24 Aug 2021

HAL is a multi-disciplinary open access archive for the deposit and dissemination of scientific research documents, whether they are published or not. The documents may come from teaching and research institutions in France or abroad, or from public or private research centers.

L'archive ouverte pluridisciplinaire **HAL**, est destinée au dépôt et à la diffusion de documents scientifiques de niveau recherche, publiés ou non, émanant des établissements d'enseignement et de recherche français ou étrangers, des laboratoires publics ou privés.

**THÈSE DE DOCTORAT DE L'ÉTABLISSEMENT UNIVERSITÉ BOURGOGNE
FRANCHE-COMTÉ**

PRÉPARÉE À L'UNIVERSITÉ DE FRANCHE-COMTÉ

École doctorale n°37

Sciences Pour l'Ingénieur et Microtechniques

Doctorat d'Informatique

par

Lina ALIOUAT

Radio resources management for Terahertz nanonetworks.

Thèse présentée et soutenue à Montbéliard, le 25 November 2020

Composition du Jury :

Noël Thomas	Professeur à l'Université de Strasbourg	Président
Hakem Nadir	Professeur à l'Université du Québec en Abitibi-Témiscamingue	Rapporteur
Guérin-Lassous Isabelle	Professeur à l'Université de Claude Bernard Lyon 1	Rapporteur
Bourgeois Julien	Professeur à l'Université de Franche Comté	Directeur de thèse
Mabed Hakim	Maître de Conférences/HDR à l'Université de Franche Comté	Codirecteur de thèse

**THÈSE DE DOCTORAT DE L'ÉTABLISSEMENT UNIVERSITÉ BOURGOGNE
FRANCHE-COMTÉ**

PRÉPARÉE À L'UNIVERSITÉ DE FRANCHE-COMTÉ

École doctorale n°37

Sciences Pour l'Ingénieur et Microtechniques

Doctorat d'Informatique

par

Lina ALIOUAT

Gestion des ressources radio pour les nanoréseaux Terahertz.

Thèse présentée et soutenue à Montbéliard, le 25 November 2020

Composition du Jury :

Noël Thomas	Professeur à l'Université de Strasbourg	Président
Hakem Nadir	Professeur à l'Université du Québec en Abitibi-Témiscamingue	Rapporteur
Guérin-Lassous Isabelle	Professeur à l'Université de Claude Bernard Lyon 1	Rapporteur
Bourgeois Julien	Professeur à l'Université de Franche Comté	Directeur de thèse
Mabed Hakim	Maître de Conférences/HDR à l'Université de Franche Comté	Codirecteur de thèse

Title: Gestion des ressources radio pour les nanoréseaux Terahertz.

Keywords: Nanonetworks, Dense Network, Terahertz band, Network Layer, control channel

Abstract:

Wireless NanoNetwork (WNN) is a wireless ad hoc network composed of a high number of sub-millimetric nodes called nanonodes. The size of the devices makes the Terahertz band (0.1–10 THz) a suitable candidate for supporting the wireless communication between nanonodes.

The intrinsic limitations of nanonodes (energy, memory, communication range, and computation capacity) and the severe path loss of Terahertz band communication, impose WNN protocols to be adapted to these stringent requirements and represent a challenge to the communication (much below one meter) among nanonodes and the overall network performance.

In this thesis, we studied different options for improving the lower networking layers (access protocols, and routing protocols) for Terahertz WNN. First, we proposed a new Terahertz pulse-based access protocol (SDMA-TSOOK) that allows to balance the radio access over the active nanonodes while reducing the co-channel and collision risks. The SDMA-TSOOK protocol is then compared with the most relevant methods such as : TSOOK, RD-TSOOK and SRH-TSOOK.

We proposed three 2.5 networking layer protocols for

reducing the density of the nanonetwork physical topology. Indeed, the high concentration of nanonodes increases the number of direct communication links. Therefore, it is important to reduce smartly the number of direct links to reduce the flooding effects and the routing complexity. First, We proposed a protocol to convert the physical topology of the network into directed-graph topology where the direct neighboring nodes of each node is reduced to a subset of its physical neighbors. We also studied cluster-based traffic regulation approach for Terahertz nanonetwork. In this case, the physical topology of the network is reduced to a hierarchical based topology that allows to prevent multiple receptions and loops effects.

Finally, We extend our work, to the study of routing protocols in ultra dense nanonetworks. We have shown that classical and dedicated ad hoc nanonetwork routing solutions are inefficient for ultra dense nanonetwork, particularly, when the nanonetwork deployment presents distortions and concave sides. We proposed then a proactive multirelay to multirelay routing protocol that takes into account the residual energy level of the nanonodes and the reliability of the routing paths.

Titre : Gestion des ressources radio pour les nanoréseaux Terahertz.

Mots-clés : Les nanoréseaux, Réseaux dense, Bande Terahertz, La couche Réseaux, Canal de contrôle

Résumé :

Wireless Nano Network (WNN) est un réseau ad hoc sans fil composé d'un grand nombre de nœuds submillimétriques appelés nano nœuds. La taille des dispositifs fait de la bande Terahertz (0,1–10 THz) un candidat approprié pour prendre en charge la communication sans fil entre nano nœuds.

Les limitations intrinsèques de nano nœuds (l'énergie, la mémoire, la portée de communication, et la capacité de calcul) et la perte sévère de chemin de la communication en bande Terahertz, imposent aux protocoles WNN de s'adapter à ces exigences strictes et représentent un défi pour la communication (bien au-dessous d'un mètre) entre les nano nœuds et les performances globales du réseau.

Dans cette thèse, nous avons étudié différentes options pour améliorer les couches inférieures du réseau (protocoles d'accès et protocoles de routage) pour le WNN Terahertz. Tout d'abord, nous avons proposé un nouveau protocole d'accès à base d'impulsions Terahertz (SDMA-TSOOK) qui permet d'équilibrer l'accès radio sur les nano nœuds actifs tout en réduisant les risques de co-canal et de collision. Le protocole SDMA-TSOOK est ensuite comparé aux protocoles les plus pertinentes telles que : TSOOK, RD-TSOOK et SRH-TSOOK.

Nous avons également proposé trois protocoles de couche réseau 2,5 pour réduire la densité de la topologie physique des

nanoréseaux. En effet, la forte concentration de nano nœuds augmente le nombre de liaisons de communication directes. Il est donc important de réduire efficacement le nombre de liens directs afin de réduire les effets d'inondation et la complexité du routage. Premièrement, Nous avons proposé un protocole pour convertir la topologie physique du réseau en topologie graphique directe où les nœuds voisins directs de chaque nœud sont réduits à un sous-ensemble de ses voisins physiques. Nous avons également étudié une approche de régulation du trafic basée sur les groupes de nano nœuds au sein d'un nanoréseau Terahertz. Dans ce cas, la topologie physique du réseau est réduite à une topologie basée sur la hiérarchie qui permet d'éviter les réceptions multiples et les effets de boucles.

Enfin, nous avons élargi nos travaux à l'étude des protocoles de routage dans les nanoréseaux ultra denses. Nous avons montré que les solutions de routage classiques et ad hoc dédiées aux nanoréseaux sont inefficaces pour les nanoréseaux ultra denses, en particulier lorsque le déploiement du nanoréseau présente des distorsions et des côtés concaves. Nous avons alors proposé un protocole de routage proactif multi-relais à multi-relais qui prend en compte le niveau d'énergie résiduelle des nano nœuds et la fiabilité des chemins de routage.

Acknowledgements

First and foremost, I would like to express my deep gratitude to Professor Julien Bourgeois for highlighting valuable research direction and providing a healthy working environment that helped me achieve this work.

I am grateful to Dr. Hakim Mabed for his valuable input and always pushing to bring out only the best of me and stepping in for guidance whenever needed. I thank him for his availability, constructive criticism, and foremost, his patience in answering my repeated questions.

A special thanks to my friend Rim El Ballouli for her support, advice, and being there every step of the way.

Last but not least, I thank my parents for their unconditional support, scarifies, and continuous encouragement that kept me driving forward despite the friction.

"Quand on veut on peut, quand on peut on doit."

-Napoléon Bonaparte-

Associated Papers

Several chapters in this thesis appeared in several papers in the form of conference and journal articles

Conference:

The following conference paper is derived from Chapter [5](#)

[1] Aliouat, L., Mabed, H., and Bourgeois, J. **2.5 layer protocol for traffic regulation in ultra-dense nanonetwork**. In *International Conference on Ad-Hoc Networks and dWireless* (2019), Springer, pp. 330–340.

The following conference paper is derived from Chapter [7](#)

[2] Aliouat, L., Mabed, H., and Bourgeois, J. **Flexible multipoint-to-multipoint routing protocol in ultra-dense nanonetworks**. In *Proceedings of the 17th ACM International Symposium on Mobility Management and Wireless Access* (2019), pp. 81–87.

The following conference paper is derived from Chapter [6](#)

[3] Aliouat, L., Mabed, H., and Bourgeois, J. **Enhanced clustering approach for traffic regulation in directional antennas based nanonetworks**. In *Proceedings of the 35th Annual ACM Symposium on Applied Computing* (2020), pp. 2121–2128

Journal:

The following journal manuscript derived from Chapter [7](#)

[4] Aliouat, L., Mabed, H., and Bourgeois, J. **Efficient routing protocol for concave unstable terahertz nanonetworks**. *Computer Networks* 179 (2020), 107375.

The following journal manuscript derived from Chapter [4](#) is under review:

[5] Aliouat, L., Rahmani, M., Mabed, H., and Bourgeois, J. **Enhancement and Performance Analysis of Channel Access Mechanisms in Terahertz Band**. *Nano Communication Networks*, August 2020

The following journal manuscript derived from Chapter [6](#) is under review:

[6] Bouchiha, M., Aliouat, L., Mabed, H., and Aliouat, Z. **Routing Framework based on Hierarchical Cluster-based Architecture in Nanonetworks**. *Computer Networks*, August 2020

Contents

1	Introduction	1
1.1	Contexte and Motivation	1
1.2	Térahertz Nanocommunication	2
1.2.1	Physical Layer Protocols	3
1.2.2	MAC sub-Layer Protocols	3
1.2.3	Network Layer Protocols	4
1.3	Thesis Contributions	4
1.4	Dissertation Organization	6
I	STATE OF THE ART	9
2	Nanonetwork	11
2.1	Introduction	11
2.2	Nanodevice Architecture	12
2.2.1	sub-millimetric nanodevices	12
2.2.1.1	Communications and energy consumption	13
2.2.1.2	Battery features	14
2.2.1.3	Memory capacity	14
2.2.1.4	Energy harvesting	14
2.3	Antennas in nanonetworks	15
2.4	Nanonetworks Application Fields	15
2.4.1	Programmable matter applications	15
2.4.2	Bio-medical applications	16
2.4.3	Industrial and consumer goods applications	16
2.4.4	Military applications	17
2.4.5	Environmental applications	17
2.4.6	Agriculture Applications	18
3	Communication in Terahertz band	19

3.1	Introduction	19
3.2	Physical Layer	19
3.2.1	OOK modulation	20
3.2.2	Pulse Position Modulation	20
3.2.3	Pulse Coding	20
3.2.4	Summary of physical layer protocols	21
3.3	Link Layer	22
3.3.1	Distributed Protocols	22
3.3.2	Hierarchical Protocols	24
3.3.3	Summary of link layer protocols	26
3.4	Network layer	26
3.4.1	Classical routing protocols	28
3.4.2	Nanonetwork routing protocols	29
3.4.2.1	Multi-path Routing	29
3.4.2.2	Single-path Routing	32
3.4.3	Summary of network layer protocols	33
II	Contributions	37
4	Improvement of pulse-based Terahertz access protocols	39
4.1	Introduction	39
4.2	Canal access protocols in Wireless NanoNetworks WNN	39
4.2.1	TS-OOK	40
4.2.2	RD-TSOOK	41
4.2.3	SRH-TSOOK	42
4.2.4	Preliminary comparison of protocols	43
4.3	Proposed protocol	44
4.4	Scenario's Implementation	45
4.4.1	Nanonodes deployment	46
4.4.1.1	Uniform deployment	46
4.4.1.2	Gaussian distribution	46
4.4.1.3	Gaussian Clusters distribution	47
4.4.2	Data traffic control	47
4.4.2.1	Constant Bit Rate (CBR)	47
4.4.2.2	Variable Bit Rate (VBR)	48

4.4.3	Density factor	48
4.5	Performance analysis and comparison	49
4.5.1	Collisions	49
4.5.2	Success Rate	49
4.5.3	Discussion of protocols performance	50
4.5.4	Analysis	52
4.6	Conclusion	54
5	Directed graph based traffic regulation protocol	55
5.1	Introduction	55
5.2	Contribution	56
5.3	Traffic regulation problem modeling	56
5.3.1	Traffic regulation constraints	57
5.3.2	Antenna steering and sleeping mode	57
5.3.3	Traffic regulation in Terahertz network	58
5.4	Distributed algorithm of traffic regulation	59
5.5	Tests and results	61
5.6	Conclusion	62
6	Clustering based protocol for traffic regulation	65
6.1	Introduction	65
6.2	Random cluster heads based Protocol	66
6.2.1	Directional Antennas	66
6.2.2	Clustering	67
6.2.2.1	CH neighborhood discovery	68
6.2.2.2	Forward Dominate Nodes	69
6.2.2.3	TDMA approaches	70
6.2.3	Simulation Results and Comparison	72
6.3	Uniformly distributed cluster heads based protocol	74
6.3.1	Spines Selection	75
6.3.2	Area Division	78
6.3.3	Clustering	79
6.3.4	The Proposed TDMA MAC protocols	79
6.3.4.1	Inter Cluster TDMA	79
6.3.4.2	Intra Cluster TDMA	81
6.3.5	CH Neighborhood Discovery	82

6.3.6	Performance Assessment	82
6.3.6.1	Nanonetwork Connectivity	83
6.3.6.2	Control Messages	84
6.3.6.3	Communication Reliability	85
6.4	Conclusion	86
7	Routing Protocol in ultra-dense WNN	89
7.1	Introduction	89
7.2	Contribution	90
7.3	Traffic characteristics in nanonetwork	91
7.3.1	Multiple sink problem	91
7.4	Multipoint to Multipoint protocol M2MRP	92
7.5	Comparison of routing protocols	95
7.6	Experimental tests	98
7.6.1	Performance comparison	99
7.6.2	Energy management	101
7.7	Conclusion	102
III	General conclusion	105
8	General conclusion	107
8.1	Contributions	107
8.2	Future works	109

Introduction

Over the last two decades, nanotechnology: A multidisciplinary technique emerging from nanoscience, has steadily attracted academics and industrialists' attention. This attraction is motivated, on the one hand, by the discovery of new materials with revolutionary properties acting at the nanometric level such as Graphene and carbon nanotubes [30] and, on the other hand, by the significant potential benefits that these exceptional materials could generate in a variety of strategic areas. This has further stimulated and encouraged the promotion of a new direction in technology research leading to the development of nanodevices working at Terahertz frequency band that traditional technology cannot enable.

These nanodevices, acting in the sub-millimeter scale, open the way to several fields of crucial interest applications such as nanomedicine, nanometric surroundings, nanometric military use, nanoagriculture, and nanorobotics, etc. Such a restrictive list of application fields is only hypothetical, as nanotechnology is still in its infancy. When the expected maturity should be reached, nanotechnology applications will cover a much larger number of domains.

In this context, nanotechnology involving the design and development of nanodevices for networking is one of the most active research areas. Whether they are wireless nanosensors, nanorobots, or others, these nanodevices can only have a significant impact within a given application if they collaborate using Wireless NanoNetwork (WNN) communications. Due to the radio antenna's sub-millimeter scale, the Terahertz frequency band appears as a promising technology. The main functionality in a WNN lies in the satisfying Terahertz communication between its nanodevices or nanonodes. This is what has devoted the work reported in this dissertation.

1.1/ Contexte and Motivation

Among the interesting nanodevices envisaged, nanorobots and nanosensors as nanocomputers with limited resources imposed by their sub-millimeter dimensions could be capable of performing simple tasks such as information sensing and its transmission, identification, actuation, and computation. Individually captured information would only be of interest if it would be transmitted to an end-user for predefined use or to the other nanodevices. Because of the energy limitation, very limited nanodevice's transmission coverage, sensing/treatment surface to be covered for collecting the interesting information, and the distance to reach micro/macro interface to the end-user, cooperative work via networking performed by a huge number of nanodevices should be required.

Thus, the cooperative grouping of a large number of nanonodes to perform complex and highly

useful tasks constitute the paradigm of wireless nanonetworks. Since this paradigm applies to an extremely miniature environment, the usual practical concepts of networks no longer apply. Therefore, it would be necessary to adapt these classical concepts to take into account the intrinsic constraints of nanonodes, as is already the case, or even better discovering new ones more relevant to this emergent paradigm.

Functionally, a network, whatever its type: macro, micro or nano, is only valuable or capable to accomplish its mission if it can ensure consistent communication between its nodes. Therefore, nanocommunication in a WNN must take into account the rigorous particularities of involved nanonodes, particularly their restricted resources and their very constraining deployment environments. More specifically, the data transmission medium used in the Terahertz frequency band has to be adapted to overcome the surrounding negative reactions. This applies, in particular, to nanocomponents used in nanocommunications, such as transceivers with their modulation/demodulation of electromagnetic waves, omni-directional nanoantennas, nanodevices for self-generation of energy, etc. Consequently, networking protocols must take into account these constraints arising from the sub-millimeter sized devices and also the highly dense resulting networks. As a result, these protocols may be able to overcome the impact of the nanocomponent weaknesses on nanocommunication.

1.2/ T erahertz Nanocommunication

Acquiring or computing information and transmitting it over a WNN to a control point or concerned nanonodes is the common goal of wireless macro/nano devices. However, the extremely severe constraints imposed by unfavorable environments, the very tiny dimensions of the nanodevices components, and their high density further complicate the design of protocols dedicated to Terahertz band nanocommunication [86, 110].

Like ad hoc network, WNN protocols address a specific layer of the multi-layer communication model, but for efficiency reasons, there is often an interaction between the neighboring layers. However, protocols acting on several layers (Cross layer protocols) have to take into account computing and storage capacity requirements that may be beyond the nanodevices capabilities. The layers often explored are: the physical layer, the MAC sub-layer and the network layer. Given the very high density of nanonodes within a WNN, accesses to communication channels are subject to strong inter-nanonode interference that creates disturbances during transmission. These disturbances are often caused by collisions and path loss that affect the transmitted signals, resulting in a reception failure requiring multiple re-transmissions.

Recognizing that channel activities are costly in terms of energy consumption, especially transmissions and receptions, and that this fundamentally crucial energy resource is available only in minute quantities and intermittently, therefore, it is essential to mandate nanocommunication protocols to address this crucial issue in terms of cost-efficiency. Furthermore, the problems generated by the environment, such as molecular absorption, path loss, etc. [109], have to be better considered by Terahertz nanocommunication protocols. The complexity of this issue poses a serious challenge to be met. Formal models specifically dedicated to the different layers and reinforced by appropriate simulation scenarios would allow a better focus on the essential aspects to be taken into account by nanocommunication protocols.

1.2.1/ Physical Layer Protocols

The physical layer defines the transmission methods of the raw bits on a communication medium. It concerns modulation, coding, error control, and other transmission methods that determine the data rate and error rate [111].

The scheme of the THz nanocommunication presents a particular combination of constraints and requirements, impacting considerably the physical layer and preventing the use of well-known techniques. This sub-millimeter dimension imposes severe restrictions on the resources available at the nanonodes and favors the use of simple and ultra-efficient modulations and coding. This is particularly limiting for applications sensitive to the intermittency caused by nanodevices powered by energy harvesting. The depletion of the renewable energy budget of nanodevices not only affects the continuity of their transmission but also poses an additional challenge in terms of reliability.

As the hardware technological maturity of THz communication is still to come, although significant progress has been made [90, 92, 31], the design of the physical layer is still affected by the THz dimension of the scheme. Moreover, for increasing distances, the THz channel faces the phenomenon of molecular absorption, which is another obstacle to nanocommunication.

In general, existing THz communication protocols favor the simplicity factors. Some work on nanocommunications mainly advocates rapid On-Off Keying (OOK) modulation to avoid energy-intensive circuits and minimize signal processing time. Other works attempt to further simplify the physical layer using impulse radio techniques, where modulations are based on the transmission of femtosecond pulses and use cross-layer strategies in an attempt to further simplify the protocol stack. Thus, in this context of pulse-based modulation, the basic idea of OOK has served as the basis for the TS-OOK cross-layer protocol, which in turn was improved by other protocols like RD-TSOOK, SRH-TSOOK, ASTH-STOOK, etc. Many other published protocols, focusing on the physical layer, have followed other research directions, namely: Pulse Coding, Pulse Amplitude, Pulse Position, and Pulse Width [111].

1.2.2/ MAC sub-Layer Protocols

The efficient THz MAC protocols design must be driven by the Terahertz band's characteristics and constraints whose frequencies are subject to particular propagation phenomena such as reflection, multipath, wave absorption by certain molecules, and thermal noise over the transmission channels [57]. This is why the behavior of electromagnetic waves in this band, which can evolve in different environments with different types of obstacles, must be well understood in order to improve the protocols' performance of this layer, particularly the throughput and delay of nanocommunications. As a result, the protocols established for the traditional Ad hoc network cannot be directly used in WNNs because they ignore the obstacles generated by the environment in THz band communication (0.1-10 Terahertz) [85]. Also, they did not aware of nanoantenna requirements and their impact on ultra-dense THz WNN.

Despite all the obstacles resulting from both the sub-millimeter range deployment environment and the technological weaknesses of nano-machines, most of the designed MAC protocols come rather from an adaptation of those already existing at the macro level, than from a design specifically dedicated to the requirements of WNNs. This probably results from the lack of evaluation of full-scale experiments due to the field's early youth. So far, most of the MAC protocols are trying to improve the nanocomponents' performance involved in nanocommunication.

MAC layer has drawn much attention and numerous protocols have been proposed addressing several issues [116] such as energy-consuming and harvesting, channel management with scheduling and random access, collisions and congestion, interference and control error, packet size and structure, data transmission and recovery, delay and throughput, adaptive bandwidth and multiplexing, nanoantennas, handshake, neighbor discovery and synchronization, etc. Each protocol focuses on one or more performance metrics, with or without cross-layer support.

1.2.3/ Network Layer Protocols

Network layer functionality enables interconnected nanonodes within THz WNN to perform data exchange regardless of the distance between them. Indeed, the extremely limited capabilities of nanonodes, as well as the Terahertz band characteristics, present a challenge to the communication between distant nanonodes and the overall nanonetwork coverage area. These communications are supported by intermediate nanonodes (hops) charged to forward information from source to destination. Therefore, appropriate routing protocols are required to ensure multi-hop communication in which nanonodes might count on identification and/or addressing methods. The routing functionality, based on common forwarding, leads to establishing paths between transmitters to corresponding receivers.

Due to nanotransceivers limitation capabilities and traditional routing protocols depending on message control exchanges to learn and distribute information about the network topology, traditional routing transmission and addressing schemes are often unusable. As a result, memory, channel, and power restrictions in WNNs impose strict routing functionality requirements. Consequently, design routing protocol could be relieved from the knowledge of WNN topology or information acquisition that is not strictly indispensable. For that reason, design of optimal selective flooding should be suggested to better comply with WNN requirements.

The performance metrics adopted in the routing protocols of this layer (and in other layers) are numerous. So far, they include throughput, packet generation rate, transmission range, bit error rate, end-to-end delay, average latency, energy consumption, memory usage, network size, failure rate, etc. However, simultaneous use of many of these metrics may be contradictory with the expected objectives of a given application. For example, satisfying the quality of service by routing protocol (ensuring reliability and/or security) may conflict with energy consumption optimization. In other words, a protocol that achieves the maximum number of performance metrics would be excessively complex and unsupported by nanonodes capabilities, and therefore unfeasible. This is why the performance objective of a protocol is imposed by the mission carried by the application executed by a WNN. This mission will, therefore, give privilege to one or a few well-targeted performance metrics.

1.3/ Thesis Contributions

Our contribution reported in this thesis dissertation, concerns proposals for new Terahertz communication protocols dealing with problems related to the data transmission among dense nanodevices. Although the different layers' functionalities are distinct, for efficiency reasons, some protocols address one layer while accessing data from another layer to exchange information and enable interaction (cross-layering). The five proposals summarized hereafter could be classified as follow. The first contribution studies the physical (modulation) and access link aspects. The second, third and fourth contributions could be classified as access link/routing protocols, while the fifth contribution corresponds to the routing layer.

1. Knowing that the main challenge with nanocommunication is the need to efficiently share the Terahertz radio spectrum in order to optimize data transmission in THz dense nanonetworks. In this context, Spread in Time On-Off Keying (TS-OOK) protocol was proposed as a channel access mechanism that uses femtosecond-long pulse-based on OOK modulation. After that, different new approaches such as RD-TSOOK and SRH-TSOOK were proposed as improvements of TS-OOK. Our first contribution is devoted to review and compare the proposed OOK based access techniques then we propose a new access protocol called SDMA-TSOOK. The proposed scheme takes into account the weaknesses of the published methods in terms of channel access balancing, co-channel collision, and networking capacity that pose a problem for concurrent channel access. We evaluated the performance of our proposal using the BitSimulator. The simulation results showed that SDMA-TSOOK ensures 100% equitable access between nanodevices, as well as a similar success rate with an insignificant number of collisions compared to the published protocols.

2. Some applications require the concentration of a very large number of nanodevices in a limited space. In this ultra-dense context and in the absence of centralized access control units, we propose to implement a distributed strategy of spatial and temporal traffic regulation to guard against the risks of congestion, interference and energy over-consumption. Forwarding is a vital networking and access channel for determining appropriate schemes of sending a packet to the next-hop along its path to the destination. Unfortunately, the pure flooding is quite inefficient, for dense nanonetwork, regarding the number of packets generated in nanonetwork that decrease its performance in terms of its lifetime, latency, and collisions.

In this context, we proposed a protocol for optimizing Terahertz radio links using directional antenna, distributed time division technique and sleep mode. The targeted aim was reducing the flow of redundant traffic over the network, smooth the volume of communications exchanged over time, and preserve the lifetime of the nanonodes. In this first approach, we targeted WNN networks working under uncontrolled environment leading to complex network topologies (concavities, instabilities, mobility, ...).

3. Unlike the previous traffic-regulation approach based on directed graph topology generation, in this new de-densification approach, we adopted a hierarchical topology. This new approach is dedicated to slightly uniformly distributed nanonetwork. It operates with Terahertz directional antennas in order to efficiently direct the radio signals towards the targeted area which significantly reduces interference. For regulating the exchanged messages, we propose a synchronous communication protocol based on a clustering approach where intra and inter cluster communications will be achieved respectively by a Time Division Multiple Access (TDMA) protocol, and a new distributed TDMA combined with Forwarding Dominate Nodes (FDN) scheme. Several scenarios have been carried out and the obtained simulation results showed that our proposition significantly reduces both the number of collisions and the number of exchanged messages required to broadcast data among nanonodes.

4. Our third de-densification protocol is based on hierarchical topology as for previous approach. This approach is dedicated for slightly uniformly distributed and stable nanonetwork. We proposed an efficient distributed access channel and hierarchical routing protocol for random dense nanonetwork. The proposal divided the nanonetwork into areas (clusters) using a pre-selected nanonodes called spines. Two communications layers are designed to overcome the broadcast storm problem: intra-area and inter-area communi-

cations based on TDMA distributed schemes. Based on simulation results, we showed that our proposal outperforms the previous proposed protocol in terms of nanonetwork connectivity, packets control exchanged, and packets loss ratio.

5. In the last contribution, we showed that classical and dedicated ad hoc nanonetwork routing solutions are inefficient and present low reliability level, supplementary delay and control traffic. Mostly of these solutions are based on point to point relaying mode, which is not adapted to the instability context and perform badly when the nanonetwork deployment presents distortions and concave sides. We propose a new routing protocol called Multirelay to Multirelay Routing Protocol (M2MRPv2), which provides a natural way to manage the residual energy levels on the nanonodes. M2MRPv2 is, to the best of our knowledge, the only approach that proposes a proactive multirelay to multirelay routing mode where the residual energy level of the nanonodes and reliability of the routing paths are taken into account. Performance of M2MRPv2 protocol is analyzed according to different multi-source to multi-sink communication scenarios. The obtained results show that M2MRPv2 protocol outperforms by far the Stateless linear-path routing (SLR) protocol [88] (The reference protocol for Terahertz nanonetworks) in terms of transmission reliability and energy management. This outperformance is accentuated when the Terahertz nanonetwork deployment presents many concavities.

1.4/ Dissertation Organization

This dissertation is composed of two parts and organized as follows:

- **Part One: State of the art** This part presents a comprehensive review of background and related works in the field of nanonetworks. It contains two chapters (chapter 2 and 3). First, an overview of Wireless NanoNetwork (WNN) system is given dealing with the development of nanotechnologies, the nanodevice architecture, the characteristics of THz nanonetwork and its problems, and nanonetworks application fields. Next, Physical layer modulation techniques, Medium Access Control (MAC) solutions and network layer protocols for WNN are reviewed and summarized.
- **Part Two: Contributions** In this part, we present the details of research contributions that are organized as follows:
 - *Chapter 4* Works related to channel access based OOK modulation are presented and reviewed. Then novel balanced channel access, that takes into account collisions and throughput is discussed. The details of the simulation and the performance of the proposed scheme are investigated, and finally we concluded the work.
 - *Chapter 5* Presents the traffic regulating problem modeling. Then we proposed an original procedure for the Layer 2.5 networking protocol that takes into account the Terahertz frequencies particularities in a dense context. Lastly, we discuss the performance evaluation, followed by conclusions.
 - *Chapter 6* We propose and show that hierarchical nanonetwork routing solutions are efficient and present a high reliability, low delay and control traffic for dense nanonetwork. Firstly, we suggested a proposal adapting the clustering approach enhanced with both a new distributed TDMA protocol and FDN scheme. Then,

we discussed the performance evaluation of our protocol via simulation compared to the flooding approach. Secondly, after observing the weaknesses of the first approach, a new protocol addressing these issues is proposed. The improvement aim is to obtain better nanonetwork connectivity, low packets control exchanged, and more packets delivery relative to the first one. Furthermore, simulation results show that last proposed scheme is more efficient in dense nanonetwork.

- *Chapter 7*. This chapter is devoted to describe the multi-relay to multirelay routing protocol for ultra dense nanonetwork. Then a complexity comparison between our method and well-known protocols is given. Last we discussed the experimental tests, and followed by conclusions.



STATE OF THE ART

Nanonetwork

2.1/ Introduction

The existence and use of a nanonetwork are only justified if its nanonodes (nanomachines) can easily cooperate to achieve a common goal (Nanonetwork mission). Indeed, nanomachines' ability is very limited and only capable of performing simple tasks on their own, in order to accomplish more complex tasks within the overall objective of a nanonetwork (Nanonetwork mission), the cooperation of nanomachines is indispensable. Different technological technologies are studied to support communications between the nanomachines. Technologies that include the following categories:

- Electromagnetic nanocommunication.
- Molecular Nanocommunication.
- Acoustic Nanocommunication.
- Nano Mechanical Communication.

Such cooperation can only be achieved if communication between the nanonodes (Nanocommunication) is established when needed at all appropriate times. Each node within a network is invested with a mission to capture/compute information relating to its local environment at the nanoscale. This information is of interest only if transmitted to a central retrieval point where a final decision will be made.

The success of a dedicated nanonetwork depends strongly on the ability of each nanonode to send its sensed/computed data, which has to reach the decision center or concerned nanonodes, whatever its distance from the sender nanonode. This means that nanocommunication between nanonodes has to be carried out in multi hops way. This is all the more true since the individual actions of the nanonodes impact also distant nanonodes.

Particularly, the timeliness of sensed/computed information diffusion may be altered. According to the targeted application, time constraints in real-time decision making can be a serious impediment. Conversely, electromagnetic nanocommunication is more suitable than molecular nanocommunication [45, 81, 32], or contact based communication [120, 34].

2.2/ Nanodevice Architecture

Due to their nanoscale dimension, nanodevices are excluded to be interconnected via wired nanocommunication medium. A wireless nanodevice, capable of doing simple tasks like sensing, computing, or actuation, includes the following units (Figure 2.1):

- Sensing unit: Various calculated magnitudes require various nanosensors for mass, force, or pressure calculation. Created from Carbon Nanotubes and Graphene Nanoribbons: Nanomaterials having high sensing capabilities [28].
- Actuation unit: Enables auto reaction of the device regarding its change. Different types of nano actuators exist: physical and chemical [28].
- Power unit: Supplying energy may be from nanobatteries made with nanomaterials offering high power, proper life time, and suitable charge/discharge periods. However, WNN may be deployed in environments that do not allow recharging nanodevices when their energy budget reaches depletion. In such situation, a nanodevice has to manage itself by self-powering which involves the paramount interest of using a self-renewal method of energy harvesting [98, 26, 40].
- Processing Unit (PU): nanoprocessors are expected to be developed from graphene-based transistors. Due to its attractive properties, the graphene nanomaterial enables developing faster switching devices like PU. As the development of PU is based on the basic elements such as the transistor [80], the extreme miniaturization of the latter will play a key role in the manufacturing of composite nanocomponents. Nevertheless, the small size of nanodevices limits the number of transistors in a nanoprocessor and the complexity of the operations carried out, thus limiting computing capacity.
- Storage Unit: Thanks to nanomaterials and new nanotechnologies, atomic memories currently being developed consider the presence of a silicon atom as storing bit 1 (or 0) and the absence of it as storing bit 0 (or 1). For programmable nanodevices, the read and write capabilities of nanoscale memory are required. As with nanoprocessors, the technology is also required to produce a huge number of very small nanosized memories [56].
- Communication Unit: The development of nanoantennas and the corresponding electromagnetic transceivers are the keystone enabling the communication between the nanodevices.

2.2.1/ sub-millimetric nanodevices

A Terahertz nanonetwork is an ad hoc wireless network where the communication between sub-millimetric nodes is carried by sub-millimeter radio waves. The choice of sub-millimeter radio waves is dictated by the use of sub-millimetric antennas. The nature of targeted applications leads to a high density of nanonodes contemplated through technologies such as Graphene antenna [51] and MEMS components [11]. Due to the Terahertz radio signal and the energy capabilities of the nanonodes, the signal range is very short (signal power of less than 1mw covering about dozens of centimeters).

Sub-millimeter node takes different states during its operating cycle according to the current task: transmission, reception, idle, sleep, etc. Each step presents a specific energy increasing

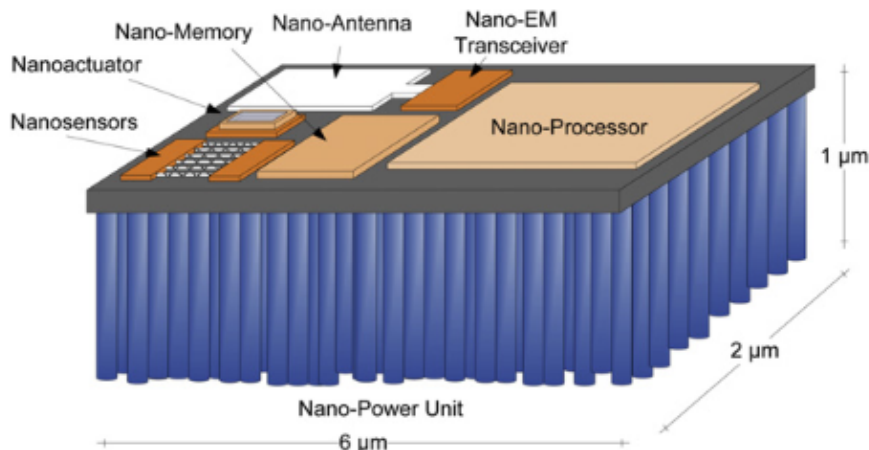


Figure 2.1: An integrated nanosensordevice [28].

or decreasing process. The characterization of the nanodevice requires the specification of the amount of energy required by each phase.

In the following study, we try to analysis the expected capacities of a sub-millimetric nanodevices at the light of current technological advances. This study is an indispensable step before any operational proposition for nanonetwork protocols.

2.2.1.1/ Communications and energy consumption

Many modeling studies were made for characterizing radio communication energy consumption [38, 63]. Authors in [66] estimated the energy required by a pulse to $E_p = 100aJ = 10^{-16}J$. However, the diffused energy of the pulse represents just a part of the energy needed to transmit a "1" symbol, E_s , that includes a power amplifier, Frequency synthesizer, etc. We notice E_f^{tx} the average energy required for transmitting a data frame of n symbols (0/1).

$$E_f^{tx} \leq n \times E_s \quad (2.1)$$

On the other side, data reception consumes energy less than energy required for transmitting data. This energy is used by the receiver components such as Low-noise amplifier (LNA). We notice E_f^{rx} the energy required for the reception of a frame of n symbols.

$$E_f^{rx} < E_f^{tx} \quad (2.2)$$

In addition to the communication task, nanonodes consume energy during their normal activity state corresponding to listening task, electronic components activities, sensing tasks, etc. The energy consumption during activity state varies over time according to the nature of performed tasks. Let E^{ac} the average energy consumption per second due to the nanonode activities. It is also possible to envisage a sleeping mode that allows nanonodes to reduce their activities and, consequently, energy consumption. We notice E^{sl} the energy consumed per second during sleeping mode.

2.2.1.2/ Battery features

The energy limitation of the nanonode is mainly dictated by the node size and, consequently, the battery size. Let d_n the volume of a node and let d_b the space consecrated to the battery ($d_b < d_n$). The maximal amount of energy stored by a battery, E_{max}^{bt} , depends on the manufacturing materials of the battery. For example, a Lithium-Ion battery presents a density of energy of 0.36 to 0.95J/g. Knowing that the volumetric mass of the Lithium-Ion battery is 0.2kg/l. We deduce that within $d_b m^3$, the energy amount of a battery is equal to:

$$E_{max}^{bt} = \text{volumetric mass} \times \text{density of energy} \times d_b \quad (2.3)$$

If the Lithium-Ion battery is of $0.2m^3$, the maximum energy is of $14 \times 10^{-6}J$ to $38 \times 10^{-6}J$

Without harvesting mechanisms and if we ignore the other tasks of the nanonode, a Lithium-Ion battery of $0.2m^3$ size and $E_{max}^{bt} = 20 \times 10^{-6}J$ can transmit up to 2×10^{11} pulses. If the energy per "1" symbol is of $E_s = 10^{-15}J$. The battery could support about 10^{12} frames of 1000 symbols. However, by taking into account the other tasks of the nanonode, the required throughput of the application, the energy consumed by receiving, and relaying frames coming from thousands of other nodes, we deduce that the battery capacity is a very critical resource that should be managed with great attention.

2.2.1.3/ Memory capacity

In terms of the sub-millimeter node's memory capacity, the current advances allow expecting a memory size of about a few dozen of MB [102]. On the other hand, the memory size impacts on the energy consumption of the nanonode (activation, pre-charging, refreshing, read, write) [77]. Each of these tasks' consumption level depends on the type of memory (DRAM, SRAM, etc.). Nanonetwork applications should limit the memory requirements. Indeed, refreshing energy, that allows keeping the data stored in the memory, is proportional to the used memory. For example, Crucial DDR4-2133 memory model presents a consumption level at the idle mode of $3.5 \times 10^{-3}J/s$ for a memory of 10MB. An energy level high enough compared to the energy provided by the nanobattery. Consequently, even though that memory of 10MB is currently possible in a sub-millimeter node, the memory size that could be supported by the battery is well below. One of the direct consequences of that is the impossibility of using some networking protocols that require high memory storage.

2.2.1.4/ Energy harvesting

Due to the constrained limitation of the nanobattery, many works pay attention to the ways to recharge the battery while the node operates [98]. The harvesting mechanism is based on a power management device that stores a part of the energy provided by an external system to supply power to the node. In [40], the authors classify the harvesting techniques according to the energy source into mechanical, thermal, radiant, and biochemical sources. For example, in [98], a solar-based harvesting system is studied, while in [26], the electromagnetic-based system is proposed. Whatever the used harvesting system, the nodes are able to restore, over time, a part of their energy. The amount of restored energy in a time unit depends on the nature of the harvesting system (in the solar-based system, it may be impacted by the brightness intensity) and the battery characteristics. Boisseau et al. [40] estimates that the restoration of 10 to $100 \times 10^{-9}W$ ($10^{-9}J/s$) is a good order of magnitude for energy harvester of about

$1mm^3$. Let $H(n)$ the recursive incremental function that returns the battery level on the node n after one-time unit.

$$H(n) = H(n) + \delta(n) \quad (2.4)$$

$\delta(n)$ designates the amount of harvested energy during the last time unit.

2.3/ Antennas in nanonetworks

The use of beam steerable antennas is vital for Terahertz nanonetworks applications due to the high path loss, signal attenuation, and energy consumption constraints. In the presence of dense nanonetwork, beam steerable antennas allow to reduce the interference by concentrating radio signal on the targeted area. The beam-steering techniques could be classified into three main categories [89]: mechanical steering, beamforming, and reflectarray antenna. Mechanical steering [6] is considered unsuitable regarding its impact of antenna size and its lack of responsiveness. Beamforming techniques [72] use a combination of signals provided by an array of antenna, leading to highly directional radio signals. Reflectarray antenna [64] techniques use an array antenna combined with a reflector. The signal provided by a field generator is reflected by a set of reflectors in a specific direction.

2.4/ Nanonetworks Application Fields

The development of nanomachines and nanonetworks is still at the conceptual stage, considerable efforts should be made to achieve an effective realization of this emerging paradigm. This does not preclude foreseeing the implementation of future applications that will provide reliable solutions to today's complex problems that current technology fails to solve.

Indeed, nanonetworks based on organic or inorganic nanomachines arisen from nanotechnology are expected to offer great potential for a wide range of application domains requiring nano-information acquisition and making the decision of acting at any scale level. At the present stage, the envisioned applications can be principally grouped into multiple areas of great importance, such as biomedical, environmental, military, industrial [24, 28, 109, 114], and agriculture.

2.4.1/ Programmable matter applications

Programmable matter is a material that has the potential to change its physical properties (shape, density, modulus, conductivity, optical properties, etc.) in a programmable way, based on user input or autonomous sensing. Therefore, programmable matter is related to the concept of a material that has the capability to process information by nature. The close integration of sensing, actuation, and computation in composite materials could then enable a new generation of intelligent material systems that can autonomously operate modification in appearance and shape.

Applications for these materials include aerodynamic profiles, vehicles, and military equipment with camouflage capability, self-reconfiguring modular robotics, etc. The latter field aims to significantly improve behaviors of many kinds of objects or systems via several new possibilities. This may come from the aptitude to change physical structure and behavior of a solution by replacing module control programs; as it could also be possible to carry out self-repairing by changing failed module [91].

At a nanoscale level, Claytronics [41] is an emerging field of engineering concerning reconfigurable nanoscale robots (claytronic atoms, or catoms) designed to form a much larger scale machines or mechanisms. The catoms will be sub-millimeter computers that will eventually have the ability to move around, communicate with other computers, change color, and electrostatically connect to other catoms to form different shapes.

2.4.2/ Bio-medical applications

The bio-medical field is one of the most promising field of nanonetworks use because the corresponding nanomachines can be designed to have required capabilities (size, control at molecular level, bio-compatibility, bio-stability, etc.) enabling them to interact with the organs and tissues of living beings, in particular humans. To this end, the following applications may be envisioned among others:

- *Immune System Enhancement.* The immune system can be strengthened by nanomachines dedicated to facilitate the process of detection and elimination of malicious agents (Viruses, microbes, etc.) and harmful cells (Cancer cells). Therefore, treatments for critical diseases would be much less exhausting and more tolerable for patients [14, 15].
- *Bio-hybrid implants.* Bio-hybrid implants and the well-controlled use of nanomachines are expected to revolutionize future medicine, in particular neurosurgery area. Bio-hybrid implants are intended to support or replace failing components such as damaged organs, nerve tracks, or tissues [16]. Thus, nanonetworks can be used to provide user-friendly interfaces between the implant and its environment. A potential application of major interest for these bio-hybrid implants would be the restoration of central nervous system tracks.
- *Drug delivery systems.* This case involves the development of systems capable of compensating deficiencies of the natural metabolism, producing certain substances or stimuli, essential to the normal functioning of the body, through regular artificial intakes via nanomachines. This is particularly the case for the treatment of diabetes through the automatic administration of insulin and neurodegenerative diseases via neurotransmitters or the administration of appropriate drugs [20].
- *Health monitoring.* Healthcare practitioners can make better use of the in/on body nanosensor networks for early diagnosis of diseases by monitoring the various metabolic reactions of patients' bodies through the examination of the levels of glycosides, cholesterol, uricemia, red blood cells, lymphocytes, etc., provided by the embedded nanosensors. This will greatly impact the quality and adequacy of treatments.
- *Genetic engineering.* Nanonetworks can be used to improve and extend genetic engineering applications through nanomachines dedicated to manipulating molecular and genetic nanostructures.

2.4.3/ Industrial and consumer goods applications

Nanonetworks can be used in the industry to contribute to the development of new materials, manufacturing processes, and quality control methods. The following applications have already been proposed:

- *Programmable matter.* Programmable matter [84] is one of the technological challenges of the future. The nanonetwork represents a group of micro-robots capable of reorganizing themselves to form different shapes. Wireless communication between these micro-robots [62] allows better efficiency and responsiveness of the reorganization algorithms.
- *Food and water quality control.* Nanonetworks can be profitably used to monitor the quality of food and water reserves. Toxic chemical or biological agents infecting food and water can be effectively detected through the use of nanosensor networks.
- *Functionalized materials and objects.* Nanonetworks can be integrated into advanced fabrics and materials to achieve attractive new functionalities. Various antimicrobial and stain-resistant objects are being developed using nano functionalized materials [18]. For example, in the context of a pandemic like COVID-19, a multitude of protective nano functionalized products available to citizens and health practitioners would significantly limit contamination and deaths. As a result, socio-economic impacts and deaths would be reduced to the impacts of a containable local epidemic.

2.4.4/ Military applications

In the military field, the deployment extent of nanonetworks depends on the application. Battlefield surveillance and maneuvering require dense deployment of nanonetworks over large areas, while nanonetworks to monitor the individual performance of soldiers are deployed over smaller areas of human body size. Some of the military applications could be:

- *Defenses against attacks by mass destruction weapons.* Nanonetworks can be deployed to cover a battlefield or targeted areas to detect dangerous chemical and biological agents and coordinate the defensive reaction.
- *Nano-functionalized equipment.* This may be focused on military equipment manufactured using advanced materials embedding nanonetworks helping to realize advanced functions like effective camouflage, self-regulating temperature underneath soldiers, signaling the location of injured and dead ones, etc.

2.4.5/ Environmental applications

As nanotechnologies are inspired by biological systems present in nature, they can also be applied in environmental fields to achieve several objectives that could not be realized with current technologies. Hereafter are some environmental applications:

- *Animals and biodiversity control.* Nanonetworks can also be used in natural environments to control animal species. Nanonetworks using pheromone messages can be used to trigger interactions in animals so that they can be monitored, studied, and controlled.
- *Air pollution control.* From time to time, some megacities suffer from severe air pollution involving drastic measures on the use of vehicles. This has a negative impact on citizens' health and means of transportation. Therefore, like quality control applications, air can be monitored using nanonetworks. When polluted, it can be purified by nanofilters developed for this purpose.

2.4.6/ Agriculture Applications

As the world population grows at a frenetic rate, its need for agricultural products is also increasing. However, although arable land is increasing at the expense of animal living space, this increase reaches its limits. Therefore, many more people would need to be able to be fed on the same arable land. This dilemma will be partially solved by the contribution of nanonetworks and nanotechnology. The use of genetic engineering with nanomachines would make it possible to develop a variety of new high-yielding and resistant plant species, while nanosensor networks can help in the early detection of crop diseases and trigger nanoactuators to eradicate the pathogen agents responsible for these diseases. Nanosensor networks can also assist in detecting and removing nanoparticles that may prevent normal crop growth prior to the seeding process [122].

Communication in Terahertz band

3.1/ Introduction

Until recently, the Terahertz band between 100 GHz to 10 THz [85] represented a "radio frequency gap" because of the lack of efficient radio transceivers using this frequency band. Terahertz band is very attractive resource, due to its availability and to the offered bandwidth. In addition, the miniaturization constraints due to the nanodevices dimension makes the Terahertz frequency band the most suitable for sub-millimeter antennas.

The cross effect of Terahertz band and ultra-dense nanonetwork raises new operational conditions, which need the revision of the network protocol stack. Current chapter addresses the major works in field of physical, link and network networking layers.

3.2/ Physical Layer

The Terahertz band communications are governed by constraints and requirements with a significant impact on the physical layer and hence need an appropriate modulation and channel access mechanism [105].

The communication system consists of three components: a transmitter, a channel, and a receiver. Transmitter and receiver terms are often regrouped in one: the transceiver term. The modulation and demodulation techniques are an important function of the transmitter and receiver. Therefore, transmitting and receiving information over the channel should be achieved without compromising the integrity of data conveyed by the signal. Also, it should be expected to maintain sufficient power at the receiver side to reproduce the original signal with minimum noise and distortion. To this end, different modulation schemes such as amplitude modulation (AM) [3], frequency modulation (FM) [2], phase modulation (PM) [1, 112], and pulse based modulation (PBM) [53, 59] may be used. The first three techniques are continuous wave modulation in opposite to the last one. The inability of nanoscale transceivers to generate a carrier signal at terahertz frequencies limits the feasibility of carrier-based modulations and motivates the use of pulse-based communication schemes in nanonetworks [85]. Hence, due to the peculiarities of dense nanonetwork, the limited transmission power of nanonodes, and the phenomena that affect the propagation, there is a requirement to model the entire Terahertz Band for distances much below one meter [43].

In pulse based modulation [36], data transmission is based on sending a sequence of electromagnetic pulses spread over the time. Several modulation techniques and channel access solutions are proposed in the literature to guarantee very large bit-rates in the short-range. The

pulse-based communication scheme is encoded either in (a) Pulse Amplitude Modulation, (b) Pulse Position Modulation, (c) Pulse Width Modulation, or (d) On-Off Keying. In following we classified the different pulse based techniques according to their main idea. On-Off Keying technique is widely used in combination with the other techniques and consists to use the electromagnetic silence to code the 0 symbols.

3.2.1/ OOK modulation

Rate division multiple access (RDMA) technique using on-off keying has been proposed in [87] for Terahertz nanonetworks. To fix the duration between consecutive time-windows, the authors propose a new scheme based on the Prime Mod algorithm, which generates a unique prime number at each nanodevice. For this, the scheme involved complexity cost due to the process of addition and factorization repeated until a different coprime factor is found.

Time Spread On-Off Keying (TS-OOK) [66] is one of the most used technique. TS-OOK is based on OOK modulation and consists to simply consider a constant inter-symbol duration of about $1000 \times tp$. Where tp is the duration of a single pulse.

In order to reduce collisions due to the unique symbol rate for all nanodevices, the authors propose an improvement of TS-OOK in [42]. The functionality of the proposal, named Rate Division Time Spread OOK (RD TS-OOK), is similar to that of TS-OOK. Except that, the symbol rate is selected among a list of coprime values during the communication announcement. The lack of the protocol is the overhead introduced by handshaking process initiated by transmitter, which would eventually result in low channel utilization.

Another TS-OOK variant in the literature is that from [94]. The authors aim to ensure symbol rate balancing. To this end, they employed pseudo-random time-hopping sequences to adjust the time between symbols that, on average, could generate similar symbol rates for nanodevices.

3.2.2/ Pulse Position Modulation

In pulse position modulation, the time position of the pulse within a cycle of T seconds is used to code a sequence of M bits. The authors in [105] proposed (TH-PPM) time-hopping multiple access (THMA) with M-ary pulse position modulation (PPM) for Terahertz band based nanonetworks as a modulation and multiple access scheme. In TH-PPM, the information is contained in the pulse position relative to a repetition time interval. This pulse position was defined by the time-hopping sequences (THSs) generated randomly.

In [106], the authors present a modulation scheme combining TS-OOK and the pulse position modulation (PPM). The new scheme is applied in nanobody networks. Contrary to TS-OOK, which sends bits one by one, the proposed scheme's basic idea is to transmit the bits as a sequence. However, slightly more time is needed to transmit the same bits, leading to lower data rate than TS-OOK.

3.2.3/ Pulse Coding

In this kind of techniques, m -bits words used by the communication is coded by a binary sequence of n 0/1 symbols. To achieve low energy consumption in wireless nanosensor networks (WNSNs), a novel minimum energy coding scheme (MEC) is proposed in [52]. Unlike the existing Terahertz communication schemes in which the whole Terahertz band is exploited,

sub-bands of the Terahertz band are chosen. Low weight channel coding is combined with OOK modulation at every sub-band to obtain efficient energy transmission. Latency is decreased according to the lengthy codewords. Therefore, the number of sub-bands used for a communication should be chosen to satisfy a certain delay requirement.

In [50], the authors adopt the OOK modulation and propose an optimal coding design in order to reduce transmission energy. The coding mechanism called low weight code. The most frequent symbols are then coded with the codes including the highest number of 0. The objective of this technique is to reduce the energy amount of the communication since the 0 are sent as a silence. It should be noted that this work only considers the transmission energy while the energy of encoding operation, conducted before transmitting the data, is not considered.

In [121], a modulation and channel sharing mechanism called Direct Sequence On-Off Keying (DS-OOK) for the Terahertz band is proposed. The direct sequence is used to distinguish concurrent transmitting. DS-OOK spreads the signal by multiplying each pulse by a user-specific spreading code. Meanwhile, its weakness rests in the fact that the receiver should know the spreading code and the expected delay.

3.2.4/ Summary of physical layer protocols

Table 3.1 gives a summary of the works discussed in this section.

Reference	Category	Features	Balancing access	Complexity of transceivers	Based OOK
[105]	Pulse Position Modulation	PPM combined with time hopping	X	Complex	X
[52]	Pulse Coding	carrier frequencies	X	Complex	✓
[50]	Pulse Coding	low-weight code	X	Complex	✓
[106]	Pulse Position Modulation	PPM and time spread pulses	X	Complex	✓
[121]	Pulse Coding	Spread codes	X	Complex	✓
[87]	OOK Modulation	Based on TS-OOK with coprime rates	X	Simple	✓
[66]	OOK Modulation	- 100-fs pulses - asynchronous transmission	✓	Simple	✓
[42]	OOK Modulation	Combining TS-OOK and coprime rates	X	Simple	✓
[94]	OOK Modulation	Based TS-OOK with coprime numbers and Simple Rate Hopping	weak	Simple	✓

Table 3.1: Summary of modulation and channel access schemes.

3.3/ Link Layer

In conventional networks, the link-layer consists of two sublayers: Media Access Control (MAC) and Logical Link Control (LLC). Usually, the MAC sublayer is dedicated to the coordination of access to the communication channels carried out by protocols belonging to that sublayer's class. Simultaneously, the management and recovery of the binary transmission errors are generally performed at the LLC sublayer level. In THz-band nanonetworks, link-layer protocols are used to establish direct communication between two standard nanonodes or between a standard nanonode and a more powerful intermediate device such as nanocontroller, nanorouter, gateway, nano-macro interface, etc.

Although the link layer in THz nanonetworks is the same as that of conventional networks, the communications protocols dedicated to it cannot be applied directly to the context of THz band transmission [79, 109]. This is justified by the nature of the Terahertz band. On the other hand, traditional link layer protocols are mostly carrier sensing techniques and are therefore too complex for THz nanocommunication regarding to the application areas.

Furthermore, nanodevices are very energy-limited, and under various situations, the use of energy harvesting systems is required over time [25, 33, 67]. The availability of nanodevice communication channels is then impacted which is not a constraint affecting the classical link layer protocols [119].

This has been widely accepted by the research community, and several theoretical MAC sublayer protocols for THz nanocommunication have been proposed. As the Terahertz nanocommunication paradigm is still in its infancy, harmonizing theoretical models with the requirements imposed by real-world constraining environments at the nanoscale remains the main exciting goal of the research community.

Up to now, communication protocols can be classified into two categories: hierarchical and distributed (see Figure 3.1). In the first category, super nanonodes (Nanocontrollers) with large resource capacities should act as pillars to support nanonetworks configuration while in distributed architecture, nanonodes act in similar way without behavioral distinction. In comparison, the main advantages of hierarchical protocols regarding the distributed ones include energy dissipation minimizing due to lowering transmission collisions and increasing nanonetwork scalability. However, these advantages are accomplished at the cost of increasing latency delivery and complexity.

3.3.1/ Distributed Protocols

Based on the assumption that nanonodes are subject to very strict resource constraints, in particular, the extreme limitation of energy and memory capacity and computing power, Akkari et al. [78] consider that new developed protocols should take precisely these limitations into account. They assume that the memory space of the nanonodes can only accommodate one data packet, which requires that the delivery of the packets should meet stringent deadlines. As a result, they proposed a lightweight distributed MAC protocol CSMA for nanonetworks. This protocol establishes optimal transmission times that allow nanonodes to have their packets delivered within precise deadlines with maximum traffic throughput. The optimization made at the transmission decision level are obtained from considerations of the incoming traffic flow and queue length of the nanonodes, their power consumption, and harvesting capacity. However, consistent time management requires a rather complicated synchronization of a large number of nanonodes that the authors have avoided addressing.

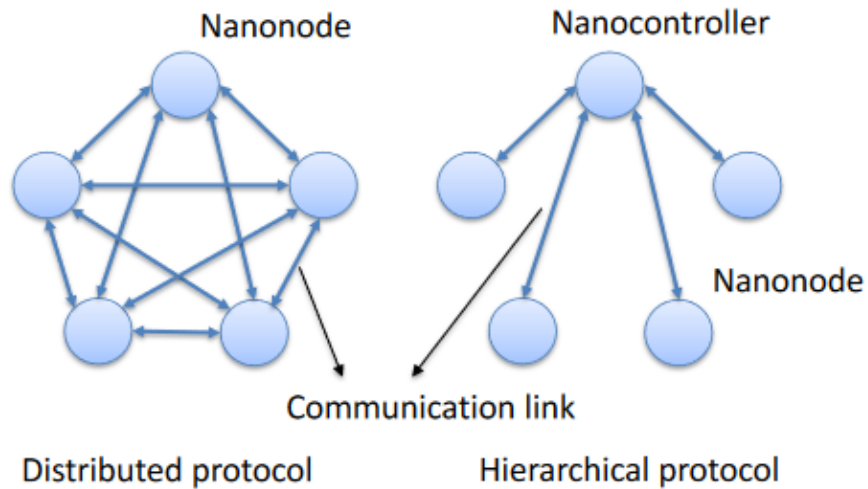


Figure 3.1: Distributed vs. Hierarchical MAC protocols [survey]

Jornet et al. [42] proposed, a distributed access link protocol called PHLAME. The protocol is built on top of modified TSOOK transmission scheme. In PHLAME, the channel coding scheme and the transmission symbol rate (the ratio between symbols) are jointly selected by the sender and receiver nanonodes. The nanonode, which has data to transmit and sufficient amount of energy to achieve transmission, begins the handshaking cycle. The transmitter sends a request packet containing the selected transmitting data symbol rate, and the error detection code. The request packet is sent using the control channel identified by a system symbol rate parameter β_0 . The recipient issues the handshaking acknowledgment upon receipt of the control packet. The transmitter then transmits a data packet using the transmitter specified symbol rate and encodes during the handshake process with the weight and repetition order specified by the receiver. The authors showed that the proposed protocol supports very high-density nanonode nanonetworks with acceptable incurred energy dissipation per sent information bit, realized throughput, and average packet transmission latency.

In Distributed Receiver-Initiated harvesting-Aware MAC (DRIH MAC) [73], the receiver initiates the communication by sending a Ready-to-Receive (RTR) packet to one or more transmitters. The RTR packet receivers send then a data packet to the receiver. DRIH-MAC Scheduling is built upon a probabilistic scheme based on the well-known problem of edge coloring, stipulating that two graph edges incident to the same node must be of different color (see Figure 3.2). In the context of communication protocol, different edge colors mean transmissions sequences. DRIH-MAC is scalable and lightweight, with minimized collision likelihood and maximized harvested energy utilization. However, the initiative for transmission belongs to the receivers, the protocol seems to be application dependent. What would happen if no transmitter is ready to transmit? As a result, these unnecessarily transmitted RTR packets would consume the vital energy of the nanonodes.

S. D'Oro et al. [71] proposed a Timing Channel-based MAC protocol that uses timing channels. The timing channels are described as logical channels in which information is encoded between two consecutive transmissions in the silence period. The authors argue that, by using timing channel-based communications, TCN enables energy-efficient low data-rate communication. Moreover, by introducing acknowledgment-based collision detection, TCN enables recovery from transmission errors. Re-transmissions are then envisioned for improving the reliability of communication.

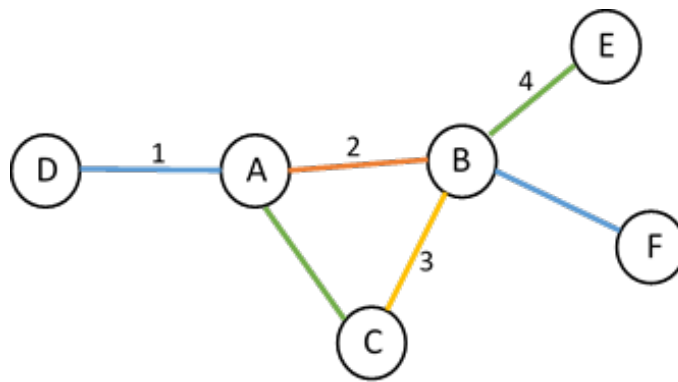


Figure 3.2: A colorful graph. Each number reflects specific colour.

In [115], the authors proposed a MAC synchronization protocol for wireless communication in the THz band. The link-layer synchronization ability is accomplished by a handshake procedure initiated by the receiver (i.e., unidirectional). The basic idea of the handshake process is to avoid data transmissions to a receiver with insufficient energy for reception and a way to guarantee synchronization between transmitter and receiver. In addition, the protocol is intended to maximize channel use and minimize the probability of packet rejection. This is achieved by using a sliding flow control window at the link layer, that is, the receiver sets the quantity of data that can be received regarding its current energy level and memory capacity.

3.3.2/ Hierarchical Protocols

As the name suggests, hierarchical protocols involve a certain hierarchy observed by nanonodes when communicating within a nanonetwork deployed to accomplish a given mission in a given environment and over a given time. This discipline related to the communication behavior of the nanonodes indeed constitutes a constraint but enables the message traffic regulation, ultimately resulting in an essential gain in energy consumption. As a result, many hierarchical protocols have been published in the specialized literature, and among them, the following relevant ones are noteworthy:

In [55], the authors have proposed an inter-layers hierarchical protocol using three types of nodes: standard nanonodes, the nanorouters, and nano interface nodes. The protocol uses two routing policies: selective flooding and random routing. In the first one, when a nanonode receives a packet, it will broadcast it to all the nanodevices within its transmission range. In the second one, if possible, a packet is sent towards a nano router, or towards a neighboring otherwise. The sender's MAC layer uses a handshaking mechanism to assess their neighbors before sending out a packet. If it finds at least one neighbor, it sends the packet to the physical interface using the TS-OOK protocol [66]. Furthermore, if the network layer has not yet found the next hop using random routing, the MAC layer will randomly select it from the neighboring nanonodes. This protocol suffers from a lack of determinism since the coordination between the three layers may fail if no immediate neighbor nanonode is selected.

In [58], the authors have proposed energy and spectrum-aware MAC protocol, a hierarchical protocol where all nanosensors can directly communicate with the nanocontroller in a single hop. Nanocontrollers manage access to communication channels by member nanonodes using TDMA approach, where a time frame layout is classified into three sub-frames: DownLink (DL), UpLink (UL), and RandomAccess (RA). Nanocontroller uses the DL subframe to send

instructions to nanosensors, while nanosensors use the UL subframe to transfer data to the nanocontroller during its time slots, and the RA subframe is required to relay data from nanosensors to nanocontroller. This protocol aims to achieve a fair throughput and ensure optimal lifetime to channel access with optimal harvesting and energy consumption. To do this, a report of critical packet transmission parameter, which is the maximum ratio allowed between the transmission duration and the amount of energy harvesting, is considered such that this collected quantity of energy is greater than the one consumed. However, the huge number of sensed data, issued by an ultra-dense nanonetwork, is not subject to an aggregation process; this raises the costly problem of redundant transmission.

Rikhtegar et al. proposed in [97] a MAC protocol under the name EEWNSN: Energy Efficient Wireless Nano Sensor Network MAC protocol for communications in the terahertz band. This protocol is designed to provide multi-hop communications of mobile nanonodes in THz-band nanonetwork environments. The authors consider a nanonetwork consisting of mobile nanonodes moving at a constant speed and fixed nanorouters (Cluster heads) and a micro interface. The protocol EEWNSN-MAC is carried out in three standard phases: cluster head election process, TDMA-based scheduling phase in which every nanorouter assigns a time slot for every cluster member, and transmission phase enabling nanonodes to send their data packets to their respective nanorouters during their time slot. The nanorouters perform the aggregation step upon receiving data, followed by its forwarding to the micro interface. A view of multi-hop communication is shown in Figure 3.3. The authors do not specify how inter-clusters communications are coordinated to avoid collisions and ignored the process of nanosensors' energy harvesting.

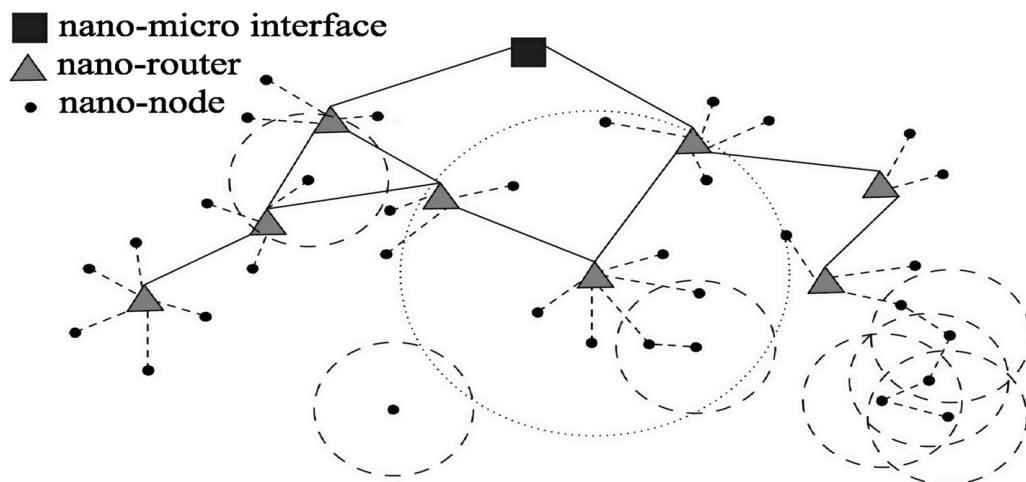


Figure 3.3: Multi-hop communication in EEWNSN-MAC [133].

In [47], the authors have proposed a hierarchical MAC protocol intended for WSNs. They consider three types of nodes: member nodes forming a cluster, a cluster head that coordinates intra-cluster communications by generating TDMA scheduling of time slots and aggregates data sensed by nodes, and a base station that receives aggregated data sent by cluster heads. The network may be regularly reclustered to choose energy-abundant devices to serve as CHs. Member nodes, to transmit packets, first send authorization requests. These requests are processed by the cluster head, which schedules the channel according to the strategy of First come - First served. However, the authors do not indicate how communications between clusters are carried out for reaching the base station.

S. J. Lee et al. proposed in [104] Slotted CSMA/CA Based Energy-Efficient MAC protocol

design in nanonetworks. A MAC protocol based on CSMA / CA communication scheme and supporting nanonodes energy harvesting. A coordinator node transmits periodically beacon packets containing the frame structure. Each nanonode regularly listens to the beacon and transmits a MAC request using slotted CSMA/CA. When a specified slot is allocated, all concurrent nanonodes wait the next time slot. If all the time slots are already allocated, the remaining nanonodes wait for the next frame beacon.

3.3.3/ Summary of link layer protocols

The Table 3.2 summarizes all Mac protocols mentioned in this section. The metrics defined for these protocols are as follows:

- **Topologies.** Previous Terahertz MAC protocols are classified generally as centralized, clustered, and distributed in network topology. Nanonetworks involve a number of nanodevices that operate together to execute basic tasks. In centralized topology, Nanodevices send their data to the controller, and the controller will process and schedule transmissions. Clustered architecture involves effective MAC protocols to maintain efficient inter and intra-cluster data relays. In distributed network architecture, nodes carry out tasks independently and make autonomous communication decisions.

- **Initiated Communication & Hand shake.** Links are an important part before a communication can be initiated, which can be used to synchronize and share information in order to explore the neighboring information. The processes for handshaking should be precisely planned to reduce the delay in constructing links while considering energy consumption. In Terahertz communication, two kinds of handshaking processes are usually handled according to either the receiver or the transmitter initiate the connection between the nodes.

Transmitter-initiated communication usually allows nodes to transmit when they have data to send. These nodes will initiate communication and perform the handshake process. Due to its simplicity and distributed nature, most Terahertz MAC protocols adopt transmitter-initiated communication. In receiver-initiated protocols, the receiver sends a Request-to-Receive (RTR) packet to inform potential transmitters of its energy status and declares its presence and ability to receive packets.

- **Neighbor discovery.** Each node informs its neighbors about its identity and availability. Nodes discovery occurs before the communication phase.
- **Energy.** Energy efficiency means using less energy to achieve the required performance. In some cases, the continuous provision of energy such as devices using low-capacity battery is challenging. Energy harvesting can be used to increase the battery life cycle in order to cope with the lack of energy provision.

3.4/ Network layer

The main aim of the network layer is to deliver packets from source nanonode to the destination or destinations when a direct link is nonexistent. To accomplish this end-to-end transport, network layer may use the following basic processes: (a) Identifying nanodevices with a unique address in order to differentiate the nanonodes and to provide a localization information.

Reference	Topologies	Channel Access Mechanisms	Initiated Communication	Hand shake	Synchronization	Neighbor discovery	Channel Access method	Energy
[97]	Hierarchical	Scheduled	Transmitter	X	X	X	TDMA	X
[58]	Hierarchical	Scheduled	Transmitter	X	X	X	TDMA	✓
[47]	Hierarchical	Scheduled	Transmitter	X	✓	X	TDMA	X
[104]	Hierarchical	Random	Transmitter	X	✓	✓	CSMA/CA	✓
[55]	Hierarchical	Random	Transmitter	✓	X	✓	Aloha	✓
[115]	Plat	Random	Receiver	✓	✓	X	-	✓
[71]	Plat	Scheduled	Transmitter	X	✓	X	TDMA	X
[73]	Plat	Scheduled	Receiver	✓	X	X	TDMA	✓
[42]	Plat	Scheduled	Transmitter	✓	✓	X	TDMA	✓
[78]	Plat	Scheduled	Transmitter	X	X	X	CSMA	✓

Table 3.2: Summary of link layer protocols

However, due to the high nanonetwork density and the highly limited memory capacity of nanodevices, individual addressing (localization) is not possible for neighbouring discovery and mapping an access path from an address or an identifier.

(b) Routing provides services to direct packets to their destinations. A packet may cross many intermediary nanodevices (hops) before reaching its destination.

The network layer services are in charge of ensuring Terahertz (THz) communication of data packets among nanonodes forming the nanonetwork deployed in an area of interest. Due to the very limited transmission range, communication between nanonodes involves a relay nanonode communication mechanism to forward data from source to destination. The forwarding ability enables data packets to be routed along paths linking source nanonodes to destinations. Nevertheless, the intended routing, in Terahertz nanonetwork, differs from the classical one because of severe requirements imposed by the scarcity of physical resources regarding transceivers, channels, storage memory, energy, and the nanonetwork density. Thus, Terahertz nanonetwork routing protocols, inspired by their equivalents in traditional wireless networks, must take into account the intrinsic specific characteristics of THz nanonetworks related to the very high density of frail nanonodes and the obstacles that disrupt transmissions such as noise and molecular absorption.

In this section, we study some of the major routing protocols for conventional ad hoc networks in order to discuss the possibility of using them in ultra-dense nanonetwork. All discussed classical approaches could be improved, taking into account the conjunction of the nanodevices characteristics and Terahertz frequencies [60, 70]. We also discuss some particular protocols proposed for nanonetwork and consider their ability to overcome the nanonetwork constraints.

3.4.1/ Classical routing protocols

Conventional routing protocols for ad hoc networks depend on the nature of the ad hoc network: MANET, VANET, WSN, etc. In Mobile [29] and Vehicular [103] Ad hoc Networks, the priority is given to managing the network variability (distances, positions) in a reactive way. While in Wireless Sensor Networks, the objective is to extend the network lifespan [46]. Some of the classical routing protocols are discussed here using their basic version.

OLSR protocol [17] is a proactive multirelay protocol. The protocol is an optimization of a classical flooding mechanism. Each node establishes a subset of neighboring nodes that will serve as relay nodes. The reduction of the relay sets allows reducing the number of exchanged messages for data broadcasting. The node relays a received message only if it is registered as a relay point of the sender.

DSR [10] is a reactive routing protocol that uses a deduction process for determining the network topology starting from the routing packet headers. When the source node has no entry for the destination in the routing table, it sends a route request packet. Once an intermediate node receives the route request, it adds its ID to the request and forwards it. When the request reaches the destination node or an intermediate node with a route to the destination, the complete route is transmitted in a route reply packet to the source node. However, several improvements have been proposed for DSR protocol [95, 61] involving topological information analysis. From the paths included in the data packets, nodes extract the sub-paths towards the intermediate nodes. Additional information on the network topology could be deduced by combining the different paths. Nodes could also use the paths obtained from their neighbors. These improvements aim to reduce the computational complexity of the protocol. However,

the topological deductions increase the risk of propagating incorrect information.

AODV [7] is a reactive routing protocol based on point-to-point routing. Each node that receives a packet computes the next-hop node using a routing table. As for DSR protocol, the node diffuses a route request (RREQ) in order to determine the path to the destination node. This request is diffused only if the node has no path to the destination or if the availability date of the route has expired. During the propagation of the path request, the intermediate nodes store the neighboring nodes that relayed the request in the routing table entry corresponding to the source node in order to establish the reverse path. Once the path request reaches the destination node, it sends a path response packet (RREP), and the intermediate nodes update the routing table entry corresponding to the destination node. Since the nodes update the routing tables according to the reverse-path principle, AODV cannot be used when the communication between nodes is asymmetric and in dense network accordingly the size routing table.

3.4.2/ Nanonetwork routing protocols

In this section, we present and discuss some of the existing routing protocols in the literature for WNN. These protocols are classified according to three principles: network topology, nanonode mobility, and routing path (Figure 3.4) [116]. The routing protocols are categorized based on the network topology that can be flat or hierarchical structure, and the nature of the routing path: multiple or single path scheme.

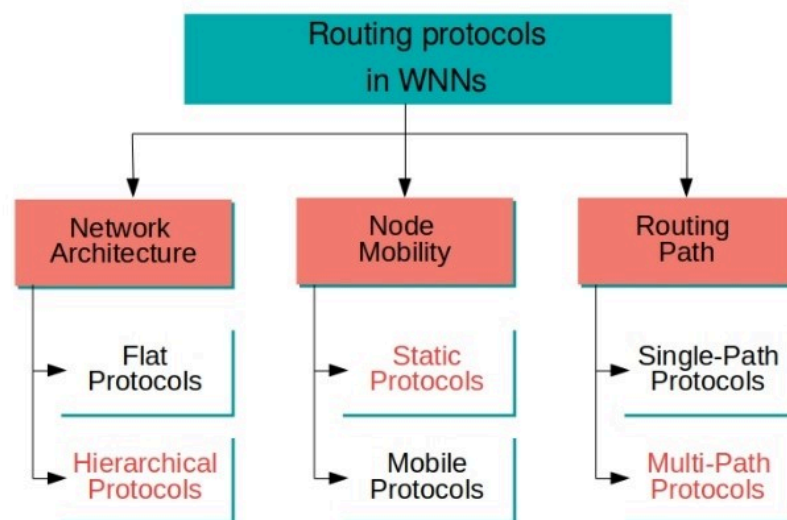


Figure 3.4: Classification of WNNs routing protocols.

3.4.2.1/ Multi-path Routing

The authors in [68] proposed a multi-path routing protocol called RADAR. The protocol is based on efficient flooding where nanonodes are uniformly distributed in a given circular area. In the center of this area, an entity rotates regularly and emits radiation at a certain angle,

as shown in figure 3.5. A nanonode located within the radiation zone is in on-state, while a nanonode located outside the radiation zone is in off-state. In the RADAR protocol, data packets are transmitted by flooding the radiation zone, which reduces the number of packets transmitted in the nanonetwork. Nanonodes that are not in on-state do not consume power. However, this protocol can suffer from packet loss since the receiver may be in off-state.

The probability of the destination node being in on-state is correlated with the radiation angle. However, the use of a large radiation angle results in high energy consumption, which requires optimization of this angle in different scenarios to find a good balance between energy consumption and packet loss. Furthermore, the more the central entity is away, the more nanonodes are in on-state. Consequently, collisions caused by a large number of packets may occur. Consequently, this lack becomes more severe in the large-scale nanonetworks.

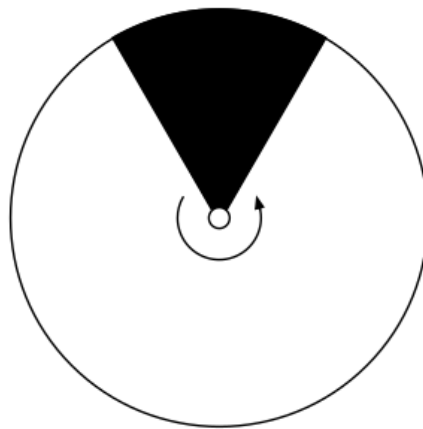


Figure 3.5: An example of RADAR routing [116].

In [75], the authors proposed and simulated a coordinate and routing system for nanonetworks called CORONA. The protocol assigns addresses to the nanonodes, which can be dynamically deployed on an ad hoc 2D nanonetwork, in the form of a coordinate system. Based on four preselected anchors and placed at the four corners of the nanonetwork area, during the configuration phase, and according to flooding packets received from these anchors, each nanonode can calculate its distance in a number of hops from these anchors (see Figure 3.6a). The network area is then subdivided into zones where each zone designates the nodes with the same coordinates. Once the coordinates have been established, the communication phase will take place. When the nanonode A wants to send a packet to another nanonode B , the nanonodes which coordinates is between the coordinates of nanonodes A and B re-transmit the packet, as shown in Figure 3.6b. The packet is re-transmitted by flooding in the area between the nanonodes source and destination.

Stateless Linear-path Routing (SLR) is an improvement of the CORONA approach. In a similar way than CORONA, the coordinates of each node regarding each anchor is computed at the initialization of the system. Nodes forward the received data packet if they belong to the direct line between the source and destination positions; otherwise, they ignore the packet. SLR offers better performance than CORONA, by reducing redundant paths. The CORONA protocol defines larger area in which the packet is forwarding until destination (see Figure 3.7). However, the number of re-transmissions in SLR could be high, as many nodes can share the same coordinates.

Unlike SLR, the authors proposed in [83] a deployable routing system (DEROUS) where nanonodes are either users or re-transmitters creating radial lines and circular patterns around a

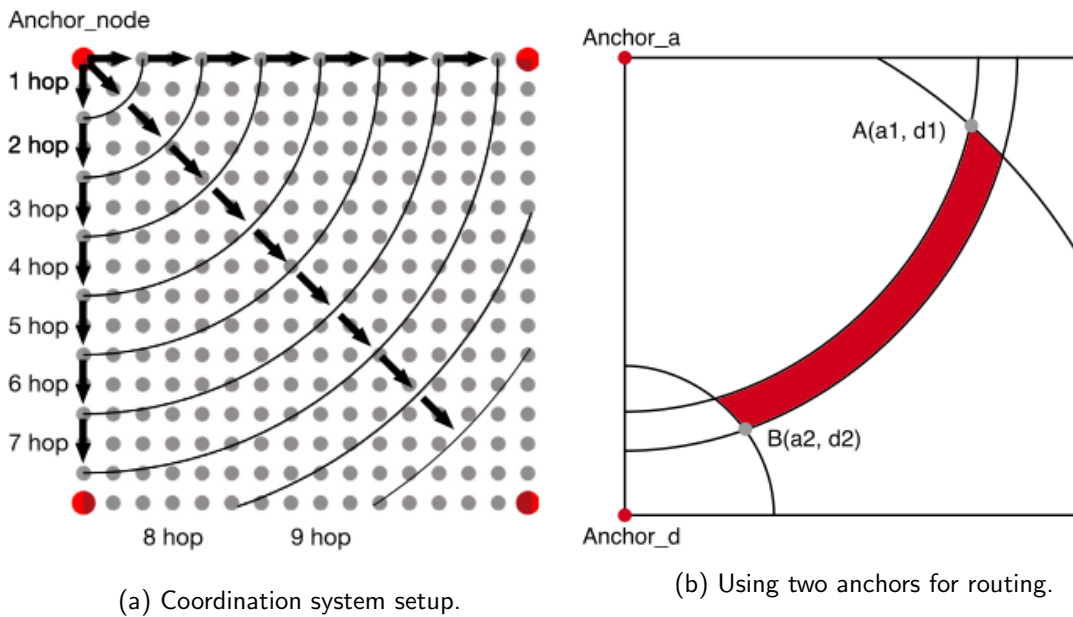


Figure 3.6: Illustration of CORONA Coordinate/routing protocol [116].

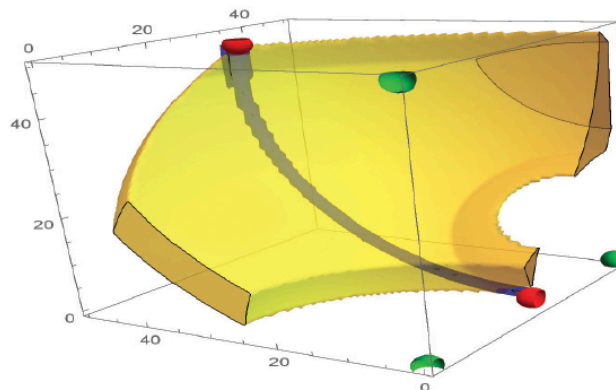


Figure 3.7: Comparison of the routing behavior of CORONA (yellow area) and SLR (dark curve) for a given communication node pair in a high resolution area [88].

BEACON-node in the center of the area. Based on this property, DERIOUS routes the communication packets along the radial and circular paths to reduce the number of forwarders. A nanonode with a radius among the sender and the receiver transmits the packet in a low-power radial direction. Furthermore, nanonode re-transmits the packet in an angular direction using standard power if its radius is the same as the sender or receiver radius. DEBOUS functioning scheme is depicted in figure 3.8 that shows four various routing cases according to the sender and the receiver positions.

Nonetheless, this approach can contribute to a high redundancy of packet retransmissions and receptions due to its failure to locate the destination node precisely. Additionally, the shortest path may not be shaped by retransmitters, resulting in an increase in transmission delay.

LaGOON [100] is one of the rare routing approaches for nanonetworks that take into account the nodes' volatility. LaGOON uses the destination MAC address of the received packet to identify the targeted relay and uses the network address to identify the packet's final destination.

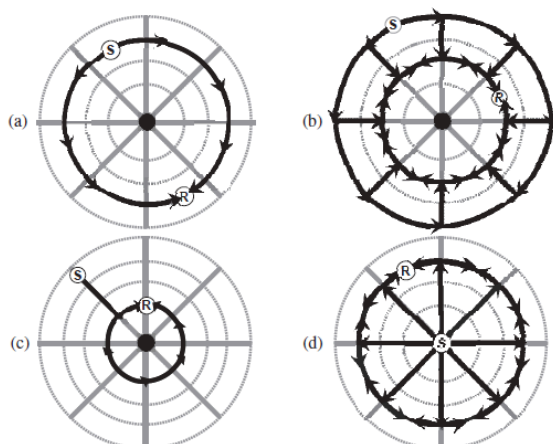


Figure 3.8: DEROUS-system routing cases. The sender (S) and receiver (R) locations can be interchanged [83].

In LaGOON protocol, when a node needs to send or relay data to a given destination node for which it has no path, it floods the message to all its neighbors. Every node receiving a message from the node, s relayed by the neighbor, v uses it to establish or update the route toward s via v . If the destination MAC address of the received message differs from the receptor's address and differs from the broadcast address, then the message is ignored. Otherwise, the message is relayed. The objective of LaGOON protocol is to eliminate the need for control messages. The routes are built using the exchanged data packets. At the starting of the nanonetwork, data transmission follows a flooding pattern. Finally, the network nodes store for every sink destination the set (or subset) of next hops to reach it. The set of good neighbors is sorted in such a manner to maintain the last direct sender on top. Therefore, the use of the last sender node can locally concentrate the traffic on one node leading to collisions and energy over-consumption. Moreover, the radio link is assumed symmetric, which is not the case.

3.4.2.2/ Single-path Routing

Afsana et al. [99], proposed an Energy Conserving Routing (ECR) protocol for wireless body sensor nanonetworks (WBSNs), using a multilayer topology based on the single-hop transmission range of the nanonodes and the distance between the nanonodes and the nano-interface (gateway). After layering phase, the highest energy nanonodes are selected as nanocontrollers (NCCs) of the first round, and after in a round-robin manner. The NCCs broadcast short-range advertising messages. Each nanonode selects the NCC with the highest Received Signal Strength Indicator RSSI and sends a join request to it. There are two types of communication intra-cluster and inter-cluster. In intra-cluster communication, only one-hop or two-hop transmissions are considered. In inter-cluster communication, the NCC transmits data to its lower layer's NCCs. However, in order to structure the network in layers, this protocol supposed an NC (placed in the center of the network), which sends a hello message to all the nanonodes of the network, without explaining how this message reaches the whole network. Besides, the NCC's election in the first round requires knowing the energy of its neighbors.

Pierobon's routing protocol [69] is a dedicated routing protocol for wireless nanosensor networks, where a set of nanosensors detect nanoscale events and send their measures to the nanocontroller nodes. Each time a nanosensor asks for transmitting data to its nanocontroller,

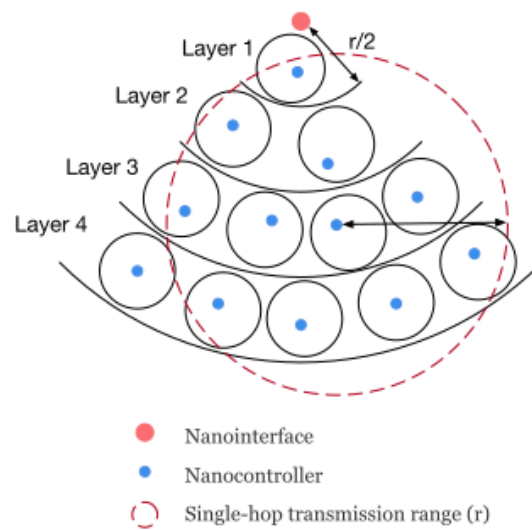


Figure 3.9: The architecture of ECR [116].

the nanocontroller checks either the direct transmission is better or the use of a multi-hop transmission (use of an intermediate node to relay the data). The decision is made according to the energy consumption estimation of each option. Pierobon's approach aims to reduce the overall transmission energy but does not take into account the residual energy at each node. On the other hand, the method assumes that the nodes are randomly distributed over the area with a constant density, ρ making the method not adapted to concave deployment topologies. The method assumes that all nanonodes can communicate directly with the nanocontroller, representing a strong restriction about the use of the method: the need for numerous nanocontrollers, a flat landscape without obstacles, etc. Finally, the method adopts a reactive routing mode where the transmission path is computed just in time, which induces some latency. This latency increases when the intermediate node refuses the reception or the re-transmission of the incoming data due to its conditions such as its residual energy, buffer capacity, and SNR (Signal to Noise Ratio).

Energy-efficient cooperative routing (EECR) protocol [117] proposes a cooperative protocol for hierarchical cluster-based nanonetworks. In random configuration, several nanonodes are distributed over a square where a nanocontroller is placed in the middle of that zone. The nanonodes of a given cluster cooperate in forwarding data to the nanocontroller (sink node). The nanonodes cooperation aims to determine the optimal path according to the energy cost. Each nanonode transmits the setup packet obtained from the nanocontroller using the highest transmitting power to the nanocontroller for the required hop counts, as shown in Figure 3.10. As with Pierobon et al. protocol, the objective is to reduce the amount of the total consumed energy without considering the residual energy level on each nanonode.

3.4.3/ Summary of network layer protocols

Table 3.3 lists all routing protocols examined in this section for a visual overview of the current routing protocols. The comparison is made according to the following criteria:

- **Routing strategy.** Routing strategy uses local or global awareness to determine a path to the destination. Thus, routing strategy is one of the essential aspects of a routing

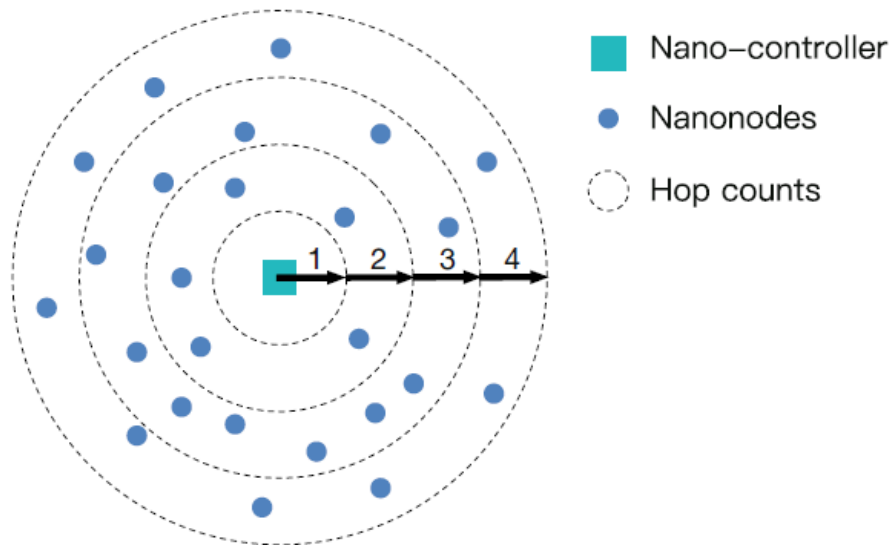


Figure 3.10: In the initialization phase, nanonodes reach the required hop counts to the nanocontroller [117].

protocol and can represent the routing protocol's working scheme.

- **Locating position.** The transmission can be controlled by a nanonode network with position knowledge, for reducing flood areas.
- **Energy-aware.** Nanonodes have limited energy instead of their small scale. Therefore, the routing protocols need to take into account the nanonodes energy. In hierarchical routing protocols, the multihop communication algorithm within the nanocontroller still considers energy aware.
- **Complexity.** Knowing that protocol complexity is related to time and space overhead and nanonodes' limited resources (computing capacity, energy and storage space), specific routing protocols are required.
- **Scalability.** Protocols are supposed to operate efficiently in small networks as well as in large ones. As the number of nanonodes grows, the routing protocol's scalability becomes "Restricted" when the network efficiency decreases rapidly. The routing protocol's scalability is "good" when a network efficiency decreases marginally.

The next part of the thesis describes our contributions, that are organized as follows:

- Chapter 4: Comparative study of pulse-based Terahertz access protocols.
- Chapter 5: Directed graph based traffic regulation protocol.
- Chapter 6: Clustering based protocol for traffic regulation.
- Chapter 7: Routing Protocol in ultra-dense WNN.

Reference	Communication	Routing strategy	Locating position	Network structure	Energy-aware	Complexity	Scalability	Coordination
[68]	Multi-path	Blindly retransmit	No	Flat	No	Low	Limited	Distributed
[75]	Multi-path	Coordinate	Hop counts to the anchor nodes	Flat	No	Low	Limited	Distributed
[88]	Multi-path	Coordinate	Hop counts to the anchor nodes	Flat	No	Medium	Limited	Distributed
[83]	Multi-path	Radial and circular paths	Hop counts to the central entity	Flat	No	Low	Good	Distributed
[100]	Multi-path	broadcasting	No	Flat	No	Low	Limited	Distributed
[99]	Single-path	Double-hop or one-hop	Layer	Hierarchical	Yes	Medium	Good	Centralized
[69]	Single-path	algorithm algorithm	Distance to the nanocontroller	Hierarchical	Yes	High	Good	Centralized
[117]	Single-path	Direction of forwarding	Distance to the nanocontroller	Hierarchical	Yes	Medium	Good	Centralized

Table 3.3: Summary of network layer protocol



Contributions

Improvement of pulse-based Terahertz access protocols

4.1/ Introduction

In pulse-based modulation [36], data transmission is based on sending a sequence of electromagnetic pulses spread over time. Several channel access solutions are proposed in the literature to guarantee very large bit-rates in the short-range [35]. This chapter focuses on the channel access techniques based on OOK modulation because of the molecular absorption noise's peculiar behavior [113, 93].

Nanocommunication's principal challenge is to efficiently share the Terahertz radio spectrum in order to optimize data transmission in dense nanonetworks. In this context, Spread in Time On-Off Keying (TS-OOK) protocol was proposed as a channel access mechanism, where all nanodevices use the same and unique time duration between transmissions.

After that, different new approaches such as RD-TSOOK and SRH-TSOOK were proposed as improvements of TS-OOK. In RD-TSOOK, the main difference remains in the time between symbols, which is various for different nanodevices. While, in SRH-TSOOK, nanodevices change the time between transmissions at each frame.

The chapter's objective is to establish a review of the existing related access techniques based on OOK modulation scheme (TS-OOK, RD-TSOOK, and SRH-TSOOK). Then, considering the weaknesses of these published protocols, we propose a new scheme called SDMA-TSOOK, where each nanodevice allocates a time slot used to send its symbols in an independent and asynchronous way.

SDMA-TSOOK aims to be efficient, provide balanced channel access, and takes into account co-channel collision and networking capacity that pose a problem for concurrent channel access. Finally, to verify the effectiveness of the proposed technique, we compare its performance with those of TS-OOK, RD-TSOOK, and SRH-TSOOK that have been all implemented in BitSimulator [101].

4.2/ Canal access protocols in Wireless NanoNetworks WNN

The nanonodes' missions are carried out using communications and have to be constrained by WNN's particularities, such as the limited capacities of the nanonodes. Besides, communication protocols are required to regulate access to channels and coordinate the transmission between

nanonodes. In this section, we will define some of these protocols, their operating principles, advantages, and drawbacks.

4.2.1/ TS-OOK

Spread in Time On-Off Keying is a protocol for sharing the radio channel among different nanodevices. This communication technique serves as both a modulation scheme and multiple access mechanism. TS-OOK protocol is based on the transmission of electromagnetic pulses of duration $T_p = 100\text{fs}$ to represent a logical "1" and silence for "0". The time between logical symbols ($T_s \gg T_p$) is fix for all communications.

In Figure 4.1, we show an example of TS-OOK communications for the case where two nanodevices, E_1 and E_2 , concurrently transmit different binary sequences to a third nanodevice R , such as:

- E_1 : First nanodevice transmitting the sequence "110100"
- E_2 : Second nanodevice transmitting the sequence "100101"
- R : Receiver nanodevice

The second transmitter is further away from the receiver than the first transmitter.

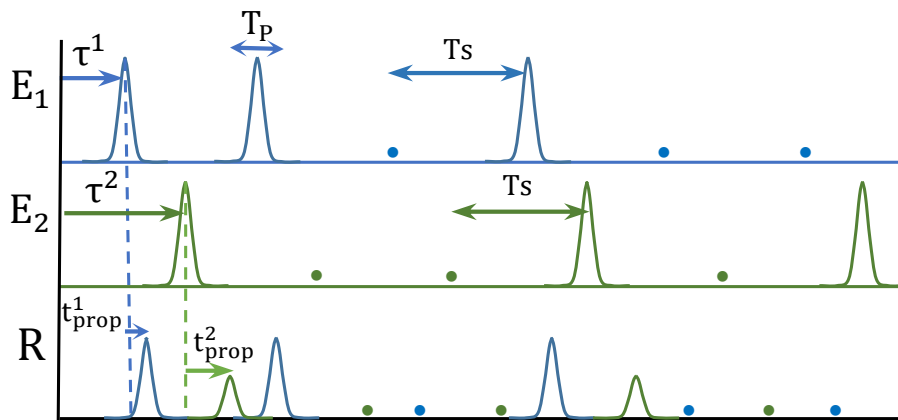


Figure 4.1: TS-OOK modulation: All nanodevices have the same symbol rate T_s .

The transmission of logical "0" does not consume energy in emission, which guarantees better energy efficiency. The multiple access mechanism does not require a global synchronization between the nanodevices. The transmitter and receiver are synchronized thanks to the packet preamble. Indeed, the receiver detects the header of the packet throughout the transmission of a specific initial sequence. The TS-OOK modulation can support a high number of nanodevices transmitting simultaneously several gigabits per second and up to a few terabits per second, since the time between transmissions T_s is much longer than the pulse duration T_p . We call symbol rate β the ratio between T_s and T_p .

$$\beta = \frac{T_s}{T_p} \quad (4.1)$$

The first drawback of TS-OOK is the complexity of finding the optimal value of the symbol rate β , in order to guarantee better flow per nanodevice according to the number of active nanodevices. If $\beta = 1$, the nanodevice sends the communication symbols in burst and the maximum throughput for each nanodevice is reached. Therefore, only one nanodevice at a time can access the channel. By increasing β , the throughput per nanodevice is reduced, but the radio resources are shared over more simultaneous nanodevices. Secondly, in the case where two senders $T1$ and $T2$ start transmitting at two different times τ_1 and τ_2 , respectively. A collision occurs between two simultaneous communications at the receiver if:

$$(\tau_1 + t1_{prop}) \bmod T_s = (\tau_2 + t2_{prop}) \bmod T_s \quad (4.2)$$

where $t1_{prop}$ (resp. $t2_{prop}$) designates the signal propagation time from $T1$ (resp. $T2$) to the receiver.

Therefore, if the transmitters and the receiver are immobile ($t1_{prop}$ and $t2_{prop}$ are fix), the collision will concern all symbols until one of the two communications is finished. The co-channel probability between two communications is then given by:

$$Prob_{co-channel} = \frac{1}{\beta} \quad (4.3)$$

4.2.2/ RD-TSOOK

Like TS-OOK, Rate Division Time Spread On-Off Keying protocol is a modulation and channel sharing mechanism based on the transmission of femtosecond-long pulses, which are transmitted following an on-off keying modulation spread in time. RD-TSOOK is an improved version of TS-OOK protocol, where the transmitter starts by announcing the used β before sending the data. The announcement packet is sent over a control channel that uses a specific fixed symbol rate β_0 .

RD-TSOOK uses different symbol rates, β , for the communications. The use of different symbol rates by nanodevices reduces selective interference effect (co-channel interference). Indeed, two communications C_1 and C_2 generate a co-channel interference if one of the used symbol rates is a multiple of the other and if the time arrival of the symbols to the receiver is synchronized. The following expression demonstrates this two conditions.

$$\begin{aligned} & C_1 \text{ is co-channel with } C_2 \leftrightarrow \\ & (\beta_{C_1} \bmod \beta_{C_2} = 0 \text{ AND } (\tau_1 + t1_{prop}) \bmod T_{sC_1} = (\tau_2 + t2_{prop}) \bmod T_{sC_2}) \\ & \text{OR} \\ & (\beta_{C_2} \bmod \beta_{C_1} = 0 \text{ AND } (\tau_1 + t1_{prop}) \bmod T_{sC_2} = (\tau_2 + t2_{prop}) \bmod T_{sC_1}) \end{aligned} \quad (4.4)$$

Thus, if a collision happens at a receiver (see Figure 4.2), the next collision between the same nanonodes could not occur before a period of $LCM(\beta_{C_1}, \beta_{C_2})$, where LCM is the least common multiple. That is why, in [42], the authors proposed to select the β value among a set of co-prime values to make that:

$$LCM(\beta_{C_1}, \beta_{C_2}) = \beta_{C_1} \times \beta_{C_2} \quad (4.5)$$

Figure 4.2 represents an example of RD-TSOOK for the case where two nanodevices start to transmit to a third common receiver, with different initial transmission times τ_1 and τ_2 .

Transmitter 2 is further from the receiver than the first emitter (the different propagation time t_{prop}^1 and t_{prop}^2). The upper plot corresponds to the sequence "110100", which is transmitted by the first nanodevice with a symbol rate T_{s1} . Likewise, the second trace represents the sequence "100101", transmitted by the second nanodevice with a different symbol rate T_{s2} . The signal received at the receiver side is shown on the third trace. In this case, the third symbol of the first nanodevice is overlapped by the second nanodevice's second symbol. Due to the use of different symbol rates, the two nanodevices' consecutive symbols do not overlap.

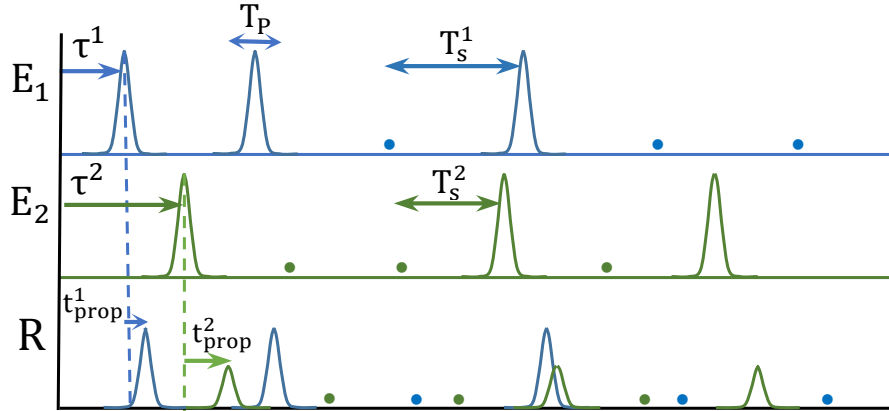


Figure 4.2: RD-TSOOK modulation: Each nanodevice has its symbol rate different from others.

RD-TSOOK suffers from two major drawbacks. First, the random selection of the symbol rate does not guarantee the uniform use of the different β . Consequently, the nodes using a $\beta \approx \beta_{min}$ benefit of a better throughput than those using a $\beta \approx \beta_{max}$, which induces an unbalancing between nanodevices. On the other side, communications with lower symbol rates are more sensitive to collisions when interfering nodes increases. Thus, data retransmission increases, which induces high energy consumption. Besides, the use of a high symbol rate when the radio channel is free (low number of active nodes) is not applicable. In addition, the protocol presents a complexity for the choice of the range $[\beta_{min}, \beta_{max}]$.

4.2.3/ SRH-TSOOK

Symbol Rate Hopping Time Spread On-Off Keying protocol is based on TS-OOK protocol. The idea is to vary periodically the symbol rate used by the communication in a pseudo-random way. This pseudo-random sequence, known by the transmitter and the receiver, is used by the transmitter to change the duration T_s . In Figure 4.3, we note that for two consecutive frames i and $i + 1$ of the same communication, different β are used ($\beta_1 \neq \beta'_1$).

Unlike RD-TSOOK, SRH-TSOOK changes β of the communication after a regular number of symbols corresponding to the transmission of a MAC frame. During the establishment of the communication, the transmitter and the receiver agree on an initial value $R_{current}$. A function, RND , is used to change the value of $R_{current}$ after each frame as follow:

$$R_{current} = RND(R_{current}) \quad (4.6)$$

The new value of $R_{current}$ is then recursively calculated without exchange between the receiver

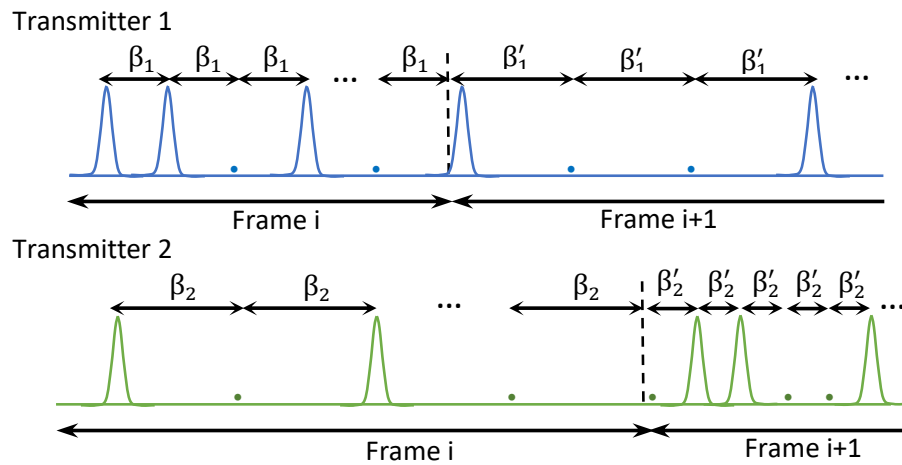


Figure 4.3: SRH-TSOOK modulation: different symbol rate β is used at each frame.

and the transmitter. After each frame, a new β is computed using the equation:

$$\beta = \frac{R_{current} * (\beta_{max} - \beta_{min})}{RND_{max}} + \beta_{min} \quad (4.7)$$

SRH-TSOOK protocol ensures that the different β are used uniformly. Therefore, all active communications ultimately have the same transmission conditions. This approach allows to spread the generated interference over the different communications and gives low similarity radio access conditions to all concurrent communications. Thus, it reduces the probability of co-channel collisions. A co-channel collision occurs when two transmitters $T1$ and $T2$ use the same initial $R_{current}$. This probability is much lower than the probability that two transmitters use the same β in RD-TSOOK and TS-OOK protocols.

SRH-TSOOK protocol does not take into account the traffic load to choose the value of β_{max} and β_{min} . Besides, high values of β can be used even when the number of active nanodevices is low.

4.2.4/ Preliminary comparison of protocols

All protocols, discussed above, are based on the exchange of very short pulses distributed over time. The difference consists in the channel access technique used to minimize the number of collisions, reduce the co-channel risk and improve radio access fairness.

Selected protocols in our study manipulate the value of β , to improve their performance. A comparative study of these protocols is given in Table 4.1 based on probabilistic analyzes. This table allows a first evaluation of the performance of these protocols.

In TS-OOK protocol, the symbol rate referred to as the interval time between two symbols is fixed and kept the same for all nanodevices in the nanonetwork. Due to the highly deployed nanodevices, the probability of collision increases significantly when multiple nanodevices transmit simultaneously. On the other hand, channel access balancing is ensured between the nanodevices. All nanodevices have fair channel access.

Regarding RD-TSOOK technique, each nanodevice randomly generates its symbol rate and kept it fix during all transmissions. So the collisions phenomena are reduced relatively to

Evaluation criteria	Protocols		
	TS-OOK	RD-TSOOK	SRH-TSOOK
Collisions	- High collision rate - The risk of chain collisions	- Few collisions - No chain collision	- Few collisions - No chain collision
Energy consumption	Very little	Relatively little	Little
Balancing Access	Yes	No	Little
Complexity	Simple	Simple	Simple
Synchronization required	No	No	No
End-to-end flow	Fixed for all nano-devices and linked to the β selected by the network	Variable from one nanonode to another linked to the β chosen by the node	Fairness of the flow between nodes according to the β changed each frame

Table 4.1: Protocol performance comparison based on probabilistic analysis

TS-OOK; this is due to the low probability that generated symbol rates be identical and transmissions starting at synchronized times. Unlike TS-OOK, RD-TSOOK is unbalanced concerning channel access because of the high variation of symbols rate among nanodevice (for example, $\beta_1 \ll \beta_2 \ll \beta_3 \dots$).

Compared to TS-OOK and RD-TSOOK protocols, SRH-TSOOK has fewer collisions than both of them. It is due to the symbol rate renewed at each frame instead of keeping it in all transmission as it does in RD-TSOOK. This symbol rate regenerated at each frame has made it better balanced than RD-TSOOK but less than TS-OOK. Collisions, considered as a significant problem in critical applications, should be greatly reduced or even avoided. In such applications, all data interfered should be retransmitted, resulting in increased latency.

To this end, we proposed a Slot Division Multiple Access scheme, called SDMA-TSOOK, that affects slot randomly to each nanodevice.

4.3/ Proposed protocol

In SDMA-TSOOK, nanodevices works in cycles, each cycle is composed by β slots of duration Tp . β is a system parameter fixed for all nodes like in TS-OOK.

The transmitter randomly generate its slot $Pslot \in [0..(\beta - 1)]$ to access the channel. For the first time, each nanodevice generates start-time τ from which it starts generating its slot. This last provides, from equation 4.8, the time slot $TSlot$ to access the channel.

$$TSlot_k = Pslot_{k,i} * Tp \quad (4.8)$$

where $Pslot_{k,i}$ is a positive integer number generated by nanodevice k to transmit symbol i and Tp is a time pulse (100 femtosecond-long).

As each nanodevice processes successively two generated values, τ , and $Pslot$, nanodevices have a low probability of achieving the same time slots. Hence, multiple nanodevices can transmit simultaneously with extremely low interference and collisions. Furthermore, our pro-

positional regulates the access channel where each nanodevice access in a cyclic manner and at a regular interval of time. So the nanodevice k transmits its first symbol at:

$$Tr_{k,1} = \tau_k + TSlot_k \quad (4.9)$$

where $k, 1$ denote the nanodevice and the first symbol respectively.

The rest symbols of the packet are transmitted as follows:

$$Tr_{k,i+1} = Tr_{k,i} + \beta \quad (4.10)$$

where β is a fixed interval symbol rate.

Since the nanodevices are asynchronous, although it is low, there is still a weak collision probability due to random channel access time even if different time slots are assigned. For example, two nanodevices 1 and 2 can have different start-time τ_1 and τ_2 such as $\tau_1 < \tau_2$, and different time slot $TSlot_1$ and $TSlot_2$ so $TSlot_1 > TSlot_2$. These two nanodevices will transmit at the same time if equation 4.11 is verified. Hence, collision at the receiver will continue to propagate in all the following symbols until the end of the packet.

$$\tau_1 + TSlot_1 = \tau_2 + TSlot_2 \quad (4.11)$$

To overcome such an issue, and minimize collision probability, nanodevice generates its slots at each frame, given by equation 4.12, as depicted in Figure 4.4.

$$TSlot'_k = ((\beta - Pslot_{k,i}) + Pslot_{k,i+1}) * Tp \quad (4.12)$$

where $Pslot_{k,i}$ and $Pslot_{k,i+1}$ are randomly generated by nanodevice.

This work aims to ensure a fair sharing access channel as well as could efficiently reduce the collision probability to achieve a highly successful packet delivery rate.

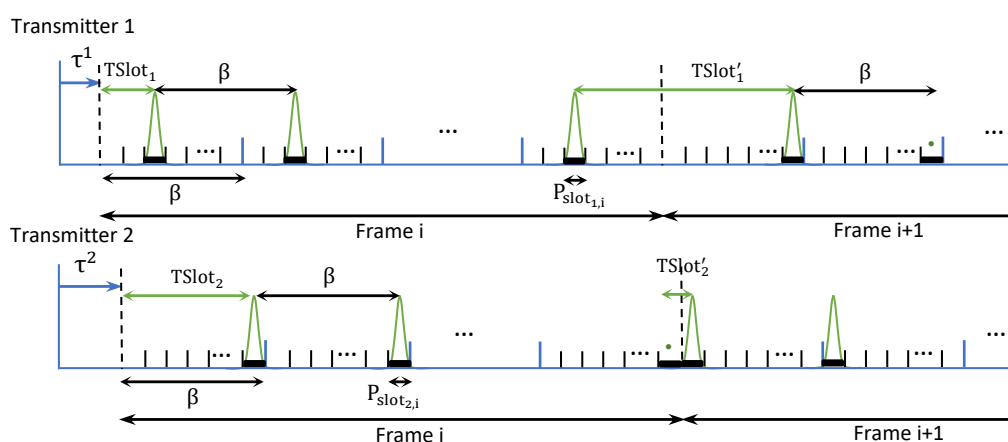


Figure 4.4: SDMA-TSOOK: different time slot $Pslot$ is used at each frame for each node.

4.4/ Scenario's Implementation

To verify the effectiveness of Slot Division Multiple Access technique, we compare its performance with those of TS-OOK, RD-TSOOK, and SRH-TSOOK that have been all implemented

in BitSimulator [101]. The comparison results show that the proposal's overall performance is better than that of the others in terms of collision, successful packet delivery, and radio access balancing. The simulation results are validated through extensive simulations in which 24 scenarios have been implemented. The different scenarios are discussed below.

WNNs are used in different applications, characterized by different topologies of traffic demand, geographical repartition of the nanodevices, and the density of nanodevices. To this end, we implemented different scenarios with different distributions of nanodevices over the network surface, different WNN densities, and different data traffic profiles.

4.4.1/ Nanonodes deployment

Nanonodes are deployed in varied ways: uniform distribution, Gaussian distribution, or Gaussian clusters distribution. Figure 4.5 presents three distribution's models of the nanodevices on a surface of 40cm*40cm.

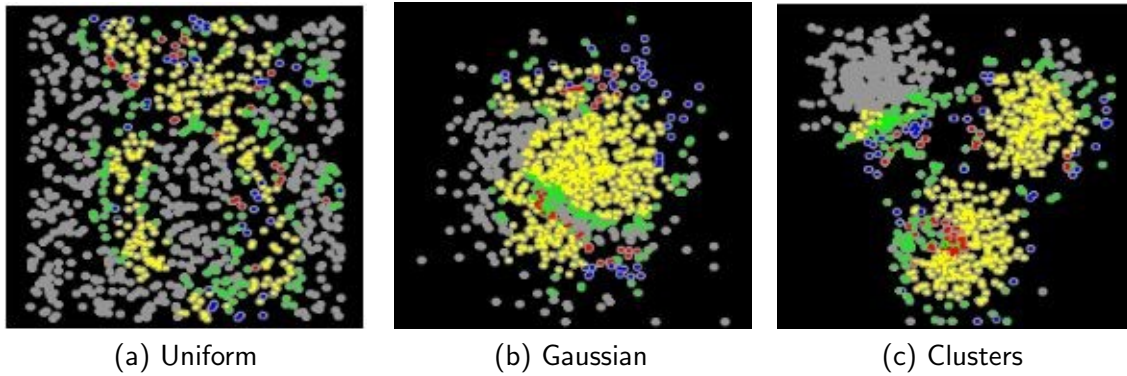


Figure 4.5: Different nanonetwork models in terms of distribution

4.4.1.1/ Uniform deployment

Bettstetter in [12] showed a relationship between nodes transmission range r_c and network connectivity as:

$$r_c \geq \sqrt{\frac{-\ln(1 - p^{1/n})}{\rho}} \quad (4.13)$$

Where p is the possibility that no nanodevice in the network is isolated, n is the total number of nanodevices deployed in the area A satisfying $A \ll r_c^2\pi$ and $\rho = n/A$ is the nanodevice density.

4.4.1.2/ Gaussian distribution

In a Gaussian distributed network, the probability that a nanodevice resides at a position with a coordinates (x, y) relatively to the center of the deployment area $(0, 0)$, follows the Gaussian

law:

$$\begin{aligned}
 X &\sim \mathcal{N}(\mu, \sigma^2) \\
 Y &\sim \mathcal{N}(\mu, \sigma^2) \\
 \mu &= \text{NetworkSize}/2 \\
 \sigma &= \text{NetworkSize}/6
 \end{aligned}
 \tag{4.14}$$

where μ is the mean of the distribution, σ is the standard deviation and NetworkSize correspond to the width of the deployment area (corresponding to a square).

4.4.1.3/ Gaussian Clusters distribution

Nanodevices deployment corresponds to a set of clusters. Moreover, their positions' coordinates in the cluster follow the law given in equation [4.15](#).

$$\begin{aligned}
 X &\sim \mathcal{N}(\mu, \sigma^2) \\
 Y &\sim \mathcal{N}(\mu, \sigma^2) \\
 \mu &= \text{num}_{cluster} * \text{NetworkSize}/4 \\
 \sigma &= \text{NetworkSize}/10
 \end{aligned}
 \tag{4.15}$$

where $\text{num}_{cluster} \in [1..\text{nbr}_{cluster}]$ and each nonodevice chooses his cluster in a random way.

4.4.2/ Data traffic control

Other parameters are added to the simulation, monitoring data traffic source-to-destination. Traffic models is a crucial factor in network simulations in order to analyze how the WNN reacts (i.e., congestion) to the traffic conditions (communication arrivals and duration). As can be seen from the analysis of [Figure 4.6](#), each transmitter (1 and 2) sends data packets every $T1$ and $T2$ time, respectively. The transmissions can be more or less overlapped according to the communication arrival and traffic amount. Therefore, data traffic behavior is analyzed through simulation using the two primary traffic techniques, CBR and VBR [\[8\]](#).



Figure 4.6: Illustration of two data traffic generation methods

4.4.2.1/ Constant Bit Rate (CBR)

The CBR technique deals with random fixed delays on the regular data packet transmission. This model is suitable for any communication network having fixed bandwidth permanently available for the entire transmission time. [Figure 4.6](#) on the left shows this type of traffic where $T1 = T2$ (i.e., all transmitters have the same transmission cycle).

4.4.2.2/ Variable Bit Rate (VBR)

The VBR traffic model uses variable random delays on data packet transmission. We will rely on the Poisson distribution to generate the value of this flow that varies over time. VBR is suitable for the real-time system that transmits data at variable flow rates over time. As shown in Figure 4.6 to the right, each transmitter has a different transmission cycle.

4.4.3/ Density factor

As discussed earlier, WNNs are characterized by high density degree. That is why, we simulated the protocols cited in Section 4.2 with different densities (100, 250, 500, and 750) nanodevices on a surface of 40cm*40cm. The density affects the behavior of the WNNs. Figure 4.7 shows the nanodevices distributions representing different WNN densities.

In the following, all these combined trilogy factors (distribution model, traffic generation method, density) will be examined to assess these protocols' performance. So we get (3*2*4) nanonetwork scenarios. For each scenario, we implement the four studied channel access protocols.

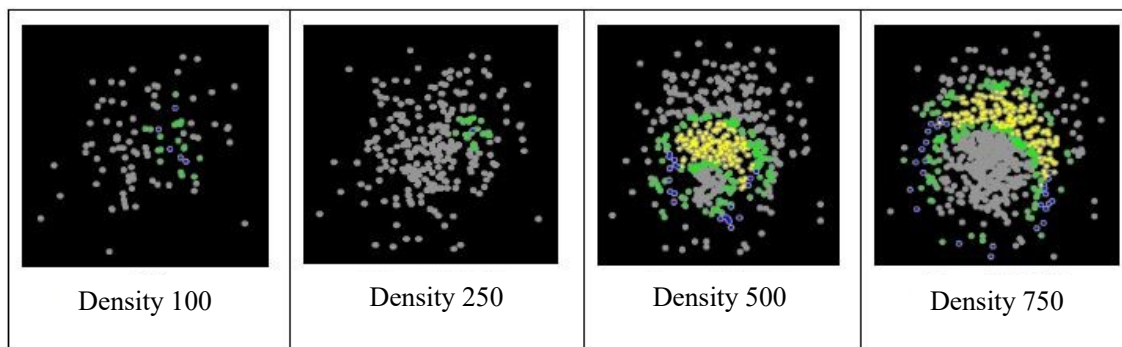


Figure 4.7: Different densities

All the tests are made using the following simulation parameters:

- Routing protocol: Stateless Linear Routing (SLR) protocol is used to transfer the data from the source to the destination nodes. [88]
- Each nanonode transmits four packets during the simulation
- Data packet size: 1000 bits
- Network size: 40cm * 40cm
- β by default equals 3000 for TS-OOK and SDMA-TSOOK while β belongs to [1000, 5000] for RD-TSOOK and SRH-TSOOK.
- Communication range of each nanodevice: 5cm
- Error rate: 10% of the packet

4.5/ Performance analysis and comparison

In this section, through extensive simulations, we exhibit the performance of SDMA-TSOOK, compared to the three discussed protocols, using the 24 scenarios presented in section 4.4 (i.e., different densities (100, 250, 500, and 750) with two traffic types (CBR and VBR) and three distributions (Uniform, Gaussian, and Gaussian Clusters)) and then we discuss the results in details. In order to illustrate the performance of the proposal, we use two evaluation metrics: number of collisions and transmission success rate.

4.5.1/ Collisions

Figure 4.8 shows that TS-OOK protocol produced a very high collision number compared to other protocols (SRH-TSOOK, RD-TSOOK, and SDMA-TSOOK). Furthermore, SRH-TSOOK generated about 30% (resp. 80%) of collisions produced in RD-TSOOK with a density of 100 (resp. 750) nanodevices. For instance, SRH-TSOOK generates less than 1030 collisions over the 250 nanodevices, with a Gaussian distribution and VBR traffic, while RD-TSOOK reaches 1391 collisions, and TS-OOK reaches 4613 collisions.

These results show the effect of density and distribution on the number of collisions in different protocols, where collisions increase over the increasing density. This is due to the high traffic in nanonetwork, and lot of nanodevices nearby, particularly in Gaussian distribution. For example, with a uniform distribution, 5 (resp. 179) collisions in SRH-TSOOK is recorded with a density of 100 (resp. 250) nanodevices, whereas, in gaussian distribution, the number of collisions reaches 46 (resp. 582) for 100 (resp. 250) nanodevices and 23 (resp. 523) with cluster distribution.

The number of generated collisions is much more reduced in SDMA-TSOOK due to the use of dynamic time-slot based communications.

4.5.2/ Success Rate

Figure 4.9 illustrates the effect of the density and distribution scheme on the success rate, i.e. the number of packets has reached their destinations compared to the total number of transmitted packets. The number of collisions does not significantly affect the success rate, which leads to convergent success rates of different protocols.

With increasing density, the preference of SDMA-TSOOK appears on other protocols (SRH-TSOOK, RD-TSOOK, and TSOOK), particularly in the Gaussian distribution where nanodevices are very close. For example, with 750 nodes and VBR traffic, SDMA-TSOOK protocol reaches a success rate of 90.3% under Gauss distribution, and 90.35% under Cluster distribution. While the success rate is about 83% for TS-OOK, SRH-TSOOK, RD-TSOOK for the two respective scenarios.

From this figure, we conclude that with the Uniform distribution, more packets reach their destinations in RD-TSOOK protocol than other protocols. However, with increasing density, SRH-TSOOK has the best success rate.

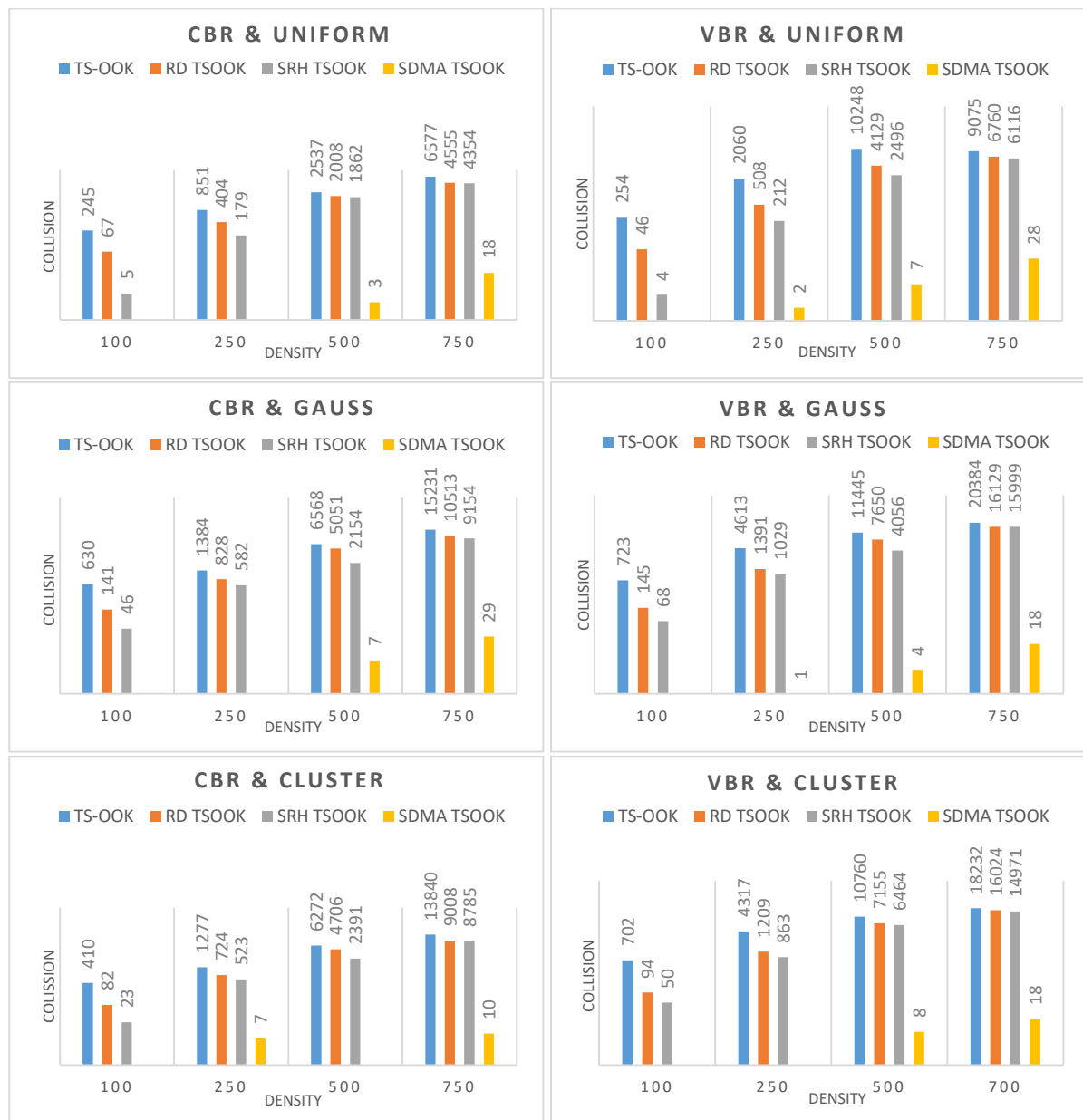


Figure 4.8: Comparison of collisions number in different scenarios

4.5.3/ Discussion of protocols performance

From the simulation results, we observe that the success rates of different protocols are convergent, even though the number of collisions is very low in SDMA-TSOOK. The latter is due to the slots' division used in SDMA-TSOOK protocol, where each node chooses a dynamic time slot. Several nanodevices can transmit their data successively one after another.

At the receiver, the number of packets accepted is limited (depending on the size of its buffer). Thus, the rest of the arrived packets are ignored (they never reach their final destination), so they will not be considered in the calculation of the success rate, that why in SDMA-TSOOK, the collision number is about 0 but the succes rate does not reach 100%.

According to the results obtained, the success rate is weak under low densities (100 and 250

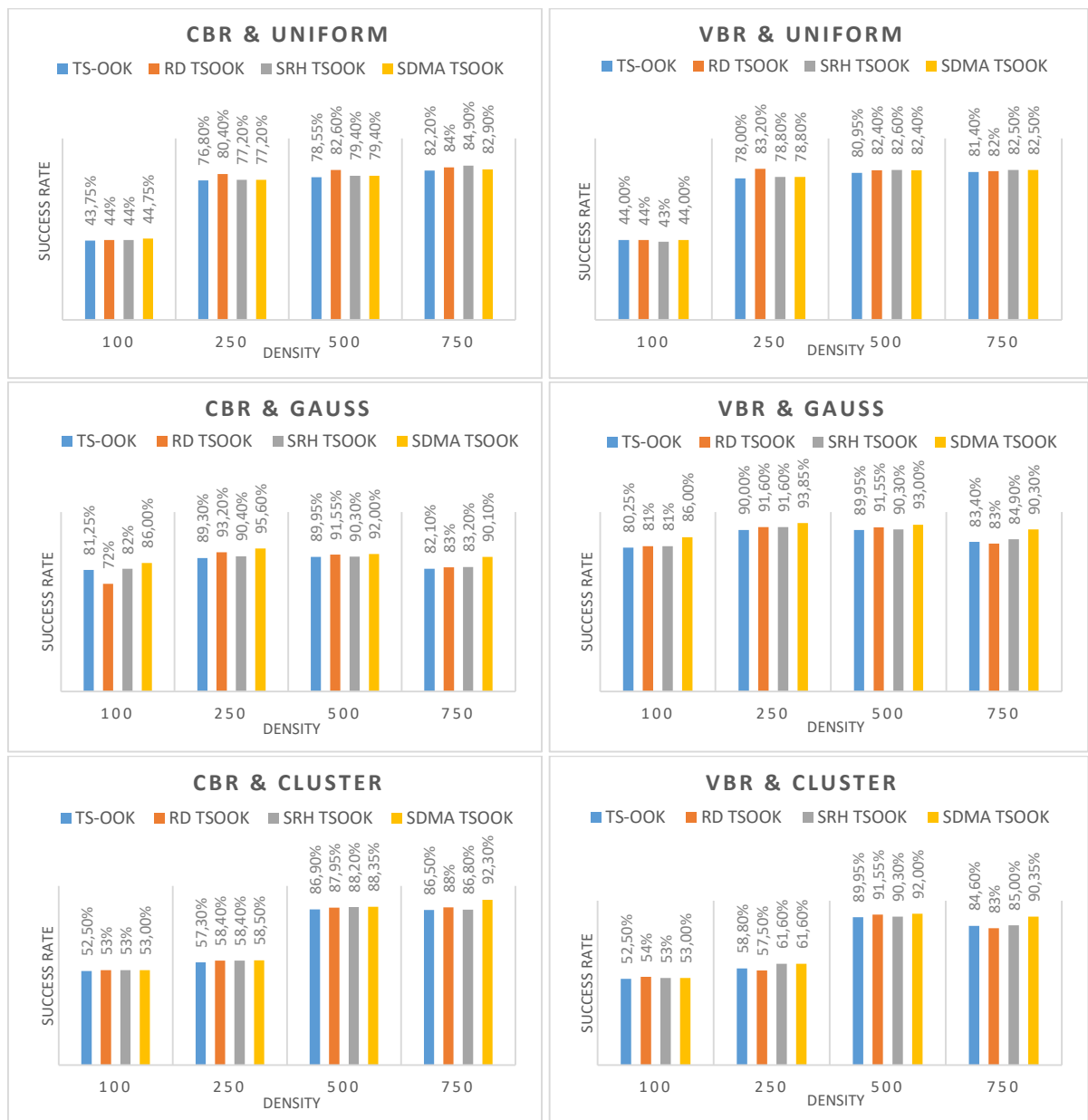


Figure 4.9: Comparison of success rate in different scenarios

nanodevices) due to the nanonetwork disconnection (the destination node is unreachable from the source node). This phenomenon is specifically observed in the uniform distribution, i.e., the nanodevices are distributed over the entire network uniformly. On the other hand, the success rate increases with the Gaussian distribution, where the nanonodes are concentrated around the deployment area center.

Also, although the high number of collisions, in the TSOOK, RD-TSOOK, and SRH-TSOOK protocols, has no major effect on the success rate. The routing protocol used in the simulation is Stateless Linear Routing (SLR), which defined linear routing paths among communicating pairs, allowing for a considerable degree of parallel transmissions within the network. Thus, a packet collided at an intermediate nanodevice can take another path to reach its destination.

4.5.4/ Analysis

All simulation results are summarized in Figure 4.10. This figure can help to select the best protocol suited according to the application priorities as follows:

- If the application purpose is the reduction of the collisions, the most suitable protocol is SDMA-TSOOK.
- If the application has a dense and concentrated network, the SDMA-TSOOK protocol is best suited.
- If the distribution is uniform with an average density, the RD-TSOOK protocol is more favored. However, RD-TSOOK leads to variable throughput from a communication to another.
- With a high density (over 500 nanodevices) and a uniform distribution, SRH-TSOOK protocol is preferable.

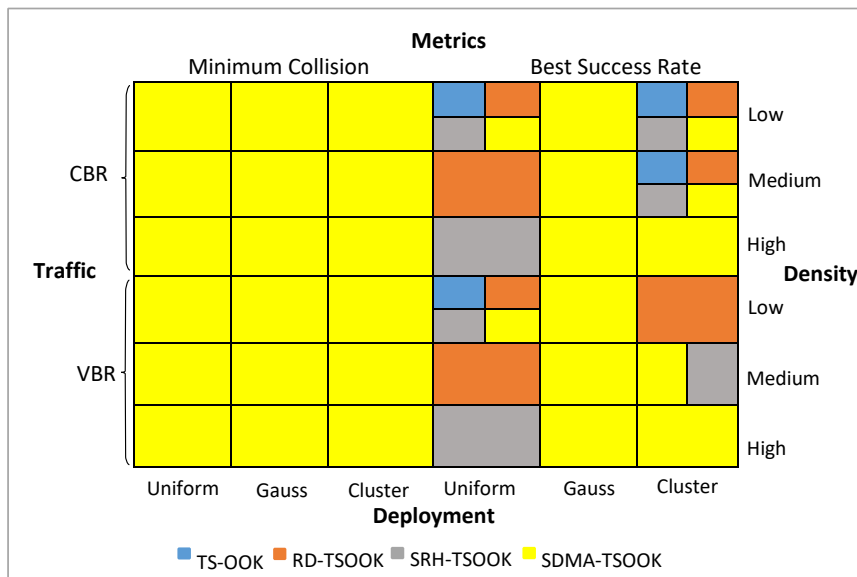


Figure 4.10: Scenarios & protocols appropriate for application types

According to this comparative study, several observations can be made. First, it turns out that nanonetworks have behaviors that only appear during the simulation. Therefore, a probabilistic study of protocols is not sufficient to validate their performance. Second, each protocol behaves differently depending on the application type in which it will be applied. Third, choosing the best protocol depends on the area and the objectives targeted by the application.

Finally, we conclude in this study that SDMA-TSOOK differs from other protocols by reducing collisions number in different performed simulations. Moreover, it ensures channel access balancing between nanodevices. RD-TSOOK showed a better success rate with a low density and a uniform distribution. However, with a high density, SRH-TSOOK protocol is preferred.

TSOOK protocol ensures a balance among nanodevices in the network with a very high number of collisions and a low success rate compared to other protocols. Success rate is higher in the Gaussian distribution than in other ones, which is due to the huge number of neighborhoods.

SDMA-TSOOK performances could be improved by adjusting the transmission cycle, represented by β . Figure 4.11 shows the results obtained by simulating 750 nanodevices network with time slots $Pslot \in [0..(\beta - 1)]$ where β has the values 750/1000/2000/3000. In each graph, three metrics (collision, success rate, and point-to-point delay) are considered. The average point-to-point delay is the average time spent by a packet from its source to its destination (given in nanoseconds).

Note that the success rate for different β values remains almost the same, while β is inversely proportional to the number of collisions but proportional to point-to-point delay.

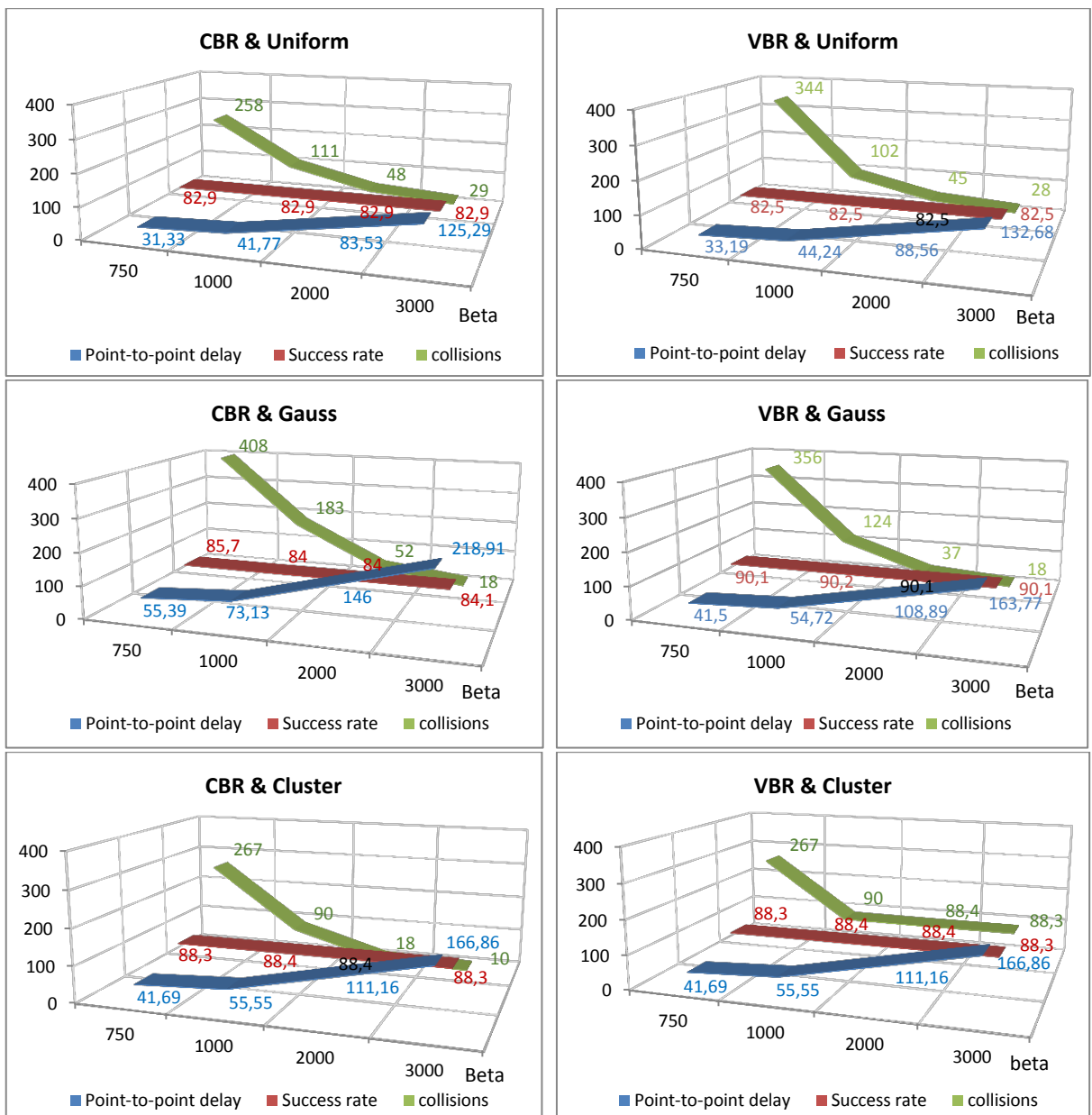


Figure 4.11: SDMA-TSOOK performance under beta and slots sequence

4.6/ Conclusion

In nanonetworks, the need for an appropriate channel sharing scheme causes a serious challenge for efficiently allow a concurrent channel access. For this, the SDMA-TSOOK protocol presents a good trade-off between the reviewed approaches concerning the channel access balancing, the success rate, and the collision rate.

First, we provided an exhaustive critical review of channel access approaches based on femtosecond-Long pulse modulation, particularly TS-OOK, RD-TSOOK, and SRH-TSOOK. This study investigated the drawbacks of each approach. Then, we proposed a Slot Division Multiple Access approach called SDMA-TSOOK to overcome these weaknesses. SDMA-TSOOK is inspired by Time Division Multiple Access technique (TDMA). Each transmitter asynchronously and independently allocates time slot used to send its symbols. To prevent the effect of co-channel interference the time slot is regularly changed, leading to highly mitigating the collisions.

We evaluated the performance of SDMA-TSOOK, compared to those reviewed approaches, in terms of channel access balancing, collision, and success rate. As a result, our proposed protocol ensured fairness between nanodevices and significantly reduced collisions while keeping the success rate.

The current chapter concerns an improvement of the Layer 2 networking protocol (link layer). In the next chapter, we turn to the study of the traffic regulation problem in Terahertz nanonetwork. A procedure that could be described as a part of the layer 2.5 networking protocol. The idea is to reduce the density of the physical topology produced by the nanodevices, by constructing a less dense logical topology describing the direct MAC links.

Directed graph based traffic regulation protocol

5.1/ Introduction

Due to the nanonetwork nodes' limited computation and energy capabilities (sub-millimeter scale), the multiple access protocols must meet simplicity and scalability requirements. In this approach, we aim to reduce the number of control messages required to channel access without resorting to centralized entities. To this end, several innovative techniques have been proposed, such as RD-TSOOK [42], SRH-TSOOK [94], HLMAC [82], DRIH-MAC [73], and our SDMA-TSOOK. However, in view of the network's extreme density, the classical multiple access protocols are not sufficient to spread the traffic load and control the multi-hop flows on the network. Indeed, given the network's density, the message broadcast causes numerous feedback loops that saturate the system (broadcast storms).

The traffic regulation protocol is seen as a 2.5 networking layer that allows to extend the access control layer missions with some routing considerations. The traffic regulation amounts to defining a logical topology of the network starting from the physical topology where any two nodes can communicate when they are within each other's range. The logical topology designates a subset of neighboring nodes that can communicate in a predetermined direction and at a predetermined time. Formally, the logical topology represents a directed sub-graph of the physical topology. The logical topology is said robust when the directed sub-graph is strongly connected. The connectivity degree of the sub-graph could be used as a measurement of the logical topology robustness. A directed graph is said k -connected if it remains connected whenever fewer than k nodes are removed.

Traffic regulation protocols for ad hoc networks have been widely studied in the literature [17, 23, 13]. One of the best known is the Optimized Link State Routing Protocol (OLSR) [17]. However, the adaptation of this protocol in the case of an ultra-dense network is complicated. OLSR is based on the exchange of neighboring lists between nodes. Those lists are heavy to transmit and difficult to store or to process due to the nanonetwork density. Other protocols aim to define a spanning tree over the network's nodes [22]. The network's logical topology represents then a tree where the nodes close to the root concentrate more traffic than nodes near the leaves. Therefore, these protocols are adapted when the network's physical structure involves different types of nodes: simple nodes and super-nodes like in Wireless Body Sensor Nanonetwork architecture [99]. In addition, such protocols present only one path to link every two nodes, which makes the logical topology unreliable. In conclusion, few works from literature deal with traffic regulation in dense homogeneous ad hoc networks.

5.2/ Contribution

Our proposed protocol has three main objectives. First, traffic load evolution presents peaks that lead to congestion phenomena. The principle of communication by appointments allows to spread the traffic and to schedule communications in time. Secondly, dense networks present various paths to transmit data from one node to another. In terms of routing (layer 3), this implies a greater complexity of choice. The risk of local congestion on the network is, therefore, higher and more redundancy is expected (multiple receptions of the same message by the same node). The use of electronically steerable antennas improves the control of the transmitted radio signals (interference).

Moreover, each node selects the subset of neighboring nodes with which it can communicate directly. Finally, communication by appointment allows nodes to plan their waking and sleeping periods. In addition, the energy consumed by communications is reduced because the emission power is channeled in specific directions at given periods. Finally, only a subset of covered nodes is selected as sources or successors nodes and messages of not selected sources are ignored (not delivered to layer 3).

In this chapter, we propose an original procedure for the Layer 2.5 networking protocol that takes into account the Terahertz frequencies particularities in a dense context. The idea is to extract a logical topology from a dense homogeneous nanonetwork (see Figure 5.1) that allows both to reduce the number of direct communication links and maintain the robustness against temporal nodes unavailability. This procedure exploits the available antenna steering techniques to schedule over time and space the data transmission. Unlike the other approaches, our method does not impose any conditions on the physical platform and presents, according to our knowledge, the first 2.5 networking layer protocol adapted for Terahertz nanonetworks.

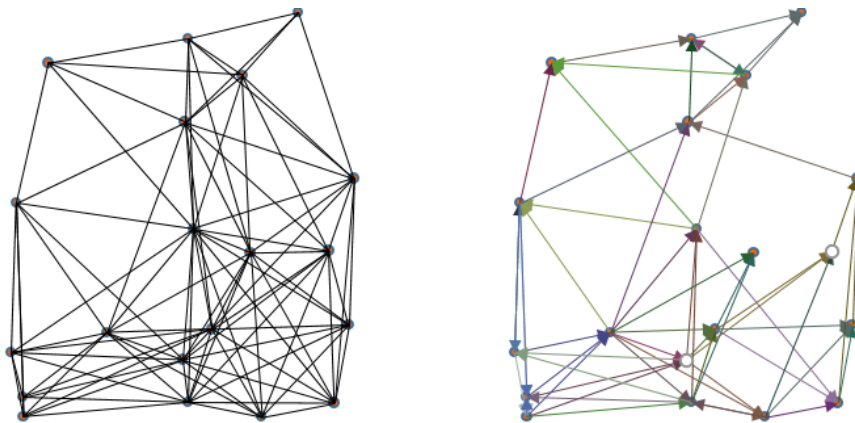


Figure 5.1: Traffic regulation problem: from physical to logical topology

5.3/ Traffic regulation problem modeling

Let W be a wireless nanonetwork composed of N nodes. Each node in the network has a reconfigurable directional antenna that can be steered dynamically to cover a particular direction. Let T_{ch} be the time needed to change the orientation of an antenna. Let $G(X, A)$ the connected graph describing the physical topology of the network with X the set of nodes ($|X| = N$) and A the communication links between the nodes. $(x, y) \in A$ means that there is

a particular configuration of the x and y antennas that makes the two nodes communicate directly.

5.3.1/ Traffic regulation constraints

The traffic control problem consists of calculating a directed sub-graph $G'(X, E)$ with $(x, y) \in E \rightarrow (x, y) \in A$ where the following conditions are satisfied:

- G' is strongly connected: given two nodes in the graph, there is a way to route the data from one node to the other in the two directions.

$$\forall x, y \in X^2, \exists \text{ a path from } x \text{ to } y \quad (5.1)$$

- G' is robust: whatever the node, there are enough ways, p , to receive the data from the other nodes and enough means, s , for the node to broadcast its data. The values p and s denote the desired level of robustness represented by each node's number of predecessors and successors. Choosing a large value of p and s allows a higher level of robustness that derives from the nodes' reliability level. When nodes are prone to a high risk of outages or if the nodes' energetic capacity regularly makes it in the charging phase, a high value of p and s is more suitable.

5.3.2/ Antenna steering and sleeping mode

Each directed edge (x, y) of the logical topology G' have two index values I_{xy} and I_{yx} designating the period of time (relatively to each node) during which x and y can communicate according to a particular orientation of their antennas. Each node changes its antenna configuration (orientation), in a cyclic manner and at a regular interval of time, $T_s; T_s \gg T_{ch}$. During the period S_1 , the node x uses the configuration $C_{x,1} \in C$ then during the period S_2 , it uses the configuration $C_{x,2}$ and so on. At the end of the period S_{NS} (NS being the number of slots in one cycle), the node x returns to the configuration $c_{x,1}$ for a new period S_1 and the cycle restarts as depicted in Figure 5.2. The duration of a complete cycle T_{cycle} is identical for all nodes (See Equation 5.2). Certain periods S_i may correspond to periods of time during which the communication devices are deactivated. Moreover, the cycle of a node can have several periods with the same parameter ($i \neq j, C_{x,i} = C_{x,j}$).

$$T_c = NS \times T_s \quad (5.2)$$

For a given period S_i , a node x is either in listening, transmitting, or sleeping mode. For each listening period S_i of x , there is one and only one node $y \in X$ such that $(y, x) \in E$, and $I_{xy} = S_i$, which means that there is only one listened node at a time. If the period S_i is a transmission period of x , then there is at least one node y such that directed edge $(x, y) \in E$ and $I_{xy} = S_i$. Sleeping mode corresponds to periods of time where the node x has no directed edge $(x, y) \in E$ or $(y, x) \in E$ with $I_{xy} = S_i$, which means that the node is not listening and not transmitting.

Given the asynchronous nature of the network, the index of a period S_i of a given node has only a local signification. The figure 5.2 shows an example of traffic regulation involving 5 nodes. The node (A) has two active periods S_1 in transmission and S_2 in reception. The period $S_1 = I_{AC} = [0.3 - 0.4]$ covers $1/10$ of the cycle time T_c between instants $0.3 \times T_c$ and

$0.4 \times T_c$. During this period, the node (A) covers the node (C) which is listening during its period $S_3 = I_{CA} = [0-0.1]$ as well as the node (E) which listens during its period $S_1 = I_{EA} = [0.7-0.8]$.

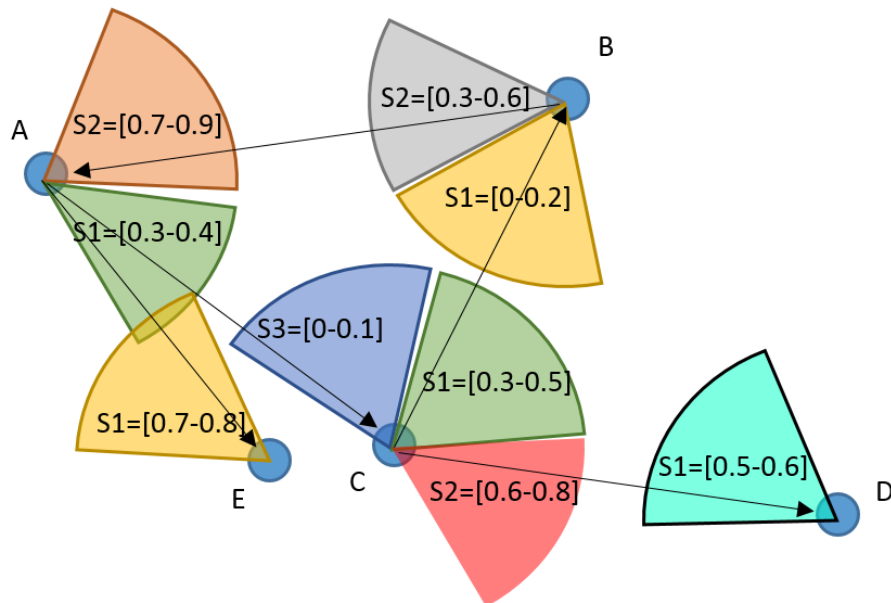


Figure 5.2: Example of TDMA synchronization: each edge (x,y) is indexed by the index of the transmission period on x (S_i) and the index of the reception period on y (S_j). Each period $S[tb - te]$ is designated by its beginning and end time (the time is given relatively to the concerned node). The colored arcs display the antenna orientation at the corresponding period.

When two edges (x,y_1) and (x,y_2) with the same tail have the same index value on x , the two incoming nodes y_1 and y_2 are then served by the same multicast stream. By the way, the edges (x_1,y) and (x_2,y) with the same head can not have the same period index on y in order to avoid interference. For all the edges $(x,y) \in G'$, the associated listening period on y must be equal to the duration of the transmitting time on x in order to maximize the sleep periods. Along with the respect of traffic regulation constraints, in particular, the connectivity and the robustness of the sub-graph G' , the traffic control algorithm must take care to maximize the useful listening and transmission times, T_i , ($T_i \subset S_i$) as well as the sleep periods of the nodes. A transmission period of a node x is said to be useful when throughout all its duration, all nodes $y, (x,y) \in E$ are at listening mode. A listening period of a node y is said useful when throughout its duration, the listened node (there is only one) is in transmission phase to y .

5.3.3/ Traffic regulation in Terahertz network

In DAMC modulation technique [65], the Terahertz frequency band is mainly subdivided into three frequency windows allocated according to the transmitter-to-receiver distance, which is either short, mid, or long. To take into account this particularity, the traffic regulation protocol associates with each active period a coverage range: short, mid, or long then, only nodes with a distance in the selected range are considered to be successors. At a given transmitting time slot, the successors of a given node are all in the same range, allowing to use the same optimal frequency window to serve them (See Figure 5.3).

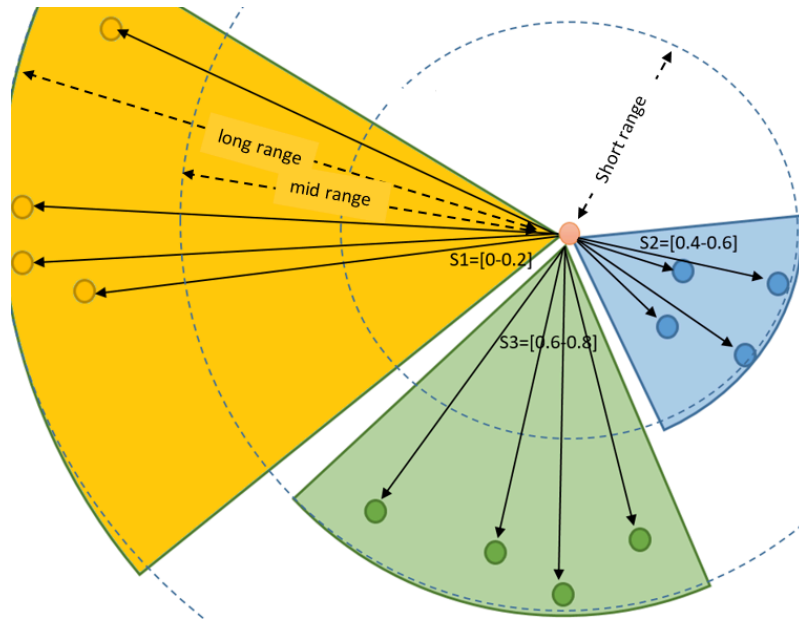


Figure 5.3: At every period, the transmitting node selects its successors according to their distance from the node in order to optimize the used frequency window. The colored arcs represent the orientation and coverage of the node at a given period.

5.4/ Distributed algorithm of traffic regulation

The algorithm **I** represents our traffic regulation protocol. The algorithm's design aims to satisfy two main constraints: a reduced computation requirement and limited messages exchange. When a node wants to join the nanonetwork, it defines for each slot a covering range (short, mid, or long). Then, the node alternates between two modes. In the first mode, the node listens to the channel and switches over configurations' set $C = \{C_1..C_{NS}\}$ with a frequency of $1/T_s$. In the second mode, the node launches invitations in different directions, looking for successor nodes and changes its configuration with a frequency of $1/T_c$. The use of two different reconfiguration speeds aims to prevent the hidden node problem. In successor search mode, the node keeps the same antenna configuration during all a cycle T_c of NS slots T_s . The value of NS depends on several parameters, such as the reconfiguration delay T_{ch} , the cycle duration, and the number of needed sources and successors. In our tests, we have set $NS = 14$.

At each period T_I , the node launches invitations. After each reception of acceptance, the source updates its useful transmission period, its coverage list and sets the period mode to 'transmission' mode. Nodes in source search mode, listen for any invitations. Based on the source's target range, the strength of the received signal, and the remaining listening time, the node chooses to accept the invitation or not. In case of acceptance, the node registers the useful listening period. Once the number of necessary source nodes is reached (parameter p), the node stops using the source search mode.

To avoid a slow start when few nodes are active, the number of listening and announcement cycles is limited to M . After every M ordinary operating cycles, a node with not enough sources (resp. successors) listens (resp. re-sends invitations) during an entire cycle. These two procedures allow nodes that start very early or late compared to the other nodes to complete their prefixed links lists.

The disconnection of the graph $G'(X, E)$ is avoided thanks to a long-term procedure which provides that each node, at a very important time interval, listens in all directions whether neighboring nodes belong to other connected components. For this purpose, the nodes of the same connected component share an identifier of the component, which corresponds to the smallest MAC identifier of the nodes belonging to the component. When a node detects a neighboring node with a different component identifier, the two nodes' connection procedure is started.

Algorithm 1: Every M successive cycles

Data: $T_s, T_c, t0, NS, P = \{C_1..C_{NS}\}, T = \emptyset, nbcycles = 0, t0 = now(), nbsec = 0,$

$nbsrc = 0 ;$

```

1 for (i ∈ {1 to NS}) do
2   rngi = rand(1..3); parami = ∅; covi = ∅; modei = ∅ ;
   /* research phase of the successors */
3 for (i ∈ {1..NS each Tc }) do
4   if (nbsuc < s) then
5     /* antenna parameters ← Ci */
6     for (j ∈ {1..NS each Ts}) do
7       if (modej = NULL) then
8         left = t0 + nbcycles * Tc + j * Ts - now() ;
9         send invit(me, left, rngj) each TI ;
10        for (each accept(n, t)) do
11          nbsuc ++; modej = 'trans' ;
12          covj = covj ∪ n; paramj = i ;
13          Tj.begin = now(); Tj.end = min(Tj.end, now() + t) ;
14        nbcycles ++;
   /* research phase of sources */
14 if (nbsrc < p) then
15   for (i=1 to NS with frequency Ts) do
16     begin = t0 + nbcycles * Tc + (i - 1) * Ts ;
17     end = begin + Ts ;
18     antenna parameters ← Ci ;
19     if (modei = NULL) then
20       while (end - now() > minCom) do
21         /* remaining time is enough */
22         for (each invit(node, t, rng)) do
23           if (distance(node, me) ∈ rng) then
24             send accept(me, min(t, end - now())) ;
25             nbsrc ++; modei = 'listen' ;
26             covi = node; parami = i ;
27             useful time Ti = [now(), now + min(t, end - now())] ;
28       if (modei = NULL) then
29         modei = 'sleep' ;
30     nbcycles ++ ;

```

5.5/ Tests and results

To study the impact of the traffic regulation algorithm over dense nanonetworks, we have established several test scenarios, which are differentiated by the number of nodes, the spatial dimension of the network, the range of the radio signal, and the density of the network. We first begin by evaluating the impact of traffic regulation on network performance in terms of interference. A first indicator of the impact on interference is the comparison of the number of edges in the graph $G(X, A)$ and the number of edges in the graph $G'(X, E)$. When $|E| \ll |A|$, the average number of signals arriving on each node is reduced considerably. Interference reduction also benefits from time division access mode, beam control antenna, and selectivity of listened sources. All these factors make it possible to reduce the risks of the massive arrival of communications simultaneously on the same node.

Figure 5.4 presents three simulations of traffic regulation using different number of nodes 200, 500, and 1000 in the same area using Microsoft Excel VBA. For each scenario, on the left, the graph $G(X, A)$ shows the physical topology of the network, and on the right, the graph $G'(X, E)$ is obtained by the traffic control algorithm 1. The traffic regulation is carried out with the maximum number of sources equal to $p = 4$ and the maximum number of successors equal to $s = 10$. For Scenario 1, the traffic regulation algorithm reduces the graph's density from 1202 edges to 744 edges, i.e., a reduction of 38%. For Scenario 3, the traffic control algorithm reduces the graph from 30891 edges to 3997 edges, which corresponds to a reduction of 87%.

We also assess the impact of traffic regulation on network data broadcasting. To this end, we have selected three evaluation criteria: The total number of receptions, including redundancies, the maximum number of receptions of the same message on one node, and the time for the total broadcasting of the message. According to the first two criteria, the traffic regulation allows improving the network's behavior when a node broadcasts a message over the network. Regarding the total number of messages received by the nodes, an approach without traffic regulation will generate for scenarios 1, 2, and 3, respectively 2404, 15082, and 61618 messages. The number of receptions with traffic control decreases to 744, 1997, and 3997 messages, respectively. The maximum number of receptions of the same message varies in the approach without traffic regulation between 24, 45, and 96 for the three scenarios. Whereas, with traffic control, it remains 4 for all three scenarios. This corresponds to the value of the maximum number of sources: parameter p .

The number of hops allowing all nodes to receive the message is also a crucial factor for the performance of the traffic control algorithm. The simulations show that the total diffusion of a message depends on the source node's position in the network. We studied four different placement of the source nodes for Scenario 1, shown in Figure 5.4 circled in red and labeled A, B, C, and D. Broadcasting without traffic regulation from node (A) requires 9 hops while 14 hops are required with traffic control. Similarly, the application of traffic control requires respectively 26, 18, and 22 hops to broadcast a message from the nodes (B), (C), and (D) instead of 12, 12, and 9 jumps without regulation traffic. For Scenario 1 which is the least dense, the number of hops for the total broadcast doubles with traffic regulation, a negligible additional cost in return for reducing the total number of exchanged messages.

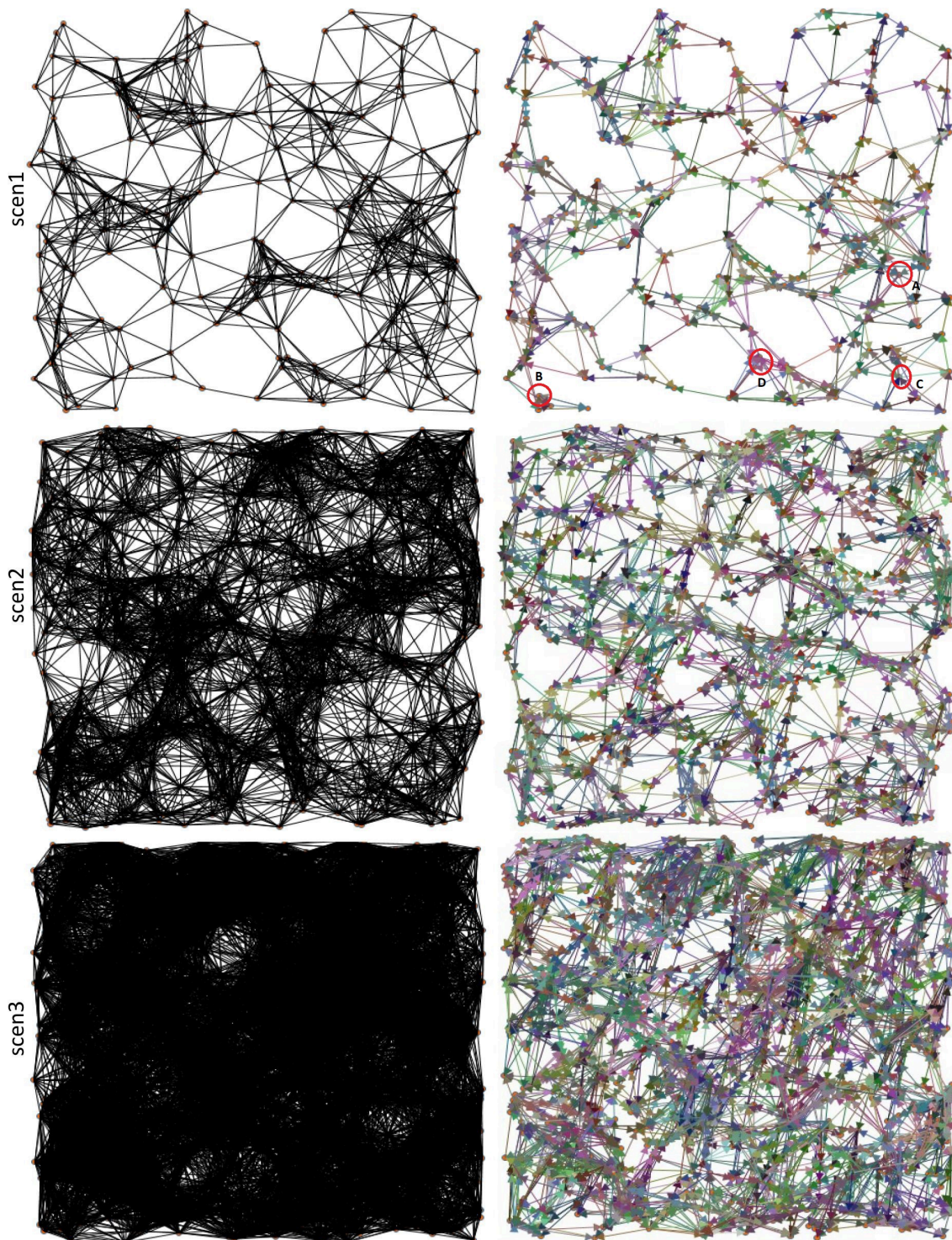


Figure 5.4: Traffic regulation for 3 scenarios: 200 nodes, 500 nodes and 1000 nodes. Tests are implemented using Microsoft Excel VBA.

5.6/ Conclusion

In this chapter, we have proposed a novel distributed protocol for optimizing the logical topology of homogeneous, ultra-dense Terahertz nanonetworks. The objective of this optimization is to

reduce the amount of interference due to the concentration of numerous nodes transmitting in all directions at random instants. The logical topology we proposed fixes for each node the moments during which it can send data in a given direction to given selected destination nodes. Each node ignores messages sent by nodes that do not belong to the predefined subset of neighbors, which reduces energy consumption.

Furthermore, the reduction of direct communication links between nodes does not impact data broadcasting coverage. Simulations show that the diminution of the broadcasting speed is limited compared to the gain in terms of transmission redundancy and generated interference.

Finally, the traffic control protocol is adapted to the DAMC protocol used for Terahertz communication. The successors of a given node in a specific direction are in the same range of distance from the transmitter. Therefore, all the nodes covered in the same direction are served by the same frequency channel. The distance between nodes and their successors varies according to the transmission direction leading to better use of the Terahertz band.

Even if the approach is very interesting when the network is ultra-dense, the method misses of guarantee about the connectivity of the obtained logical topology (see section [5.3.1](#)). An additional discovering procedure should be implemented to allow the detection of graph discontinuity in order to establish additional links between connected components. One way is to associate each connected component with a number corresponding to the lowest ID of its nodes. The number of the connected component is regularly broadcasted by all nodes. When a node detects a neighboring node with a different component number, it establishes a new link with it. The major drawback of the approach remains the slot distributed management that leads to variable communication duration. In the next chapter, we studied a hierarchical based topology that allows the assignment of synchronization tasks to specific selected nodes called cluster heads.

Clustering based protocol for traffic regulation

6.1/ Introduction

In the precedent chapter, we addressed the problem of de-densification of Terahertz nanonetwork. This approach is well adapted for unstable nanonodes based nanonetwork where the nanonodes suffer from unpredictable unavailability periods. Such applications are characterized by an austere environment like in Body Area Network (WBAN) [39]. Therefore, a high value of p and s parameters (see Algorithm 1) expresses the need for high link redundancy. We propose, in this chapter, another de-densification approach adapted to stable nanonodes based nanonetwork. In this case, nanonodes are deployed in under-controlled area like in Terahertz intra-chip communication for multi-core machine [96].

The clustering approach is widely studied in the field of ad-hoc wireless networks [9, 21]. However, Terahertz nanonetwork has specific features due to Terahertz signal characteristics, including propagation phenomena such as molecular absorption [66], very large bandwidth, and various communication ranges [58]. We present how the Terahertz band can be better managed by varying the used frequency sub-bands within each cluster. In addition, we consider the case of ultra-dense WNN up to thousand of neighbors per node.

Major works on clustering approaches ignore the antenna steering. Link in directed graph-based traffic regulation, we suggest using directional transmission/reception antennas as a way to regulate and reduce collisions resulting from concurrent accesses on communication channels.

The hierarchical based topology of the network offers better control on the data flooding over the network. Furthermore, contrary to the directed graph approach, cluster-based protocol for traffic regulation assigns a constant duration time slot for each nanonode, which allows balanced access to the radio channel.

In this approach, the nanonetwork nodes are organized into clusters [44] to regulate the traffic messages, save nodes' energy, and reduce interference. Each cluster includes a set of nanonodes (members) and a Cluster Head (CH). A CH is an ordinary node responsible for scheduling its members' data transmission during the current cycle/round. This scheme of accessing channel is the well known Time Division Multi-Access (TDMA) [74]. Data received from member nanonodes are multiplexed and sent to the neighbor CHs. Indeed, in random access protocols and CSMA/CD protocols, the number (not the size) of communications increases collisions' probability, making time scheduling-based approaches benefit.

In this context, we propose two hierarchical based protocols for nanonetwork de-densification. In the first one, the clustering process begins by randomly selecting the CHs, then forms the clusters, where nanonodes join the nearest CH.

Conversely, the second protocol begins to form the clusters (geographical areas) and then selects one CH node among each cluster's members. Thereafter, each member node communicates with its CH during the time slot defined by its identity. In both, only one nanonode will be able to communicate during its time slot in the cluster. Therefore, intra-cluster collisions are avoided leading to less re-transmissions, better energy consumption, and higher throughput.

The two discussed approaches propose different trade-off between the computational vs. communication complexity and the efficiency of the clustering procedure. The second proposed clustering protocol presents a higher complexity but overcomes the drawbacks of the random selection of CHs. Indeed, with random selection of the CHs, the CHs are not uniformly distributed in the network, which causes (a) isolated nodes that cannot reach all other CHs, (b) some CHs may be faced to unbalanced load and, in the worst case, singleton CHs are formed without cluster member. These situations generate low network connectivity and hence, high energy consumption and low successful delivered packets.

6.2/ Random cluster heads based Protocol

The clustering protocol is run periodically at the beginning of a new round. We assume that the beginning of a new round is announced by a base station covering all the nanonodes using a broadcast signal (see figure 6.1). A round is composed of two phases. The clustering phase performs the CH selection, *ADV*, *JOIN*, *FDN* and *intra/inter TDMA*. The second phase ensures data transmission. In order to reduce collisions, each node uses its directional antenna to communicate with the others. For this, the following section describes the directional antennas configuration that takes place before the two precedent phases.

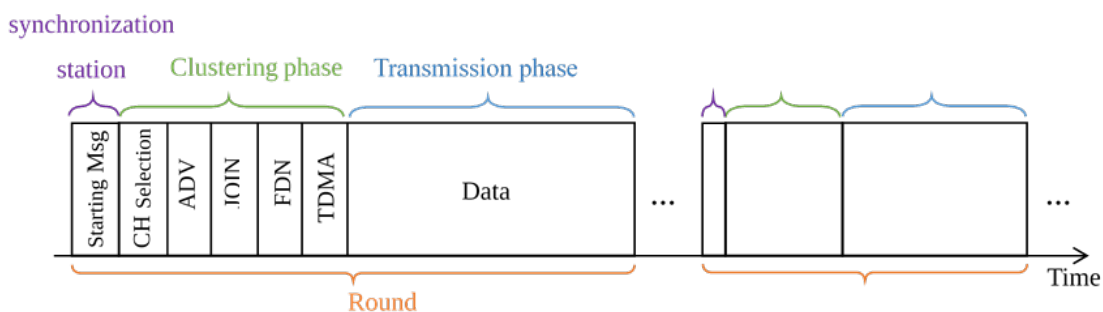


Figure 6.1: Clustering and communication phases

6.2.1/ Directional Antennas

In this work, we assume that each node has a reconfigurable directional antenna. The latter can be dynamically directed to cover a particular area using D specific configurations. A node changes its antenna's parameters in a cyclic manner and at a regular interval of time, among a set of D possible directions.

In the beginning, the synchronization station sends a message to start the clustering phase.

At the end of this phase, the nanonetwork is subdivided into clusters; each one contains a CH node and cluster member nodes, named ordinary nodes. The duration of a complete cycle TC , i.e., the time to cover all possible directions, depends on the node type (CH or member node). The reconfiguration frequency of CH node is D times slower than the reconfiguration frequency of ordinary nodes.

$$TC_{CH} = TC_{Ordinary} \times D \quad (6.1)$$

The period TP_X is the time during which the node of type X keeps the same antenna configuration. The duration of a period, TP_{CH} , is D times longer than when an ordinary node keeps the same configuration, which means that CH nodes keep the same configuration during a complete cycle of an ordinary node.

$$TP_{CH} = TC_{Ordinary} = TP_{Ordinary} \times D \quad (6.2)$$

We deduce then that :

$$TC_{CH} = TP_{Ordinary} \times D^2 \quad (6.3)$$

The use of two different period durations TP_{CH} and $TP_{Ordinary}$ prevents the hidden node cases, where two close nodes are not seeing each other because they are always directed in the same direction. During a given period, a node is either in listening, transmitting, or sleeping mode as in the directed graph-based protocol (chapter 5).

6.2.2/ Clustering

The CH selection is done in a distributed, independent, and random decision way. When a node becomes CH, it will advertise (message ADV) the neighboring ordinary nodes of its new rank during a complete cycle TC_{CH} .

In [65], authors stated that Terahertz bandwidth should be adapted according to the distance between communicating nodes. Three frequency windows are then proposed to carry-out short-range, mean-range, or long-range communications. The CH nodes select randomly a target range indicating the targeted distance from covered ordinary nodes. The ADV message is then sent using frequency window associated with the selected range. On the other hand, ordinary nodes work with a shorter cycle of duration $TC_{Ordinary}$. Ordinary nodes retrieve ADV messages sent by neighboring CHs and decide to join one of them according to the quality of the received signal. Also, as indicated in figure 6.2, the ADV message can be received by other CHs, which allows to discover its CH neighbors (described in section 6.2.2.1).

Each member node informs the selected CH of its membership decision by a $JOIN$ message. Subsequently, communications within a cluster are done using the TDMA technique and the selected frequency sub-band. For this, each CH establishes a TDMA schedule for its members to coordinate their communications. Communications between Cluster Heads are managed by the proposed distributed TDMA protocol and Forwarding Dominate Nodes algorithm (FDNs). FDN is described in section 6.2.2.2

As indicated in figure 6.3, switching from one antenna direction to another can take $D \times TP_{Ordinary}$. So the ordinary nodes are ensured to receive an (ADV s) message from all neighboring CHs. When a CH takes an antenna direction AD_i , it has to send regularly D times ADV messages. The duration between sending ADV s messages is the same as $TP_{Ordinary}$.

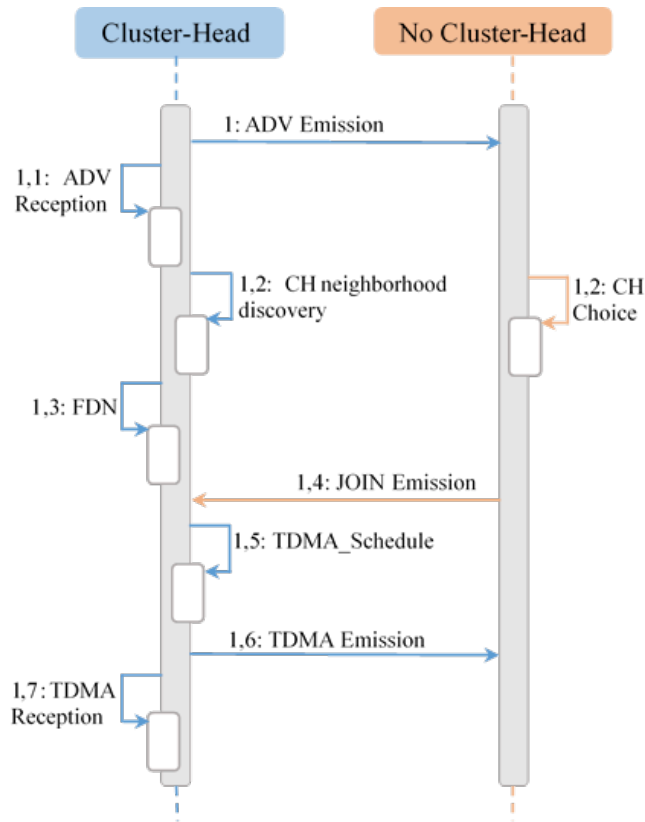


Figure 6.2: Sequence diagram of clustering phase

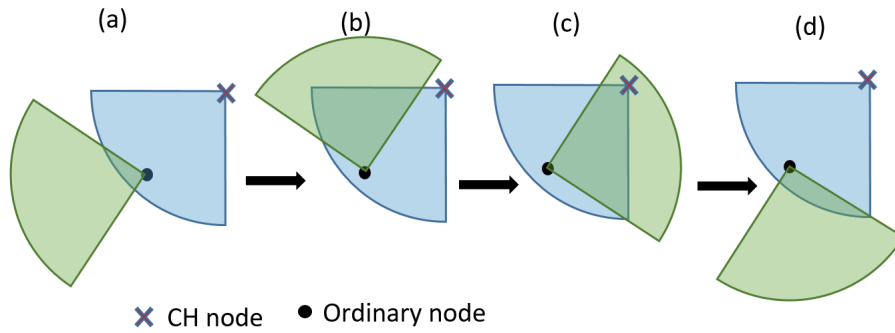


Figure 6.3: Switching Antennas in ADVs step. At (c) step, the ordinary node receives the ADV message.

6.2.2.1/ CH neighborhood discovery

Upon the reception of an *ADV* message, the receiver CH_j adds the sender CH_i to its neighbouring CHs list named $N1_{CH_j}$. This list includes all CHs directly linked to CH_j (accessible with just one hop). After receiving the *ADV*s of different Cluster Heads, each Cluster Head, CH_j , sends its $N1_{CH_j}$ list to its neighboring Cluster Heads. At the end, each CH_i can apply algorithm 2 and chooses its Forwarding Dominate Nodes (FDN_{CH_i}) among its neighbors. The FDN_{CH_i} is described by the following formula:

$$FDN_{CH_i} = \{CH_j \in N1_{CH_i} / CH_j \text{ relays data received from } CH_i\} \quad (6.4)$$

The FDN_{CH_i} list is then sent to the neighboring Cluster Heads, $CH_j \in N1(CH_i)$. Upon the reception of the FDN_{CH_i} list, the neighboring Cluster Head, CH_j checks if it belongs to FDN_{CH_i} , if so, it adds the transmitter CH_i to its selectors S_{CH_j} list.

For each Cluster Head, CH_i , S_{CH_i} list includes neighboring Cluster Heads that have choosing CH_i as a FDN node. S_{CH_i} is defined by:

$$S_{CH_i} = \{CH_j \in N1_{CH_i} / CH_i \in FDN_{CH_j}\} \quad (6.5)$$

We deduce that the sets FDN and S are linked by the following expression:

$$CH_i \in S_{CH_j} \Leftrightarrow CH_j \in FDN_{CH_i} \quad (6.6)$$

Therefore, during transmission phase, each data packet transmitted by CH_i will be forwarded by only nodes CH_j such that $CH_i \in S_{CH_j}$.

For example in figure 6.4, data packet of CH node 4 will be forwarded by only CH nodes 7, 11 and 15 to finally reach all nodes.

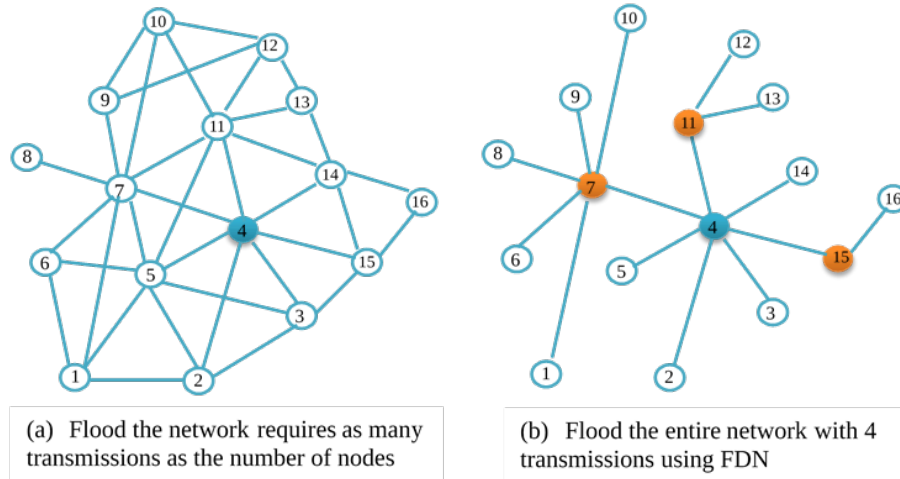


Figure 6.4: Flood diffusion (left) and optimized diffusion (right)

6.2.2.2/ Forward Dominate Nodes

The Forwarding Dominate Nodes is a distributed process that determines the subset of neighboring CH nodes that will act as relay nodes. The use of this subset of nodes enables to reduce the number of redundant re-transmissions for broadcasting a packet over the nanonetwork. A packet is re-transmitted only by relay nodes (CHs), contrary to a naive flood approach.

Let CH_i , $N2_{CH_i}$ be a set of two hops CHs neighbors and FDN_{CH_i} the relaying nodes set of CH_i . FDN_{CH_i} is initially empty.

- If a neighboring $CH_j \in N1_{CH_i}$ covers all the nodes of the set $N2_{CH_i}$, we define the node CH_j as member of FDN_{CH_i} and we stop searching for other relay nodes for CH_i .
- If there are nodes $CH_k \in N2_{CH_i}$ which have one and only one link with a node $CH_j \in N1_{CH_i}$, we add CH_j to the FDN_{CH_i} , and we remove from $N2_{CH_i}$ all the nodes connected to the added node CH_j ($N1_{CH_j}$).

- If a node $CH_k \in N2_{CH_i}$ is linked to several CH nodes forming a subset $E \subset N1_{CH_i}$, then the node $CH_j \in E$ which covers a maximum number of nodes in $N2_{CH_i}$ is added to FDN_{CH_i} . If several nodes cover the same number of nodes, the added CH is the one with the highest degree (number of neighbors $|N1|$). All nodes directly linked to the added node CH_j are then removed from $N2_{CH_i}$.
- The search for new relay nodes stops when the set $N2_{CH_i}$ becomes empty.

Algorithm 2: Forwarding-Dominate-Nodes

Data: *NeighborNeighborlist*, $N2 = \emptyset$, *ChNeighbor* ;

NeighborNeighborlist : Map of neighbours of a node and their neighbours

/* Fill the list N2

*/

```

1 for (it = NeighborNeighborlist.begin() to NeighborNeighborlist.end()) do
2   for (it' = it → second.begin() to it → second.end()) do
3     i = find it' in N2? ;
4     j = find it' in ChNeighbor? ;
5     if ( !i and !j ) then
6       N2.insert(it');
7 N2.erase(myId); it = N2.begin();
8 while (!N2.empty()) do
9   /* research if N2 elements are linked to a single N1 node */
10  for (it2 = NeighborNeighborlist.begin() to NeighborNeighborlist.end()) do
11    findElement = find it in it2 → second;
12    if ( findElement ) then
13      k ++ ;
14      findFDN = it2 → first;
15      fdnChoice.insert(it2 → first, it2 → second);
16 /* If it exists insert Node N1 to EnsFDN */
17 if (k == 1) then
18   EnsFDN.insert(findFDN);
19   Delet all Neighborlist of findFDN from N2;
20 else
21   i = find Node N1 witch cover most of N2;
22   if (i) then
23     EnsFDN.insert(Node);
24     Delet all Neighborlist of Node from N2;
25   else
26     /* severel nodes cover same number of N2 */
27     choose one with highest degree;

```

6.2.2.3/ TDMA approaches

The TDMA-Schedule avoids collisions (Transmission channel access conflicts) between nodes and therefore minimizes nodes' power consumption by reducing the re-transmission effort. In addition, it allows node to turn off its communication interface outside its reserved time slot

that is used to transmit its sensed/computed data.

TDMA is a temporal multiplexing technique where each served node uses a particular time slot. In our approach, the TDMA scheme is used at two levels: Distributed inter-cluster and centralized intracluster scheduling.

Intra Cluster TDMA: After the construction of clusters, each CH builds the TDMA-Schedule and informs its members by their rank in this TDMA-Schedule. The member node's rank indicates the time slot during which the node sends its sensed/computed data to its CH. An ordinary node, n , calculates its time slot TS_n as follows:

$$TS_n = rank_n * Ts \quad (6.7)$$

Where Ts is the slot duration.

Inter Cluster TDMA: Each Cluster Head runs the algorithm 3 to fix the time slots for communicating with its direct neighboring CHs, $N1_{CH}$. First, the CHs with the smallest identity number among their direct neighbors begin the computation of their TDMA-Schedule and transmit it to their neighbors (See steps 1.5 and 1.6 in Figure 6.2). Once the TDMA-Schedules of all the neighbors with smaller identities are received (step 1.7 in Figure 6.2), the CH schedules its TDMA-Schedule according to the schedules already done.

Algorithm 3: Distributed TDMA scheduling

```

Data:  $idNode, idNeighbors$  ;
1 if ( $idNode < all\ idNeighbors$ ) then
2   Create  $TDMA\_Schedule$  ;
3   Send  $TDMA\_Schedule$  to neighbors ;
4 else
5   while ( $Receive\ TDMA\_Schedule\ from\ idNeighbors < idNode$ ) do
6      $position = TDMA\_ScheduleNeighbors(idNode)$  ;
7     /* find  $idNode$  position in  $TDMA\_ScheduleNeighbors$  */
8      $TDMA\_Schedule[position] = idNeighbors$ ;
9   Create  $TDMA\_Schedule$  for the rest of neighbors taking into account the remaining
    slots ;
10  Send  $TDMA\_Schedule$  to neighbors ;

```

Figure 6.5 shows an example of time slots planning over 13 CHs. In the beginning, each CH checks if it has the smallest identifier regarding its neighbors. CH1, CH2, and CH8 start the construction of their TDMA-Schedule in first. When they send their tables to their respective neighbors, the other CHs establish, in turn, their TDMA-Schedules. CH3, CH6, CH7, and CH10 have been released by their neighbor CH1 while CH12 has been released by CH1 and CH8. This process is repeated until all CHs obtain a TDMA-Schedule.

After the clustering phase, the CH nodes return to the cycle of $TC_{ordinary}$, while the ordinary nodes keep the same antenna configuration all the time (the direction corresponding to the selected CH). Thus, the transmission phase starts. Each node transmits its sensed/computed data. These data received by the covering CH are then aggregated and transmitted to other neighboring CHs, which in their turn, send them to their CH neighbors and their members according to the FDN lists.

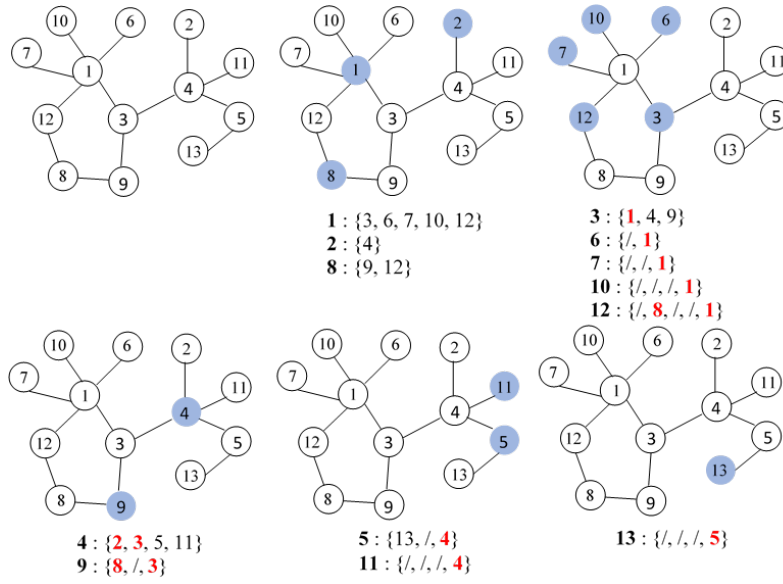


Figure 6.5: Distributed TDMA inter cluster scheduling

6.2.3/ Simulation Results and Comparison

To assess the performance of proposed traffic regulation protocol, simulations were done using BitSimulator platform [101]. BitSimulator presents a good testing framework because it provides high accuracy (at a symbol level) and high calculation performances (simulation of dense terahertz nanonetworks).

The high density of a nanonetwork necessarily generates huge messages traffic. The lack of regulation of the traffic will negatively affect the overall behavior of the nanonetwork. As well, to consider the contribution of our clustering algorithm dedicated to the Directional Antennas Nanonetwork, we used several test scenarios, including the number of nodes and the number of directional antennas. This enabled to assess the impact of clustering and TDMA schedules on the nanonetwork's performance in terms of generated interference. So we compared the number of messages generated by our proposal with the flooding approach.

Figure 6.6 shows the results obtained on several scenarios with different number of nodes deployed over an area of $60cm \times 60cm$ with a communication range of $5cm$.

For each scenario, we give the number of sent messages in the flooding and our clustering approach. The curves show that the performance of our proposal outperforms that of the flooding. Our proposal presents a significant gain of about 15% of the total messages used by flooding approach. This result is interesting, knowing that the very high nodes density in a nanonetwork is the prime source of messages traffic perturbation.

The number of messages generated by broadcasting data over the network with the flooding approach can be computed as follows:

$$NbMsg = \sum_{i=1}^C N1_{n_i} \quad (6.8)$$

Where C is the total number of nodes and $N1_{n_i}$ is the number of neighboring nodes of the node, n_i .

In the clustering approach, the maximum number of messages generated by data broadcasting from an ordinary node, n , to all the nodes is given by the following recursive formula:

$$NbMsg(n) = 1 + \alpha_{Ch_i} + NbMsg(Ch_i / n \text{ is covered by } Ch_i)$$

$$NbMsg(Ch_i) = \sum_{Ch_j \in N1_{Ch_i}} \left\{ \begin{array}{ll} NbMsg(Ch_j) & \text{if } Ch_j \in FDN_{Ch_i} \\ D & \text{else} \end{array} \right\} \quad (6.9)$$

where $\alpha_{Ch_i} = D + N1_{Ch_i}$ and D is the number of antenna directions.

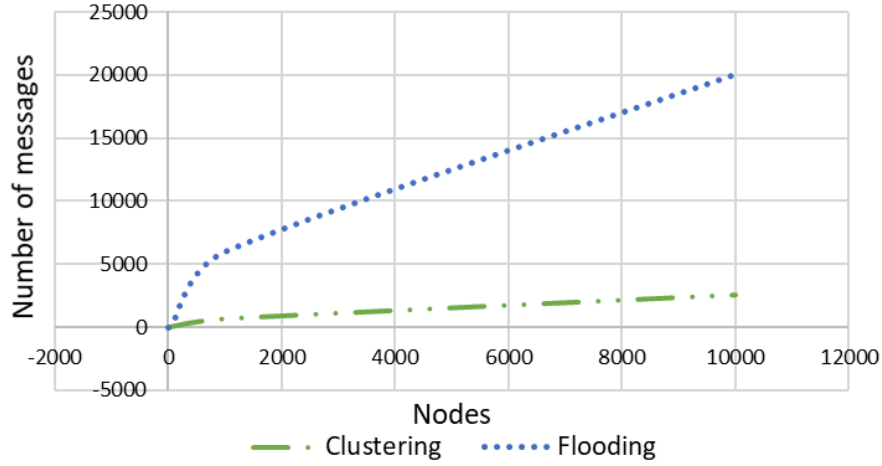


Figure 6.6: Clustering vs Flooding regarding number of messages generated. Tests are made with different network densities.

We now study the impact of Cluster Heads' number on the performances of the clustering method. Too much or too little Cluster Heads number impacts on the nanonodes lifetime. So it has great significance to select the optimal Cluster Heads number for the nanonetwork. The higher the number of CHs, the more energy will be consumed. This is due to the increase of communications number between Cluster Heads (see eq. 6.9). Furthermore, the number of clusters is inversely proportional to the clusters' size. Thus, the latency driven by TDMA protocol is directly proportional to the size of clusters.

Figure 6.7 shows two curves obtained from simulation over a nanonetwork of 1000 nodes. The first curve indicates the variation of exchanged message number according to the number of CHs (given as a percentage). We note that the number of messages increases with the percentage of CHs until a given threshold. When the percentage of CHs exceeds 75%, the number of messages decreases, because messages between CHs and their respective members disappear.

Furthermore, when the number of CHs is small, the number of nodes receiving the data is small too (see the dotted curve in figure 6.7). For example, with 2% of CHs only 40% of the nodes received the data. This is due to the fact that, when the CHs percentage is low, some individuals or groups of nodes become isolated. Beyond 10% of CHs, we note that the data reaches the entire network.

With regard to collisions, intra-cluster collisions are impossible. Therefore, under the condition that data generated by each node are not voluminous and relatively less frequent while the number of simultaneous messages generated by all nodes is high, the TDMA method performs better than random access approach or CDMA/CD method.

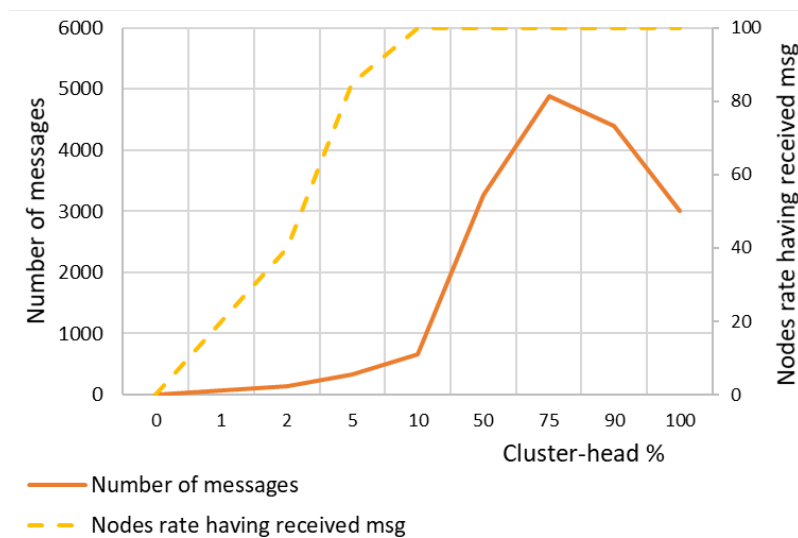


Figure 6.7: Optimal CH rate for covering the entire nanonetwork

6.3/ Uniformly distributed cluster heads based protocol

In this section, we present our second protocol based on a uniform selection of the cluster heads over the deployment area. In this approach, we propose dividing the nanonetwork area into zones, where each zone consists of selected cluster head (CH) nanonode and ordinary nanonodes, based on an established choice of spines among nanonodes. So we begin with the spines' selection process, then the area division using these spines. After that, we propose two distributed TDMA MAC protocols for intra and inter cluster communications.

As shown in Figure 6.8, the proposed protocol proceeds in rounds following globally the same scheme as that described for random cluster head based approach. It begins with synchronization, using a specific broadcasted signal from the base station. The initialization phase is run only during the first round. It includes four main sub-phases called: Spines Selection, Area Division, Clustering, and TDMA schedule. The following two phases are repeated in all rounds: (a) setup phase performs the CH selection, CH neighborhood discovery, and FDN process followed by, and (b) the data transmission phase.

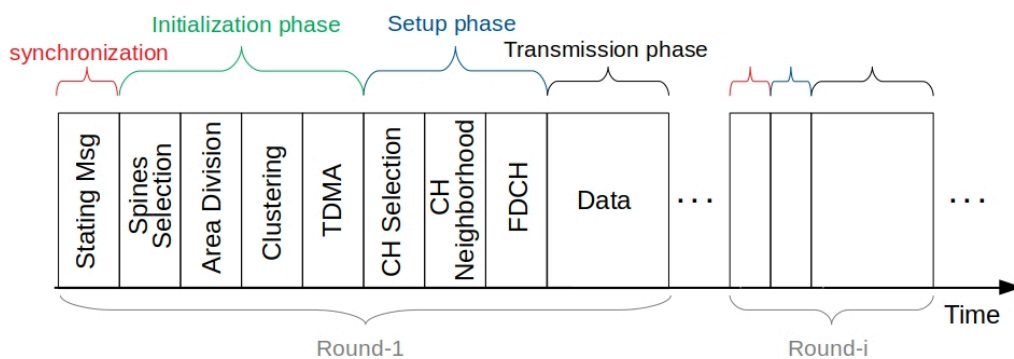


Figure 6.8: The proposed protocol phases.

6.3.1/ Spines Selection

The spines selection phase consists of selecting SP nanonodes used for dividing the nanonodes into small areas or clusters. The spines nanonodes allows to locate each network nanonode, n , using the coordinates (x_1, \dots, x_{SP}) , where x_i designates the number of hops between the nanonode n and its spine.

A cluster corresponds then to a set of nanonodes with the same coordinates. The spines selection must provide a uniform partitioning of the nanonetwork, i.e., small areas with nearly the same size. That is why the spines nodes should be selected among the peripheral nodes. In the absence of geographical information about the nanonodes' positions, we use a metric called weight. The weight of a node corresponds to the number of its direct neighbors according to the signal range. A nanonode is said local lowest weighted if it has the lowest weight among its direct neighbors.

Figure 6.9 illustrates that the set of local lowest weight nanonodes (blue nodes) shows a good sampling (distribution) of the network deployment edges. However, some local lowest weight nodes are located in the center of the nanonetwork area. That is why the local lowest weight nodes, i , compute their rates according to the equation:

$$rate_i = \frac{weight_i}{\sum_{j=1}^n weight_j} \quad (6.10)$$

Where n is the number of neighbors of the node i . A high rate means that the nanonode has low-weight neighbors, i.e., probably near the corners, while a low rate means that the nanonode has high-weight neighbors, i.e., probably near the center of the nanonetwork.

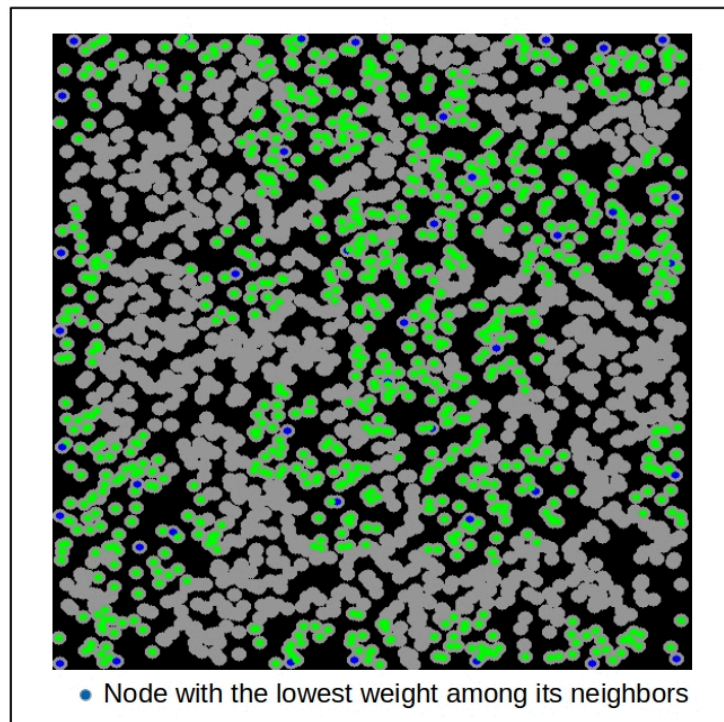


Figure 6.9: Positioning of the nanonodes with the lowest weight (in blue) among their direct neighbors.

The selection phase begins with the neighborhood discovery, where each nanonode will send a *HELLO* message to discover their neighboring nanonodes. Upon receive a *HELLO_j* from neighbor *j*, the receiver *i* update its $weight_i$. After that, each nanonode will send its weight to its neighbors. At the reception of $weight_j$ from the neighbor *j*, the receiver *i* updates its weight sum $S = S + weight_j$, and then checks whether $weight_j$ is less than its $weight_i$, if so, then receiver *i* will be directly a non-candidate for being spine node. Once all neighbor weights are received, each candidate node follows the proposed algorithm 4 to decide whether it will be a spine or not.

Algorithm 4: Spines Selection.

Data: *idNode* , *weightNode* , *weightNeighbors* , *rateNode* , *Threshold* , *isspines* , *mapspines* ;

```

1 Init: rateNode  $\leftarrow$  0, isspines  $\leftarrow$  false, mapspines  $\leftarrow$   $\emptyset$  ;
2 if weightNode < all weightNeighbors then
3   | rateNode  $\leftarrow$  weightNode/sum(weightNeighbors) ;
4   | if rateNode  $\in$  [Threshold, 1[ then
5   |   | isspines  $\leftarrow$  true ;
6   |   | mapspines.insert(idNode, rateNode) ;
7   |   | Send rateNode to neighbors ;
8 upon receive ratespine from spine j do ;
9 if isspines then
10  | mapspines.insert(Idj, ratespine) ;
11 else
12  | Send ratespine to neighbors ;
13 end do
14 if isspines then
15  | Pick (id1, rate1), (id2, rate2)  $\in$  mapspines which have the highest rates ;
16  | if (idNode, rateNode)  $\notin$  [(id1, rate1) ; (id2, rate2)] then
17  |   | isspines  $\leftarrow$  false ;

```

So the spines that will be selected are those with a high rate. Once the rate is calculated, the nanonode checks whether it is higher than the threshold, and then broadcasts a message containing its rate. The threshold is used to reduce the number of transmitted messages. It can take several values; initial value depends on the distribution and the density of the nanonetwork. For example, if uniform distribution is used, its value is $3/D$, where D is the nanonetwork density (see Figure 6.10). If the nanonetwork has a grid distribution, the formula is unused because the nanonodes with the smallest weight are the four nanonodes situated at the four corners.

First of all, we need to determine the number of spines used to get better partitioning. Several scenarios have been carried out using various numbers of nanonodes deployed over an area of $60cm \times 60cm$ with a communication range of $5cm$. The results of the simulation are summarized in Table 6.1

The table shows that using two spines instead of three or four spines gives a smaller number of clusters and, therefore, fewer transmitted messages among the CHs. Moreover, the use of two spines gives fewer clusters without members and, accordingly, less CH that will be used just as a gateway. Then the optimal number of spines that can be used is two spines.

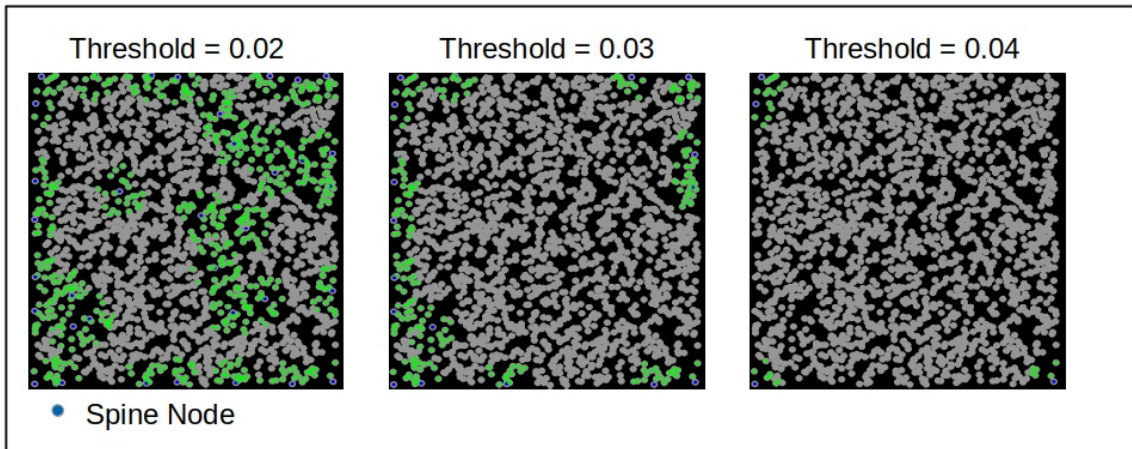


Figure 6.10: Selected spines after the first step under different threshold values.

Table 6.1: Number of Clusters obtained using different spines.

Spines	Number of clusters	Clusters without members
2	200 – 225	5 – 30
3	350 – 400	40 – 130
4	400 – 550	60 – 170

The second step of the selection is choosing exactly two spines with the highest rates through a consensus process. The spines selection process is illustrated in Figure 6.11.

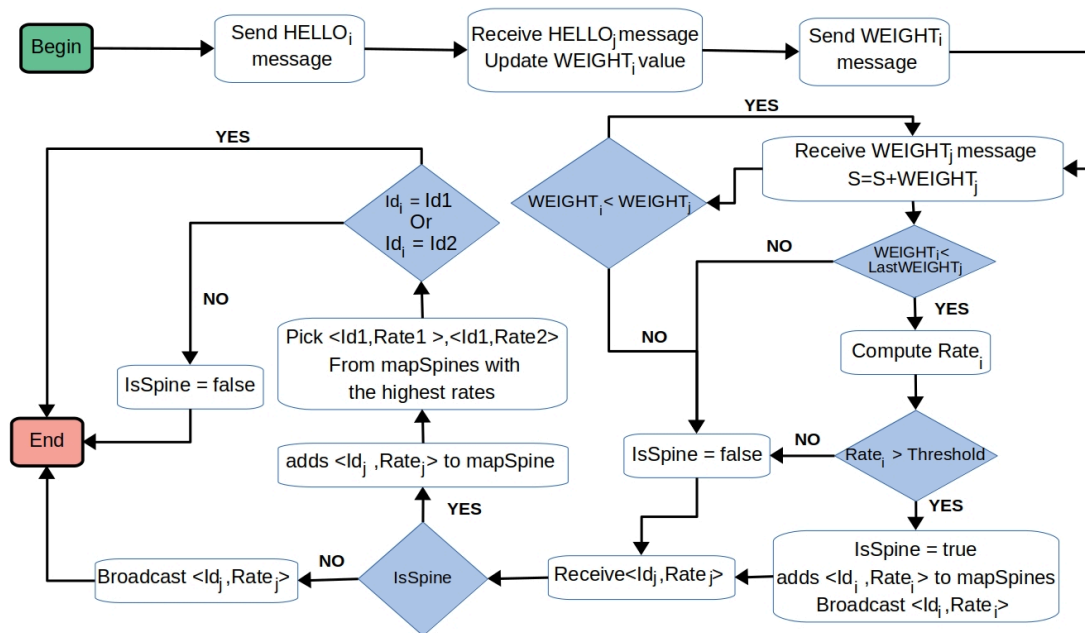


Figure 6.11: Spines selection phase.

6.3.2/ Area Division

The second phase of our protocol is the nanonetwork partitioning i.e., dividing the network into sub-areas or clusters. Figure 6.12 shows that the use of two spines located at the corners of the nanonetwork results in a better area division.

In this phase, the two spines selected in the previous phase will begin the division process by executing the algorithm (5). Then the two spines will send a setup packet that contains the hops count with a value equal to 1. At the reception of this packet, nanonodes memorize the hops count from the corresponding spine, update and forward it. Once the two packets from the two spines are received, the nanonodes define the hop counts from the two spines as their respective coordinates (x, y) .

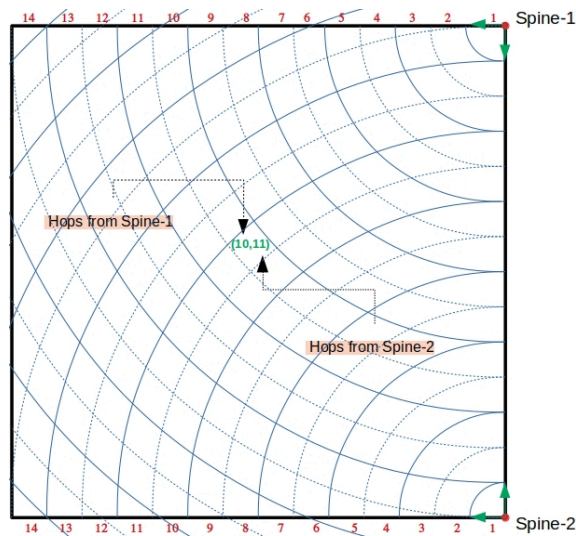


Figure 6.12: Area division using two spines.

Algorithm 5: Area Division.

Data: $hopsNumber$, $mapCoord$, x , y ;

```

1 Init:  $hopsNumber \leftarrow 1$  ,  $mapCoord \leftarrow \emptyset$  ,  $x \leftarrow -1$  ,  $y \leftarrow -1$  ;
2 if isSpine then
3   | Send  $hopsNumber$  to neighbors ;
4 else
5   | upon receive  $hopsNumber$  from spine  $j$  do ;
6     |  $mapCoord.insert(Idj, hopsNumber)$ ;
7     |  $hopsNumber \leftarrow hopsNumber + 1$  ;
8     | Send  $hopsNumber$  to neighbors ;
9     | end do ;
10  |  $It1 \leftarrow mapCoord.begin()$  ,  $x \leftarrow It1.second$  ;
11  |  $It2 \leftarrow It1 + 1$  ,  $y \leftarrow It2.second$  ;
12  |  $mapCoord.clear()$  ;

```

6.3.3/ Clustering

In this phase, nanonodes discover their sub-area neighbors using the algorithm (6). Hence, each nanonode broadcasts a specific message containing its coordinates (x, y) . A receiver node, i , counts the number of nodes, $idPosition$, belonging to the same cluster (with the same coordinates) and having an identifier smaller than its identifier. After receiving all neighbors' messages, each nanonode in a specific sub-area determines its numerical order, $idPosition$, relatively to its neighbors in the same cluster (see Figure 6.13).

The ascending order of $idPosition$ is used to determine the round during which the node will be CH. In each cluster, the nanonode with the smallest $idPosition$ becomes CH in the first round.

Algorithm 6: Clustering.

```

Data:  $idNode$  ,  $isCH$ ,  $x$ ,  $y$ ,  $idPosition$  ,  $k$  ;
1 Init:  $isCH \leftarrow false$ ,  $idPosition \leftarrow 1$ ,  $k \leftarrow 1$  ;
2 Broadcast  $(x, y)$  message;
3 upon receive  $(x_j, y_j)$  from Neighbor  $j$  do ;
4 if  $x == x_j$  and  $y == y_j$  then
5    $k = k + 1$  ;
6   if  $idNode > Id_j$  then
7      $idPosition = idPosition + 1$  ;
8 end do ;
   /* CH Switching */
9 upon receive  $roundCount$  from BS do ;
10 if  $(roundCount \bmod k) == idPosition$  then
11    $isCH \leftarrow true$  ;
   /* CH Begins the setup phase */
12 else
13   if  $isCH$  then
14      $isCH = false$  ;
     /* CH of the previous round be an ON */
15 end do ;

```

6.3.4/ The Proposed TDMA MAC protocols

TDMA approach is used to both schedule the communications occurring between the cluster members and their CH (Intra Cluster) and for scheduling communications occurring between CHs (Inter Cluster). Hereafter, we discuss these two procedures.

6.3.4.1/ Inter Cluster TDMA

Each nanonode subdivides the time into frames of fixed size S_f . The frame cycles are synchronized over the nanonodes thanks to the base station. Let n a nanonode belonging to the cluster C_0 and let C_1, C_2, \dots, C_8 the surrounding clusters. The frame is subdivided into 9 equal periods where each period is dedicated to one of these clusters $\{C_0, C_1, C_2 \dots C_8\}$. In other words,

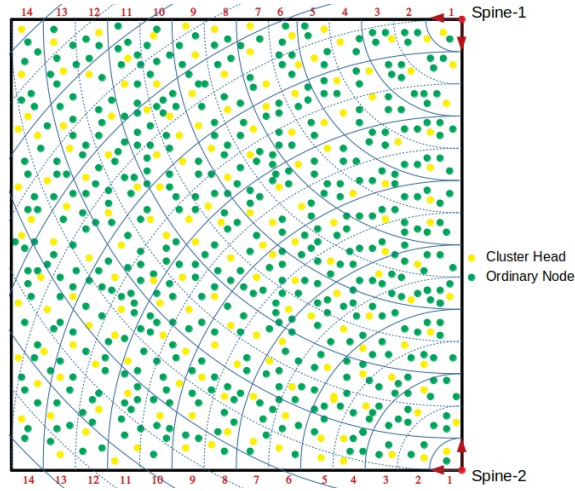


Figure 6.13: Nanonetwork topology after the clustering phase.

if the cluster C_0 is associated with the 4th period, the nanonodes belonging to this cluster will communicate only during this period. The scheduling of nanonodes communications within the same cluster (same period) is discussed in the intra TDMA section.

The time domain architecture of the Inter Cluster is shown in Figure 6.14. The nanonodes of the same cluster are concerned by the same period, P , computed according to the coordinate x, y of node following the formula:

$$\begin{aligned} Rank &= (\alpha x + \beta y) \pmod{9} + 1 \\ P &= Rank \times D_a \end{aligned} \tag{6.11}$$

Where, x and y are the nanonode coordinates regarding the two selected spines, and α and β are constants that are initially fixed for all nanonodes. $Rank$ designates the index of the period during which the nodes of the same cluster communicate. D_a is the duration of period and is equal to $D_a = S_f/9$. P is the start time of the period associated to the node's cluster.

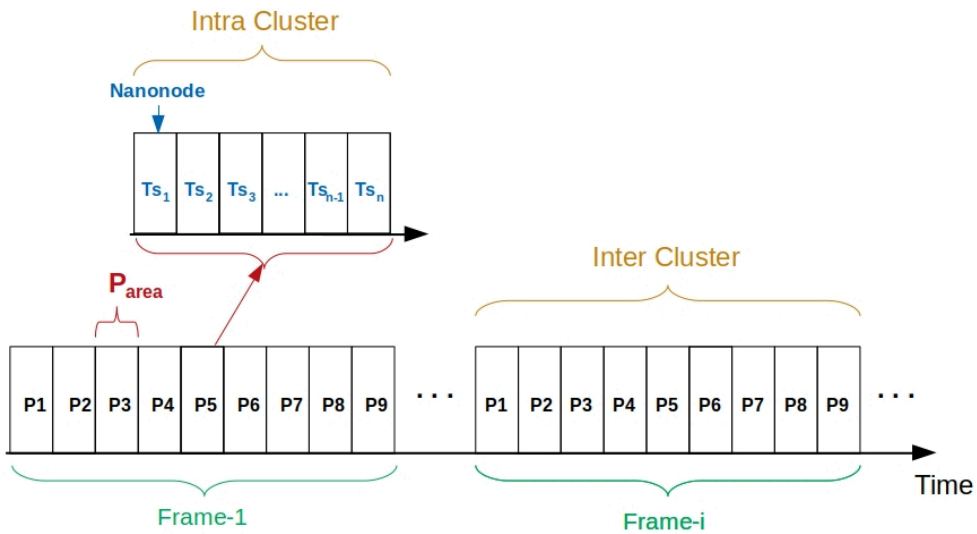


Figure 6.14: Time domain architecture of the Inter Cluster TDMA

As shown in figure 6.15a, each sub-area (cluster) has at most eight neighboring sub-areas. Therefore, at least nine different periods should be used. We used α and β to avoid getting the same rank value for two adjacent sub-areas that have the same inverted (x, y) coordinates. The results of several test scenarios using different α and β values show that, more than 93% of the sub-areas have different rank values than their adjacent sub-areas. Figure 6.15b shows the obtained results with $\alpha = 2$ and $\beta = 3$. The use of different periods by adjacent clusters allows the elimination of the inter-cluster interference.

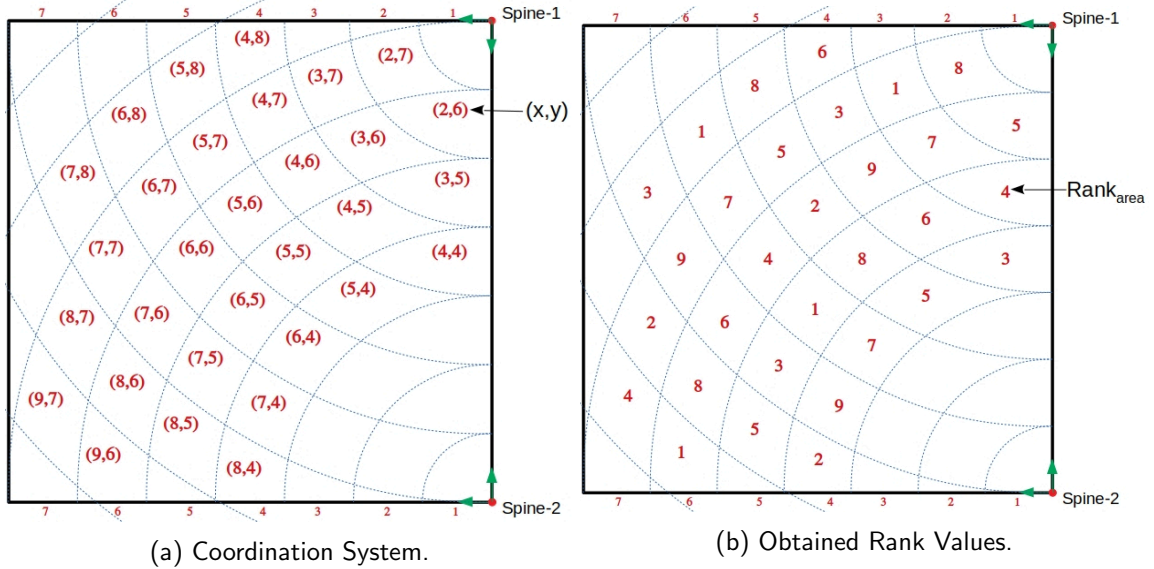


Figure 6.15: Illustration of The Inter Cluster TDMA Algorithm.

6.3.4.2/ Intra Cluster TDMA

During the communication phase, each nanonode n waits for its period P (the period associated with its cluster). Outside this period, the nanonode remains in standby mode. The period associated to the cluster is subdivided into n time slots, where CS is the number of nanonodes of the cluster. Therefore, the duration of the time slots, TS , may vary from one cluster to another.

$$TS = P_{area}/CS \quad (6.12)$$

Each nanonodes compute its transmission order in the intra cluster TDMA-Schedule. To that end, the nanonode, n , calculates its time slot TS_n using equation 6.7 as for the random cluster head based approach where $rank_i = idPosition_i$. This time slot is used sending the node sensed/computed data to its CH. The last time slot is used to send the CH's data to its cluster member and CH neighbor nanonodes.

If the nanonode becomes CH in a specific round, it will occupy the last time slot, i.e. the highest rank. Accordingly, the CH will receive the data packets from all its members before broadcasting its packet to its CH neighbors.

6.3.5/ CH Neighborhood Discovery

This step is responsible of defining the communication links between the cluster heads. The objective is to define the links followed by the packets to exchange data between distant nanonodes.

At each round, the selected cluster heads discover their CH neighboring nanonodes by sending a *HELLO-CH* message using the same communication range. Each receiving CH_i nanonode will add the sender CH_j to its CH neighbors list named $N1_i$. This list includes all CHs directly linked to CH_i (accessible with just one hop). After receiving the *HELLO-CH* from different Cluster heads, each cluster head CH_i sends its $N1_i$ list to its neighboring cluster heads. Upon the reception of $N1_j$ from CH_j , the receiving nanonode CH_i adds the couple $\langle CH_j, N1_j \rangle$ to its two hops neighbors list called $N2_i$. Once the two hops neighbors list is built, each CH nanonode can select its forwarding dominating CH (FDN) among its direct neighbors ($N1$) using the algorithm (2). Furthermore, the *HELLO-CH* message can be received by the sub-area neighbors, i.e. the cluster nanonodes, allowing them to determine their CH at each round.

During the data transmission phase, each data packet transmitted by CH_i is forwarded by only successor nanonodes CH_j ($CH_i \in S_{CH_j}$). For example, in Figure 6.16, the data packet of CH nanonode 7 is forwarded by only CH nanonodes 2, 3, 6, and 10.

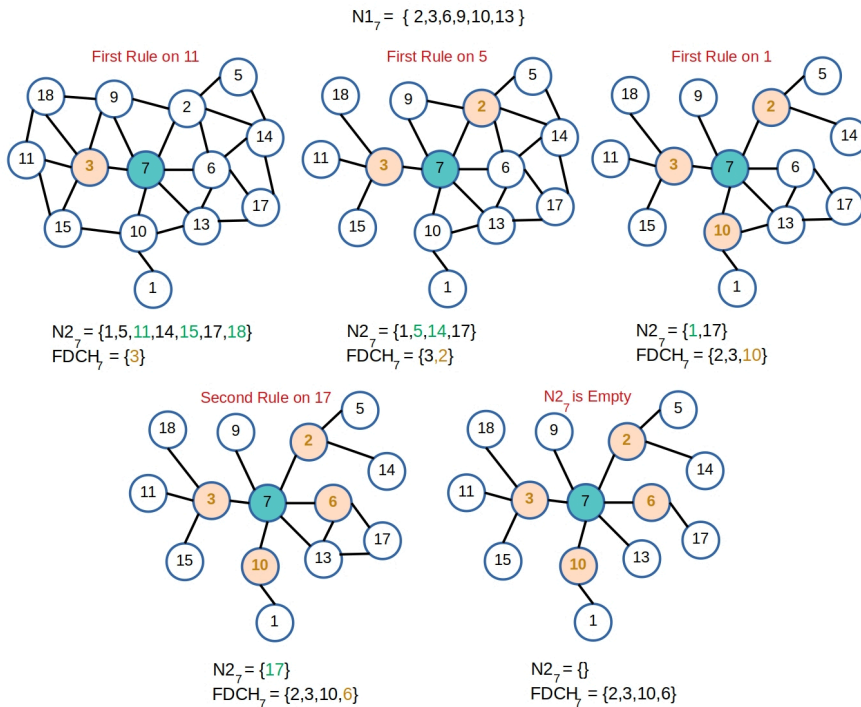


Figure 6.16: Illustration of the FDN selection algorithm.

6.3.6/ Performance Assessment

In this section, we evaluate our second proposed protocol (called Uniform based cluster head protocol) in comparison to the first one detailed in section 6.2 (called random cluster head based approach) regarding the nanonetwork connectivity, control packets, and communication

reliability. In order to evaluate the performance of the proposed protocol, simulations were performed using the BitSimulator platform [101].

6.3.6.1/ Nanonetwork Connectivity

Several test scenarios with different nanonetwork density were performed to evaluate the Uniform based cluster head approach compared to the random one [6.2]. More specifically, assessing the impact of both approaches on the nanonetwork connectivity in terms of isolated ordinary nanonodes and limbless clusters obtained.

Figure 6.17 shows the results obtained from several scenarios with different number of nanonodes deployed over an area of $60\text{cm} \times 60\text{cm}$ with a communication range of 5cm . According to Figure 6.17a, there is no isolated Ordinary Nanonodes (ON) in uniform based approach since areas with a single node are automatically considered as a singleton cluster. In contrast, the random based approach presents many isolated ordinary nanonodes due to the big distances between these nanonodes and the nearest selected CH. Finally, uniform based approach presents a better coverage of network area than the random approach.

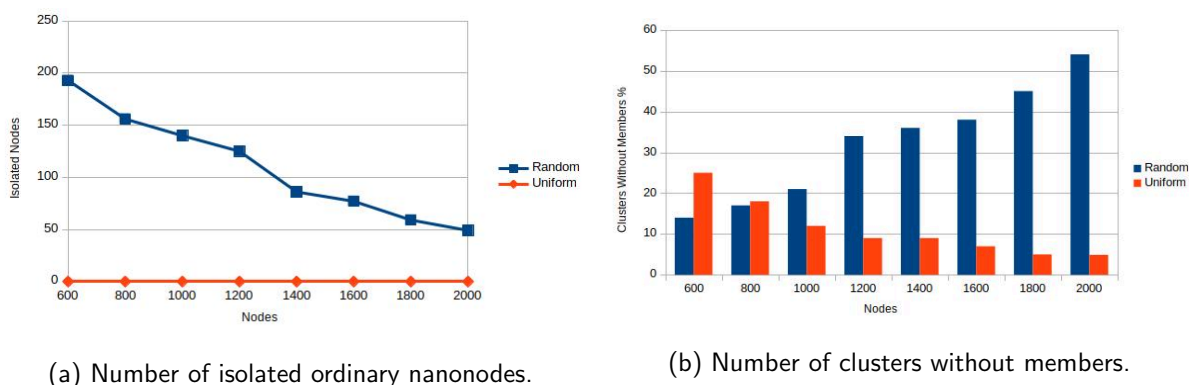


Figure 6.17: Impact of the used clustering approaches on the nanonetwork connectivity.

The number of clusters that contain only the CH i.e., without members nanonodes, is shown in Figure 6.17b. The uniform based approach presents a lower number of singleton cluster than random based approach. Furthermore, the more the density of the nanonetwork increases, the more this number increases in random based approach contrary to the uniform based approach. This is caused by the random distribution of CHs on the nanonetwork. An example of obtained cluster head distribution is given in Figure 6.18. Random cluster head selection leads to regions with few cluster heads and others with a large number of cluster heads. Uniform based selection presents better distribution of cluster heads over the nanonetwork area. Therefore a small number of clusters without members is obtained.

We further calculated the percentage of isolated cluster heads using different communication ranges. As shown in Figure 6.19, the use of a short communication range (5cm) in uniform approach results in a percentage of less than 2% of isolated cluster heads regardless of the nanonetwork density. On the other hand, the random approach requires higher ranges to achieve the same percentage, which will significantly increase the energy consumption at each CH. As a result, Uniform based approach offers a better degree of connection than Random approach when the same communication range is used.

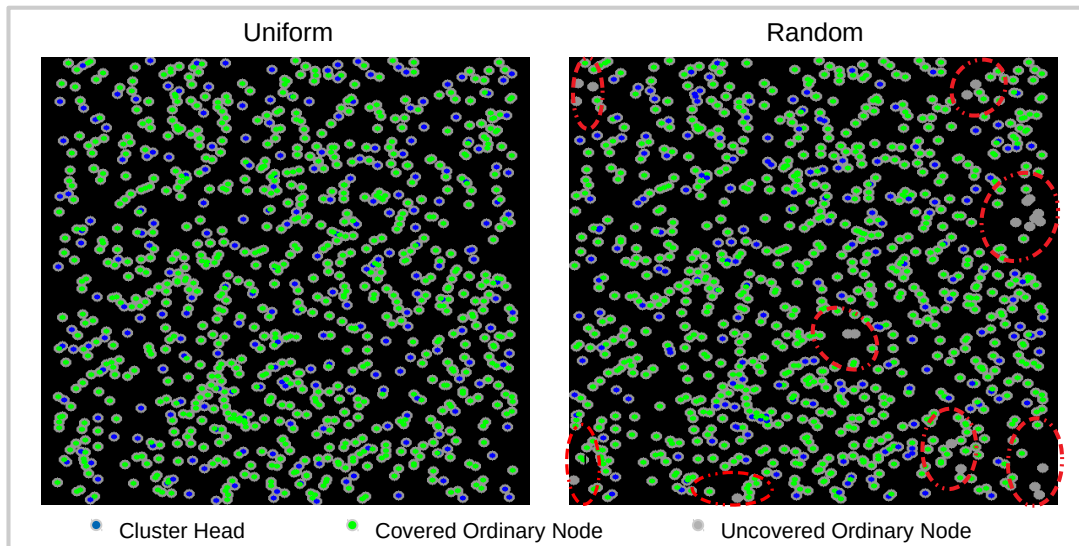


Figure 6.18: Comparison of cluster heads distribution between uniform based approach and random based approach

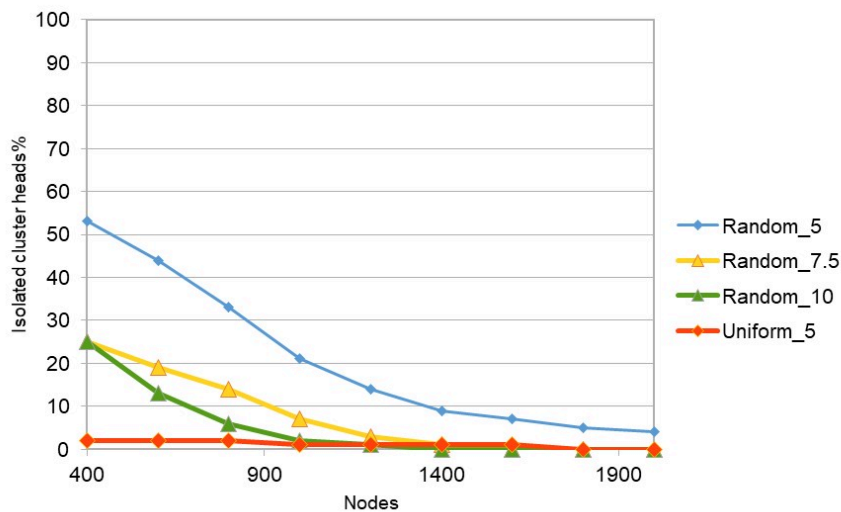


Figure 6.19: Percentage of isolated CHs obtained in each approach.

6.3.6.2/ Control Messages

We evaluated the complexity of uniform cluster heads selection protocol compared to random protocol, in terms of the generated control packets. As described in [6.3] uniform approach performs the clustering phase only one time during the first round, as opposed to random approach, which repeats this phase at each new round. Figure [6.20] shows the number of clustering messages needed at each round, which can be estimated by the following formulas:

- For Area protocol :

$$N_{CM} = packet_{SS} + packet_{AD} + packet_{AN} \quad (6.13)$$

Where $packet_{SS}$, $packet_{AD}$ and $packet_{AN}$ are the control packets required for spines

selection, area division and area neighbors discovery respectively.

- For Random protocol :

$$N_{CM} = packet_{ADV} + packet_{JOIN} \quad (6.14)$$

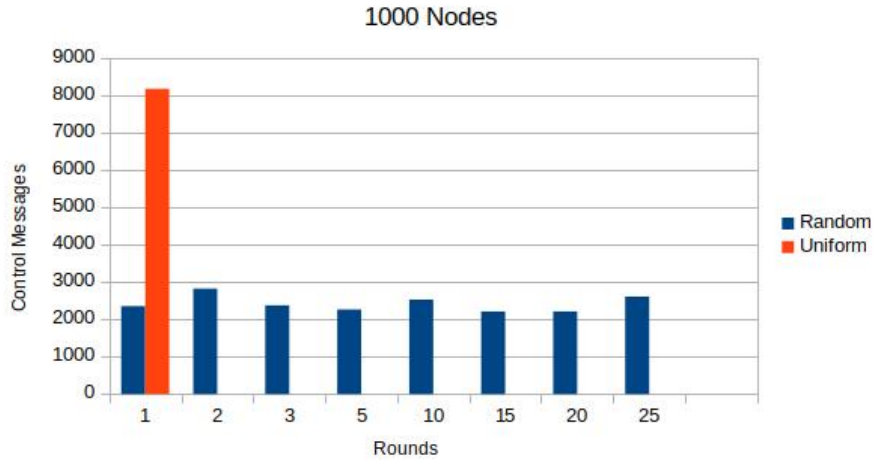


Figure 6.20: Required clustering messages at each round in each approach.

Figure 6.20 shows that uniform CH selection generates more control packets in the first round, 60% of which is needed for spines selection process. Random based approach requires control packets in each round. Thus, excluding the first round, the setup phase in the random approach is much longer than uniform one. Therefore, in uniform based protocol, little time is wasted during the first round, but a lot is saved during the following rounds. Besides, we measured the total number of generated control messages arriving at a specific round as follows:

- For Area protocol :

$$TN_{CM} = N_{CM} + \sum_1^n packet_{N1} + packet_{N2} + packet_{FDN} \quad (6.15)$$

Where $packet_{N1}$, $packet_{N2}$ and $packet_{FDCH}$ are the control messages required for one-hop neighbors discovery, two-hop neighbors discovery and FDCH list sending, respectively.

- For Random protocol :

$$TN_{CM} = \sum_1^n packet_{ADV} + packet_{JOIN} + packet_{N2} + packet_{FDN} + packet_{TDMA} \quad (6.16)$$

As shown in figure 6.21, by the 3rd round, the total number of generated control packets in random approach exceeds that of uniform protocol, which means that Area protocol is less complex in the long run.

6.3.6.3/ Communication Reliability

We assess communication reliability as the proportion of clusters heads that do not receive a broadcasted packets due to collisions or network disconnection. This is noted Packet Loss

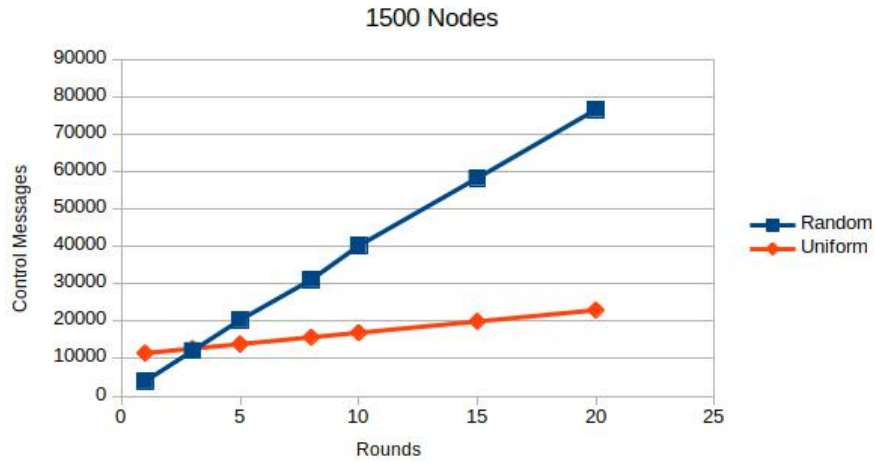


Figure 6.21: Generated control packets arriving at a specific round.

Ratio (PLR) and measured as follows:

$$PLR = 1 - \frac{NP_{received}}{N_{CH}} \quad (6.17)$$

Where $NP_{received}$ is the number of cluster heads that receive the broadcasted packet, and N_{CH} is the number of cluster heads in the nanonetwork. Average results from the simulation of a nanonetwork of 1000 nanonodes using different slot duration ($5 \cdot T_d$, $10 \cdot T_d$ and $15 \cdot T_d$) and different communication ranges (5cm , 7.5cm , 10cm) are presented in Table 6.2. T_d is the packet transmission delay (size = 128bits, pulse duration = 100fs , interval between pulses = 10ps using TSOOK protocol).

Table 6.2: PLR of Area Protocol and Random Protocol.

Approach	$5 \cdot T_d$	$10 \cdot T_d$	$15 \cdot T_d$
Random – 7.5cm – 10%CH	93.6%	92.5%	92.5%
Random – 7.5cm – 20%CH	69.0%	68.5%	68.3%
Random – 10cm – 10%CH	58.5%	56.3%	56.0%
Random – 10cm – 20%CH	20.5%	19.5%	18.0%
Uniform – 5cm – 218CH	6.3%	6.2%	6.2%

Uniform based protocol presents lower PLR (better reliability) than random one, in all cases, even when the communication range used in random approach is equal to 10cm, = which is the double of that used in uniform based protocol. Also, uniform based protocol perform well even with short range communication, which allows the CHs to minimize their energy consumption. The remaining packet lost, in uniform approach is due to the small probability that two adjacent clusters obtain the same rank (hence use the same period).

6.4/ Conclusion

With very high density WNN, efficient coordination of communications allows to significantly reducing the costly conflicting channel accesses and ensures traffic regulation by assigning

a time slot for each nanonodes. Consequently, collisions and node energy consumption are minimized, and the channel access is balanced too.

In this chapter we studied dense nanonetwork applications under a controlled topology and environment. The nanonodes positions over the geographical area is assumed well distributed. To this end, our proposals consist of organizing the nanonetwork into clusters and controlling multilevel nanonode communications. The first level concerns communications inside clusters with the use of centralized and distributed TDMA approach in the first and the second proposal respectively. The second level is dedicated to inter-cluster communications with the help of forwarding dominate nodes and uses a new distributed TDMA scheme. This multilevel approach allows minimizing delay and regulating large data amount transmissions over the network.

The first proposition proceeds in a cyclic manner, where each round is composed of the clustering and transmission phase. The first phase performs the CH selection and construction, then the intra/inter TDMA scheduling. The second phase ensures data transmission. In order to reduce collisions, each node uses its directional antenna, dynamically directed to cover a particular area and to communicate with the others. The proposal's performance exceeds that of the flooding approach by a gain of approximately 85% of the total forwarded messages in the nanonetwork. This result is interesting, knowing that the very high density of nodes in a nanonetwork is the prime source of traffic disturbance messages.

The second proposal overcomes two main drawbacks of the first one : logical topology disconnection and interference between intra-cluster communications carried on different clusters. The initialization phase is composed of four steps: the spines selection, area division, the FDN selection, and data transmission. The last one, including intra and inter communication, is performed by the proposed distributed TDMA MAC protocols to achieve high channel capacity while avoiding collisions. The protocols complexity in terms of exchanged control packets is evaluated. Based on simulation results provided by BitSimulator, the uniform cluster head based selection outperforms the random cluster head selection protocol with better nanonetwork connectivity, lower control packets, and higher packets delivery rate. Furthermore, the proposed scheme is more efficient in dense nanonetwork.

In Table 6.3, we summarize the main features of the three approaches of traffic regulation or de-densification. The table shows that globally each approach presents some features making it more suitable for some kind of applications. The two first features relate to the nature of targeted application. The third and fourth features relate to the physical layer based mechanisms used for improving the radio efficiency of the protocol. Finally the fifth and sixth features relate to the traffic conditions, where traffic capacity designates the number of simultaneous communications, while traffic intensity designates the required throughput per node.

Table 6.3: Synthesis of the features of the three studied de-densification approaches

Characteristic	Directed graph	Hierarchical+random CH	Hierarchical+uniform CH
Nanonodes	mobile, volatile	fix, stable	fix, stable
Topology	any	convex, uniform	convex, uniform
Antenna	directional	directional	omni
Frequencies	frequency windows	frequency windows	none
Gateway	none	needed	needed
Traffic capacity	low	low	high
Traffic intensity	high	high	low

Routing Protocol in ultra-dense WNN

7.1/ Introduction

Terahertz nanonetwork domain is giving birth to new ad hoc network topologies composed of a huge number of sub-millimetric nodes with unprecedented density.

By comparison, Internet network involves up to billions of terminal nodes with an average connection degree of about 6 connections per node [54], while ultra-dense nanonetworks can present an average degree (number of neighboring nodes per node) higher than 1000 nodes. The devices' sub-millimetric size leads to energetic and memory limitations, and the use of Terahertz band frequencies represents a real issue for data communication. Moreover, it is not always possible to control nanonetwork's global shape that may present some concave sides. An example of the nanonetwork topology distortion is given in figure 7.1, where the nanonodes are deployed inside a human bowel. The nanonodes distribution is dictated by the bowel shape.

The routing problem in ad hoc network is widely covered by the literature. Mainly, the classical routing approaches could be classified into proactive and reactive protocols [49]. In reactive protocols such as AODV [7], DSR [10] based on a chain of re-transmissions (one node every time) are a risky strategy in terms of communication reliability. The path followed by the communication data is computed in real-time by exchanging route requests (flooding mechanism), which leads to additional latency and additional control traffic. The flooding impact is



Figure 7.1: Wireless Body Area Network (WBAN) is deployed inside a bowel. The nanonetwork deployment follows the bowel shape and consequently forms a concave shape.

accentuated by the high density of the network.

In proactive protocols (OLSR [17], Babel [4], DREAM [5], and DSDV [37]), each node computes and stores in advance the optimal paths or just the next node in this path, towards one, several, or all nodes. These approaches suffer from a lack of responsiveness in case of nodes failure requiring the path recalculation.

New routing paradigm was proposed in [75] and [88] (see section 3.4.2). These approaches are based on multipoint-to-multipoint paths and offer a more reliable connection, especially under the high volatility context of nanonetworks. The data are transmitted from the source node to the destination node by crossing successive areas. At each hop, all the current area nodes re-transmit the packet to the next area and so on until the packet reaches the area containing the destination node. The successive areas passed through by the packet correspond to those located on the direct line between the source and the destination nodes.

Major recent protocols dedicated to the nanonetworks such as LaGOON [100], Pierobon [69], EECR [117], and TSCR [108] also adopt the point to point relay mode. Besides, the node's energy management consists of reducing the overall consumed energy without considering the residual energy on the nanonodes [69, 117]. In contrast, in multirelay to multirelay routing protocols, such as Flooding method [76], OLSR [17], and SLR [88], every node forwards received data to a subset of neighboring nodes. This way, communication reliability is improved since the data transmission does not depend on a single node. However, no multirelay to multirelay approach does deal with the energy aspect. Also, the shape of nanonetwork topology is ignored, which makes difficult the adaptation of the multirelay to multirelay approaches such as CORONA [75] and SLR [88].

7.2/ Contribution

In this chapter, we propose a proactive multipoint-to-multipoint routing protocol for ultra-dense nanonetworks with volatile nodes. The density of the network is exploited in order to increase communication reliability. Packet routing follows a sequence of multipoint-to-multipoint links (see Figure 7.2), which offers better protection against packet loss. Two versions of the multirelay routing protocol called (M2MRP and M2MRPv2) are discussed in this chapter.

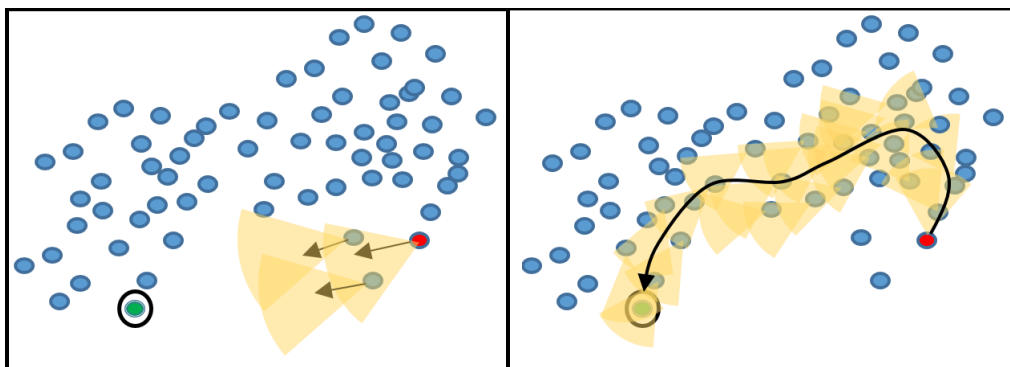


Figure 7.2: Comparison between direct line multipoint-to-multipoint approach (left) and M2MRP protocol (right). The surrounded node is a sink and the dark one is the source. The direct line approach fails to route the message until the sink node, whereas M2MRP approach succeeds.

Unlike direct line routing protocols [88], the M2MRP uses adaptation mechanisms that allow to continuously adjust the circulation flows of data according to network deployment (mobility), nodes availability (curative adaptation), and energy state (preventive adaptation). This way, the adequacy of a node to serve as a relay point varies over time according to its energy state and its neighboring nodes' state. Additionally, unlike other methods, M2MRP(v2) uses the Terahertz beam steering technology [19] to improve the spatial coverage of nodes (node radiates in a specific direction corresponding to the targeted reception nodes), leading to more efficient use of energy, better interference control and a reduction of short multiple reception loops (reception of the same packet several times). M2MRP(v2) allows every node to determine the best reception and transmission directions that optimize traffic flow from any node to the sink nodes. Therefore, the flooding effect and cumulative interference are significantly reduced.

Every *original* received packet (received from a node situated in the reception direction) is just sent in the transmission direction without checking the sender or the destination identity. Finally, M2MRP(v2) protocol leads to efficient use of wake-up receiver technology [27], since the energy generated by transmitters is steered in one direction to activate only a part of the physical neighbors corresponding to the next-hop nodes. This procedure provides a low-latency communication environment when nodes are activated just in time to receive a packet and to re-transmit it.

Furthermore, we present a critical analysis of the routing protocols dedicated to nanonetworks and highlight their lack of reliability and adaptability. Special attention is given to multirelay routing approaches and a comparison of their performances is done to assess the way nodes' energy is managed.

We considered the multi-source to multi-sink routing problem where nanonodes produce data that should be sent to the sink nodes representing gateways towards the decision unit. We show the efficiency of M2MRPv2 compared to SLR and classical flooding methods. The tests are achieved on a set of nanonetwork scenarios presenting different network topologies, energy harvesting processes, and traffic patterns while major works in this field assume naive CBR traffic [8] with homogeneous topology.

7.3/ Traffic characteristics in nanonetwork

The study of the routing protocols performance needs to identify in advance the targeted application types. The nature of the application determines the probabilistic model of the occurring events. Exhaustive identification of these applications represents a tremendous work and is still somewhat premature. However, we distinguished in our work two case studies. The first case assumes that the nodes are independent and each node is regularly a source of data packets. This case fits well with sensor networks case, where every sensor (node) senses the environment and diffuses the measures. In the second case, we consider that occurring traffic leads to relatively simultaneous data packets sent by the nodes near the event location. This case well represents positioning and tracking applications, where the nodes close to the foreign object detect and help to compute the object's position.

7.3.1/ Multiple sink problem

Routing in nanosensor networks is a very common problem [48, 107]. The nanosensors measure environmental conditions such as temperature or pressure and forward the data to particular

nodes called sinks. We assume that sink nodes are not affected by the volatility phenomena and represent gateways to the decision unit.

7.4/ Multipoint to Multipoint protocol M2MRP

M2MRPv2 is an improved version of the M2MRP routing protocol. We start by describing the common operating scheme between M2MRP and M2MRPv2, then we discuss the difference between them, which mainly concerns the computation of the orientation of the nodes antenna (equation [7.1](#)).

The idea of the M2MRP(v2) protocol is to bring out a communication flow pattern defining how the data are transferred from any ordinary nanonode to one of the sink nodes, as shown in Figure [7.3](#). So the flows' circulation structure corresponds to a distributed data structure that stores, in every ordinary node, the steering directions for receiving and sending data. The nanonodes are assumed to use directional antennas [\[123 118\]](#).

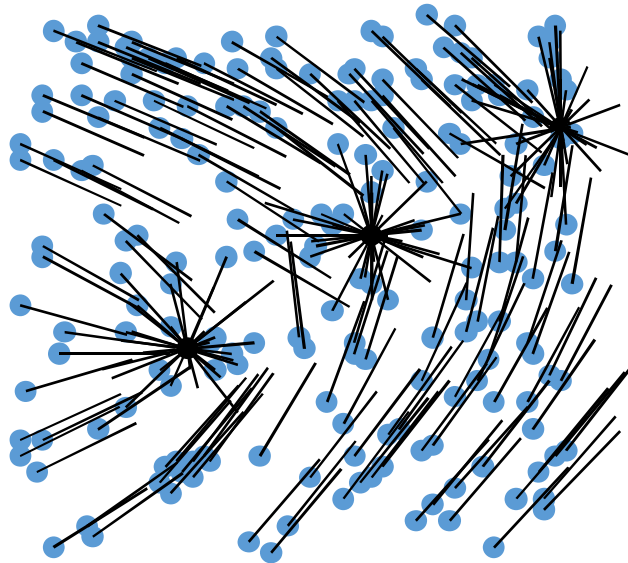


Figure 7.3: An example of M2MRP(v2) data flows pattern describing the trajectory of data from any source node towards one of the three available sink nodes.

For that end, M2MRP(v2) draws on electrostatic physics to determine how the nanonodes compute the best direction (and not the best path) to reach one of the sink nodes. Three main principles govern the protocol functioning:

- the attractiveness effect: this principle states that every node attracts all nodes within a given range.
- the distance effect: this principle states that the attraction level of a given node on another one is proportional to the received signal power.
- the attractiveness vector (direction) of a given node is a weighted sum of the attractiveness vectors of its direct neighbors.

The third principle means that the attractiveness vector of a given node is measured according to the attractiveness vectors of its direct neighbors. Therefore, by propagation effect, the

attractiveness of each nanonode impacts the attractiveness of farther nodes by the effect of intermediate nodes. The distributed propagation process leads to the formation of circulation lines defining the data circulation flow from ordinary nanonodes to the sink nodes.

More formally, let N be a nanonetwork composed of a set of ordinary nodes, O and a set of sink nodes, S . Each node involves a directional antenna that can be steered in a direction $d \in D$ with a fixed opening angle α . The M2MRP protocol proceeds by periodic updates of the circulation flow to reflect the evolution of nodes state availability and energy level. In asynchronous way, each node proceeds per cycles (See Figure 7.4) called *routing cycle*. The *routing cycle* duration is $10^{12} \times Tp = 100ms$ and is subdivided into 1000 *data cycles* of a duration $10^9 \times Tp = 0.1ms$. The last *data cycle* is dedicated to the routing update procedure and forms the *listening cycle*. During the *listening cycle*, each ordinary node, $o \in O$, captures the *control packets* sent by the neighboring nodes (the antenna is used in omnidirectional mode). The *control packets* are particular packets with a specific signature and contain the attractiveness vector of the transmitter node and its energy level. The signal power of the received control packets and the attractiveness vectors of all neighbors are processed in order to determine the main sending direction, $\vec{d}(o)$, of the node o .

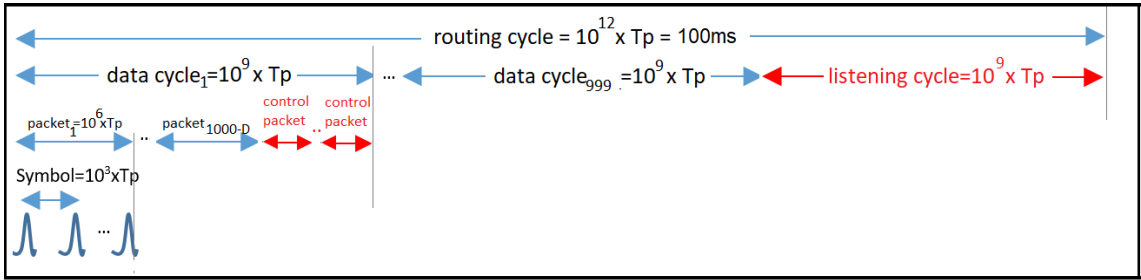


Figure 7.4: Routing cycle: every 100ms, the node recomputes its attractiveness vector (the transmission direction).

Ordinary *communication cycles* are subdivided into 1000 *data packet cycles*. The $1000 - |D|$ first packets are used to eventually send data packets in the main direction $\vec{d}(o)$ of the node. During the last $|D|$ data packet cycles, the node sends $|D|$ control packets each one in a different direction $d \in D$. Therefore, during the *listening cycle*, the node is ensured to detect all the *control packets* of its available neighbors in all directions.

Every 100ms, an ordinary node o updates its attractiveness vector using the received *control packets* during the *listening cycle* (0.1ms). Let $V(o)$ the set of neighboring nodes of o . We notice $pow(v, o)$ the power of the received signal from the node v at the node o . If o receives different *control packets* from the same neighbor v with different antenna directions, the strongest signal is then selected.

The attractiveness vector of the node o is then updated according to the expression 7.1. An illustration of the attractiveness vector calculation is also given in figure 7.5.

$$\vec{d}(o) = \left\{ \vec{d}^*; \forall \vec{d} : P(o, \vec{d}^*) \geq P(o, \vec{d}) \right\} \quad (7.1)$$

with :

$$P(o, \vec{d}) = \sum_{v \in V(o)} pow(v, o) \times \max\left(0, \cos\left(\vec{d}, \vec{d}(v)\right)\right) \times E(v)$$

Sink nodes, $s \in S$, present a specific case where the sent attractiveness vector $\vec{d}(s) = (\infty, \infty, \infty)$.

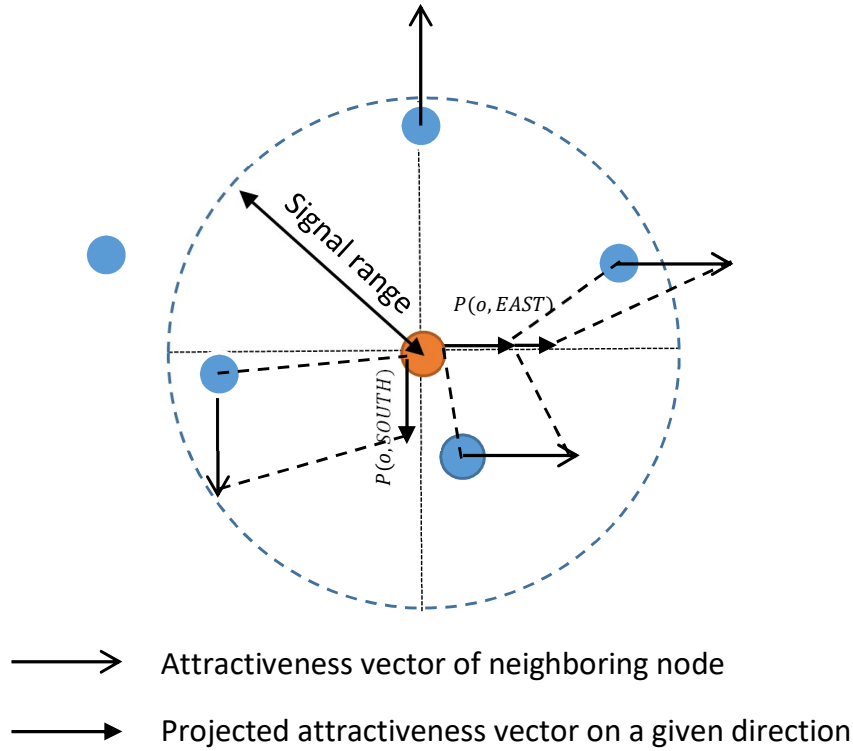


Figure 7.5: The computing of the attractiveness vector of the reference node in the center. For simplification, only cardinal directions are considered. The computation of $P(o, EAST)$ and $P(o, SOUTH)$ are given. $P(o, WEST)$ and $P(o, NORTH)$ are equal to zero. The East direction (the best direction) is selected as the attractiveness vector. The node located in the extreme West is ignored since it is out of coverage of the reference node.

When an ordinary node o receives one or several control packets with attractiveness vector (∞, ∞, ∞) , it sets its own attractiveness vector in the direction of the sink node (current direction d) and ignores the equation [7.1](#). The functioning scheme of the protocol is summarized in figure [7.6](#).

M2MRPv2 shares the same global scheme as M2MRP. The computation of the attractiveness vector represents the key characteristic of the algorithm. In the precedent version (M2MRP), the attractiveness vector is computed using the equation [7.2](#):

$$\begin{aligned} \vec{d}(o) &= \left\{ \vec{d}^*; \forall \vec{d} : P(o, \vec{d}^*) \geq P(o, \vec{d}) \right\} \\ \text{with :} & \\ P(o, \vec{d}) &= \sum_{v \in V(o)} pow(v, o) \times \cos(\vec{d}, \vec{d}(v)) \end{aligned} \quad (7.2)$$

The main difference between equations [7.1](#) and [7.2](#) consists in the computation of the weight of each direction $P(o, \vec{d})$ in order to determine the best one. In the new version (equation [7.1](#)), the neighbors with a negative contribution regarding the direction \vec{d} are ignored in the computation of $P(o, \vec{d})$. To illustrate the impact of this change on the behavior of the method, let us take the example illustrated in figure [7.7](#).

The reference node o , in the center, computes the $P(o, \vec{d})$ for each possible direction. We

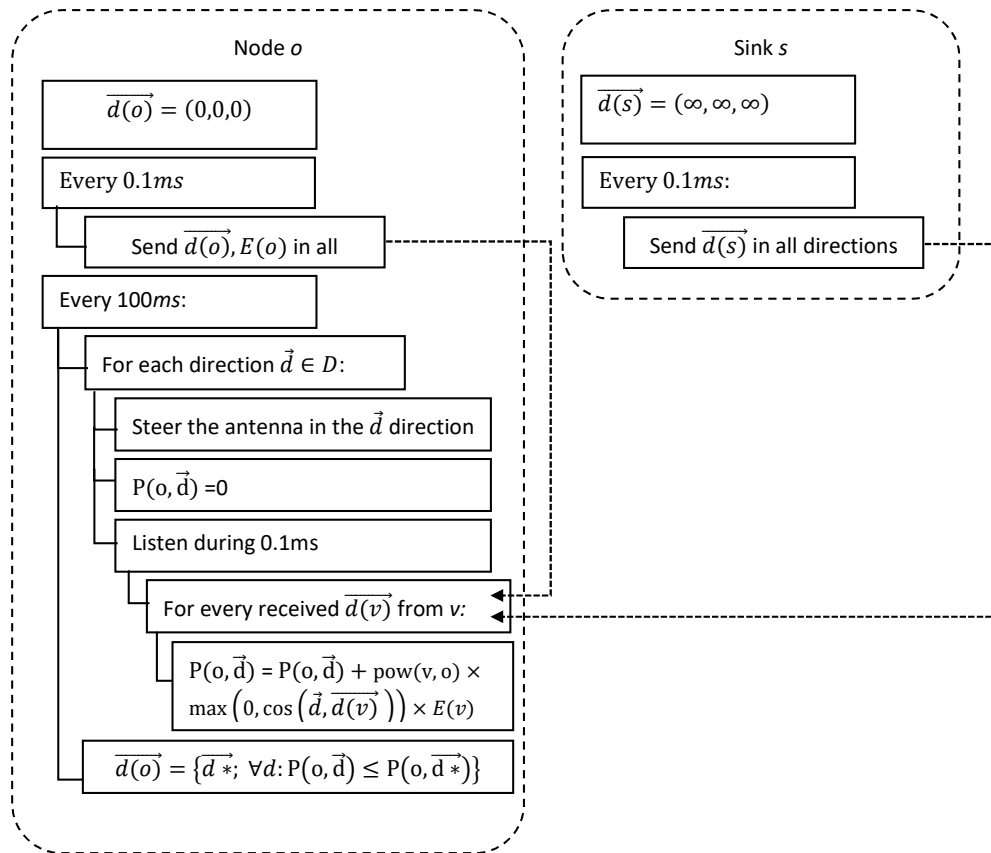


Figure 7.6: Block Scheme of the multirelay to multirelay routing protocol including an ordinary nanonode o and a sink node s .

assume, for the explanation, that the set of possible directions is $D = \{N, S, E, W\}$ corresponding to the four cardinal directions. The node o is surrounded by a set of 13 nodes, 6 on the East side, 6 on the West side and one node on the North side. The nodes on the East and West sides present a perfect symmetry and attractiveness vectors received by o from the 12 nodes offset one another. Using the equation 7.2 of the precedent algorithm version M2MRP, the attractiveness of the East direction, $P(o, EAST)$, and the West direction, $P(o, WEST)$ are null. Therefore, the North direction will be selected even if there is only one node on the North side, which is far from o . In contrast, with equation 7.1 the computation of $P(o, EAST)$ ignores the nodes on the West side of o and vice versa for $P(o, WEST)$. Consequently, in M2MRPv2, either the West or the East direction would be selected, which increases the method's robustness.

7.5/ Comparison of routing protocols

In this section, we analyze a set of major routing methods used in the literature. For this purpose, many criteria are considered:

- The space complexity of the protocol corresponds to the amount of stored data necessary for the protocol operation.
- The routing efficiency corresponds to the time needed for transmitting the data from the source node to one of the sink nodes. This criterion allows to appreciate the quality of

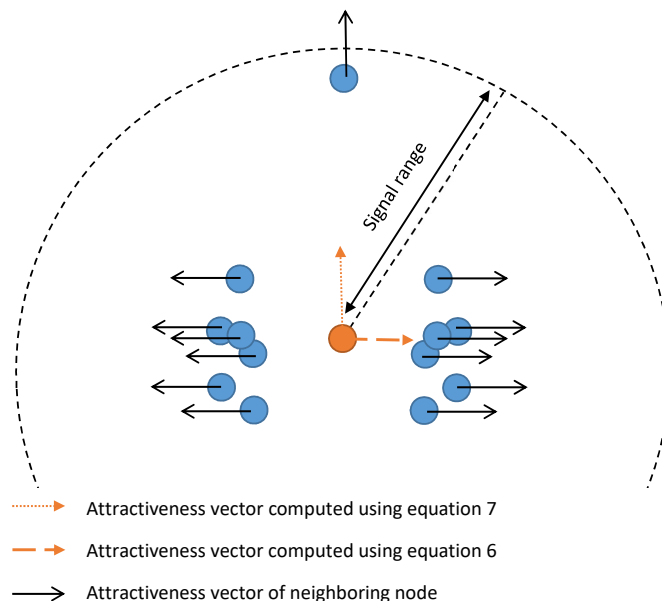


Figure 7.7: Comparison between the computation of the attractiveness vector in M2MRP and M2MRPv2 methods. Reference node is in the center.

the routing path.

- The communication complexity corresponds to the number of sent messages required to broadcast one message from a source node. This number gives an idea of the global amount of energy consumed.
- Number of received messages that correspond to the number of received messages by all nodes but not necessarily resent. The number of received messages impacts on the amount of generated interference.
- Number of control messages corresponds to the number of exchanged messages before selecting the routing path.
- The need for checking the source and the final destination nodes of the received messages allows to appreciate the additional delay and energy consumption required by the protocol.

Table 7.1 gives a comparison of the 8 discussed methods according to the 7 criteria listed above, where $|V|$ is the average number of neighbors, S is the set of sinks, $|E|$ is the number of pairs of neighbor nodes, and $|D|$ represents the number of steering directions of the antenna.

We observe that M2MRPv2 method is the only protocol that does not need control messages, nor checking the source or the destination of the packets, which reduces the routing latency. We also observe that only M2MRPv2 selects the routing path on the basis of the density of the crossed areas, which contributes to the reliability of the protocol.

The complexity of AODV and LaGOON presents a lot of similarities. Though contrary to AODV, LaGOON protocol eliminates the need for control messages. If the route is unknown,

Method	O(mem)	O(t)	#sent mess	#rcv mess	#ctrl mess	check src	check dst
AODV	$ S $	shortest	r	r	upto E		x
OLSR	$ V ^2$	> shortest	$< D \times N$	$< V \times N$	0	x	x
Flooding	1	shortest	$ D \times (N - S)$	$ V \times N$	0	x	
Pierobon	1	lowest energy	$< r$	$< r$	$< 2 \times r$	x	x
EECR	1	lowest energy	$< r$	$< r$	$< 2 \times r$	x	x
LaGOON	$< S \times V $	shortest	$[r.. D] \times (N- S)$	$[r.. V] \times N$	0	x	x
SLR	1	direct	$Z \times r$	$Z \times 4 \times r$	0	x	x
M2MRPv2	1	denser	$\ll N$	$\ll V \times N$	0		

Table 7.1: Complexity comparison between routing techniques for ad hoc networks and nanonetworks.

the message is diffused to all direct neighbors using omnidirectional or directional signals. Suppose the node's antenna is omnidirectional, then $|D| = 1$. LaGOON presents higher memory complexity than AODV since a set of next-hop nodes are stored for each sink. In ultra-dense nanonetwork, the set of stored next hops is more probably equal to neighbors' set. Pierobon and EECR protocols present good memory complexity since they are proposed for nanonetworks. However, these two approaches compute the transmission path in real-time, which leads to additional control traffic and more latency.

Concerning the multirelay to multirelay approaches, even if the flooding approach ensures the fastest transmission of data, but it leads to a high amount of exchanged messages and consequently, a high level of energy consumption and interference. M2MRPv2 and SLR generate less exchanged messages than the flooding method, but the efficiency of SLR method depends on the average density of a zone Z . Dense zones can lead to a high level of exchanged messages, while blank zones can lead to communication failures.

In table 7.2, we compare the different features of routing protocols proposed for nanonetworks. Among all the algorithms, we observe that only our protocol M2MRPv2 allies the use of the multirelay to multirelay mode with the optimization of the residual energy level of nanonodes. Both features contribute to the improvement of communication reliability.

Method	mode	Energy saving	Reliability	constraints
Pierobon	reactive	total consumed energy	point to point relay	- homogene topology - direct link between nanonodes and sinks
EECR	reactive energy	total consumed	point to point relay	clusters computation
LaGooN	reactive	-	point to point relay	symmetric links
Flooding	reactive	-	multirelay to multirelay	-
SLR	reactive	-	multirelay to multirelay	convex topology
M2MRPv2	proactive	residual energy	multirelay to multirelay	-

Table 7.2: Comparison between nanonetworks routing protocols.

7.6/ Experimental tests

In this section, we focus only on the studied multirelay protocols, since Point-to-Point protocols are ineffective for unstable networks. The OSLR protocol is ignored because it is very demanding for memory space ($O(|V|^2)$). Three routing protocols are then compared, corresponding to the naive broadcasting approach, SLR protocol, and M2MRPv2 protocol. The three approaches are compared on two network scenarios representing square and tie bow topologies with 100, 300, 500, 700, and 1000 nanonodes, among which three sink nodes (see figure 7.8). The nodes are deployed over an area of $100\text{cm} \times 100\text{cm}$ and the radio signal range is 20cm , which guarantees the high density of the network. For each network scenario, we tested two traffic profiles representing both independent events and location-based events.

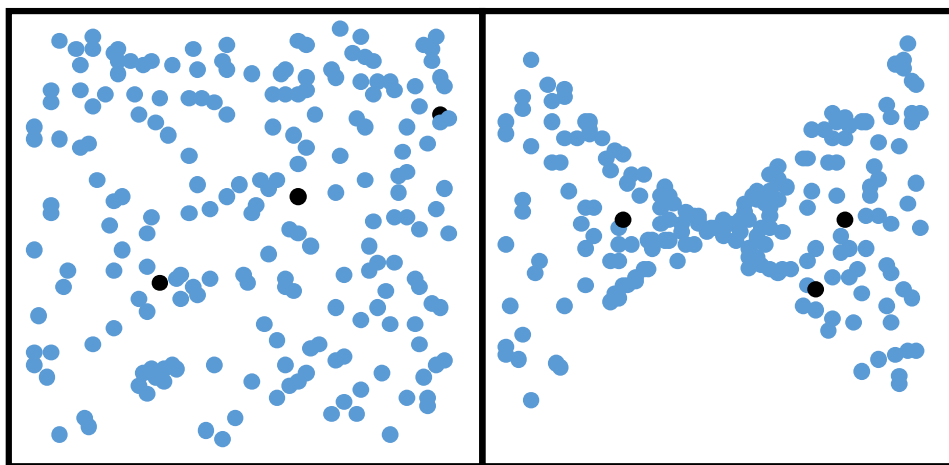


Figure 7.8: Two classes of nanonetwork topologies: square and tie bow. Black nodes represent sink nodes.

Finally, we tested several traffic load levels to analyze the performances' evolution when traffic increases. The traffic load, Lo , designates the average number of packets generated per node per communication cycle of 0.1ms . We tested 5 different values of the traffic load 0.1, 0.2, 0.3, 0.4 and 0.5. In independent events scenarios, the number of packets generated by a given node during a given communication cycle is computed using the formula: $-\log(\text{rnd}) * Lo$ where $\text{rnd}()$ is the function that returns a random value in $[0..1]$. In location-based events scenarios, at each communication cycle, a sequence of several random positions are selected. For each random event location, the nanonodes that are less than 5cm from it, generate each a packet. The selection of event location process is stopped once the average number of packets per communication cycle is reached. One packet contains 1000 bits, and once a packet is generated, the packet routing is simulated within the same cycle.

We note that collisions between received packets are not simulated in this work. The parameter settings used in the simulations are summarized in table 7.3.

The simulated traffic (chronology and source of packets) is the same in all scenarios with the same topology, the same traffic profile, and load. This way, we guarantee that protocols are tested under the same conditions. The scenarios use 3 sink nodes corresponding to the 10th, 20th, and 30th nodes.

Parameter	Value
Maximal stored energy: E_{max}^{bt}	$100\mu J$
Energy consumption for one packet transmission: E_f^{tx}	$0.05\mu J$
Energy consumption for one packet reception: E_f^{rx}	$0.005\mu J$
Energy harvesting rate per 0.1 sec: $\delta(0.1sec)$	$0.05\mu J$
Energy consumption by nanonode activities or inactivity: $E^{ac} + E^{sl}$	$0J/s$
Communication cycle duration	$0.1ms$
Routing cycle duration (frequency of attractiveness vector computing)	$100ms$
Packet size	1000 bits
Number of simulated routing cycles	1000 (100s)
Radio range	20cm
Network size	$100cm \times 100cm$
Number of sink nodes	3

Table 7.3: Simulation parameters

7.6.1/ Performance comparison

The performance of each approach is assessed according to the number of sent messages (both generated and forwarded packets) and according to the success rate. The success rate measures the percentage of generated messages (from the source) that reached at least one of the sink nodes.

In figure 7.9, we present the obtained results. The left column compares the three approaches according to their success rate. First, we observe that M2MRPv2 protocol outperforms the two other approaches in all cases, especially when the generated traffic by nanonode is low. This is explained by the fact that the M2MRPv2 protocol succeeds in sharing the relaying effort on all nodes. However, when the generated traffic per node exceeds the harvesting rate, data transmission towards the sink nodes fails from the start. In this case, the routing strategies cannot provide a solution.

SLR performs slightly better than the naive broadcast method. However, the number of needed messages is significantly reduced by SLR method. We observe that for tie bow topology, the broadcast approach presents a better success rate when the energetic constraints are weak (low traffic). Indeed, SLR uses the direct line between the source and sink nodes, making it less reliable than the broadcast method when the energy limitation is not a problem. Simultaneously, when the traffic load increases, SLR reduces the number of sent messages and therefore manages better the energy limitations of nanonodes, leading to better reliability.

In applications with position-based events, the efficiency of all protocols decreases. The traffic is less well distributed over the network nanonodes and generates a temporal peak of traffic on localized parts of the nanonetwork. However, the M2MRPv2 protocol is much better than SLR and broadcast approaches.

The number of sent messages shown in figure 7.9 is higher in M2MRPv2 protocol for overloaded networks. That does not mean that M2MRP generates more redundancy, just that the energy is better managed, leading to better traffic spreading and, therefore, to more successful transmissions (i.e., more packet forwarding). Whereas in Broadcast and respectively in SLR, all or respectively some nodes are overused and can no longer relay the data.

In other words, even if the multi-received packets are relayed just one time, the multi-reception

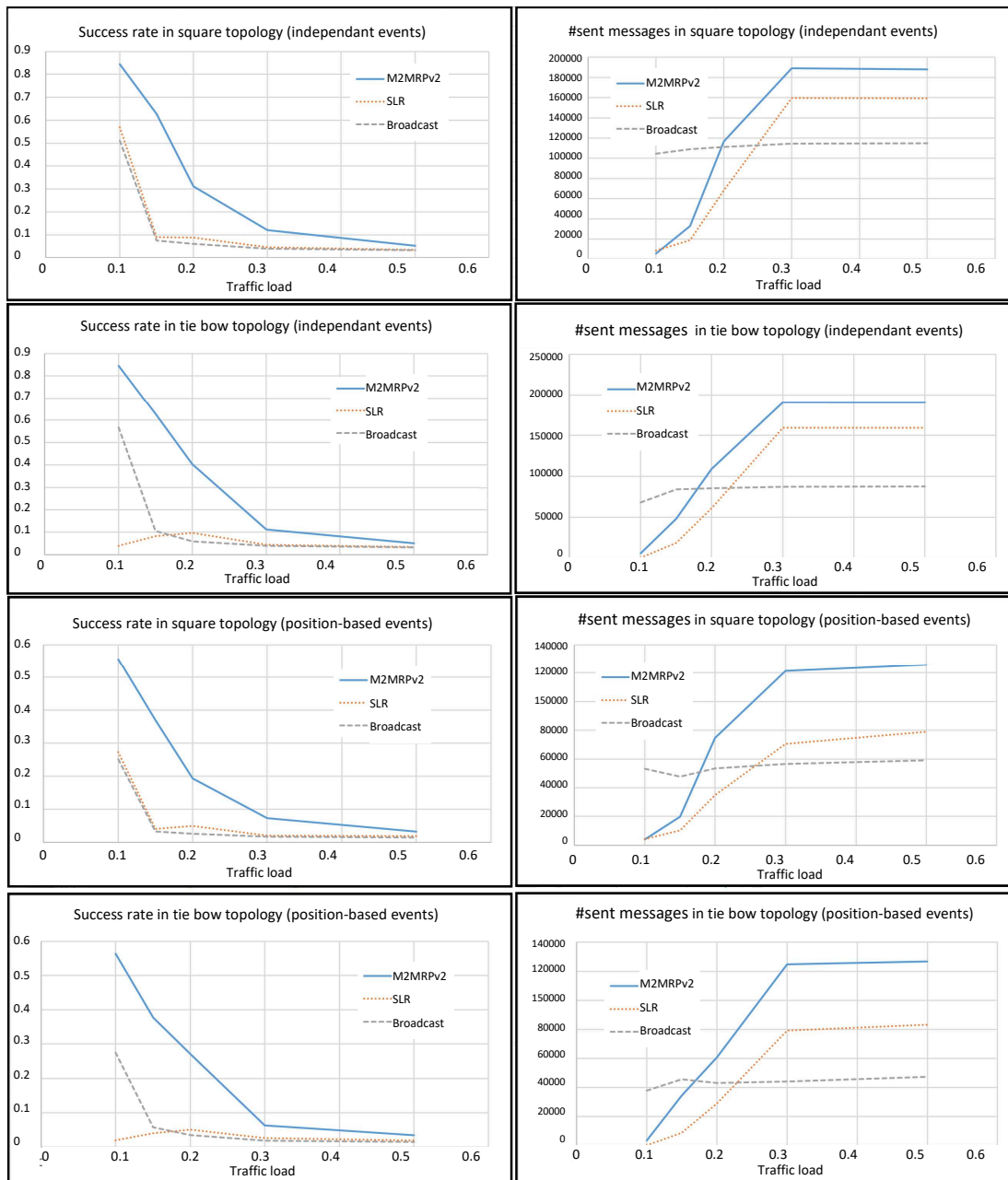


Figure 7.9: Comparison of broadcast, SLR, and M2MRPv2 routing protocols over two network topologies and under two traffic profiles. A comparison is given according to the success rate and the number of sent messages. The traffic load measures the average number of new packets generated each 0.1ms.

of the same data impacts the state of charge of the nodes causing their temporal unavailability and then transmission failure. Consequently, under moderate traffic (0.1 packet per node per 0.1ms), the exchanged traffic remains high in the broadcast approach due to the network density and the number of re-transmissions and receptions of the packet.

In the broadcast method, the received packets are relayed by all nodes, and nodes exhaust rapidly their battery leading to temporary unavailability. Broadcast method hits rapidly saturation, which results in the observed stagnation of the number of sent messages when the

traffic load increases. SLR and M2MRPv2 approaches provide more sent packets. Indeed, SLR and M2MRP provide a better success rate, which means that packets are relayed farther than in broadcast in order to reach the sink nodes. The difference between the sent messages and received messages is given in figure 7.10.

Figure 7.10 displays the percentage of relayed packets among the received ones, as well as the number of receptions over all nodes for each method. The relaying rate is a good indicator of the efficiency of the routing policy. A low value means that the protocol leads to a high level of redundancy with a lot of received packets that have already been received or that should be ignored (For example, in SLR, according to the source and the destination nodes). We observe then that M2MRPv2 leads to extremely higher efficiency compared to SLR and broadcast methods with 51% of received messages that are retransmitted with 200 nodes and 75% with 100 nodes. This can be explained by the use of beam steering devices in M2MRPv2 protocol, which improves the targeting of the next-hop nodes.

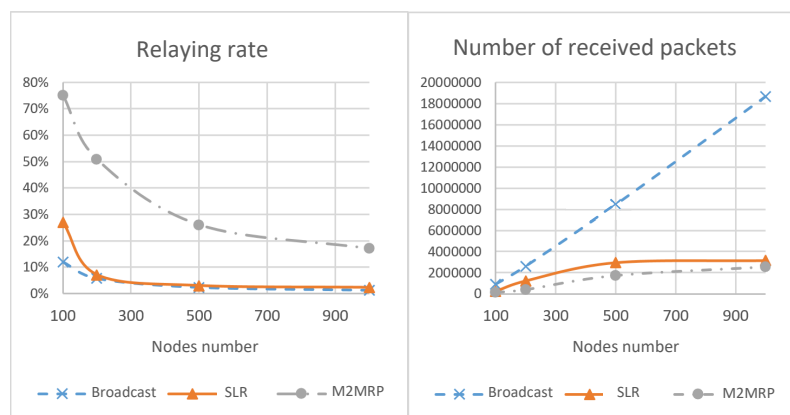


Figure 7.10: Comparison between Broadcast, SLR, and M2MRP protocols according to the number of received messages and relaying rate. Test parameters are the same as above and traffic load is of 0.2 packets per communication cycle per node.

Furthermore, the number of received messages in M2MRPv2 is significantly lower than in SLR and Broadcast protocols. We conclude that the performances of M2MRPv2 could be even better than those presented in figure 7.9 if the ratio between energy consumption for reception and emission is higher (10% in the test).

7.6.2/ Energy management

Figure 7.11 shows the energy level of the network nanonodes starting with fully charged batteries after 4 routing cycles. We observe that the charge of batteries falls below 10% for all nodes with the broadcast method. Indeed, major nodes are used to relay every message. Whereas, SLR and M2MRPv2 protocols succeed in reducing energy consumption, which results in less discharged nanonodes with less than 70% of the full charge. However, we observe that M2MRPv2 protocol reduces the number of critical nanonodes presenting less than 10% of the charge, which underlines the quality of energy control in M2MRPv2 method.

Figure 7.12 shows the energy level cartography over the scenarios of figure 7.12 after 100 routing cycles. As shown in tests of the figure 7.9, M2MRPv2 succeeds to route 4 more times packets than SLR and Broadcast methods, which means more exchanged messages. Despite this, the energy level of nanonodes in M2MRPv2 is relatively identical to SLR approach and

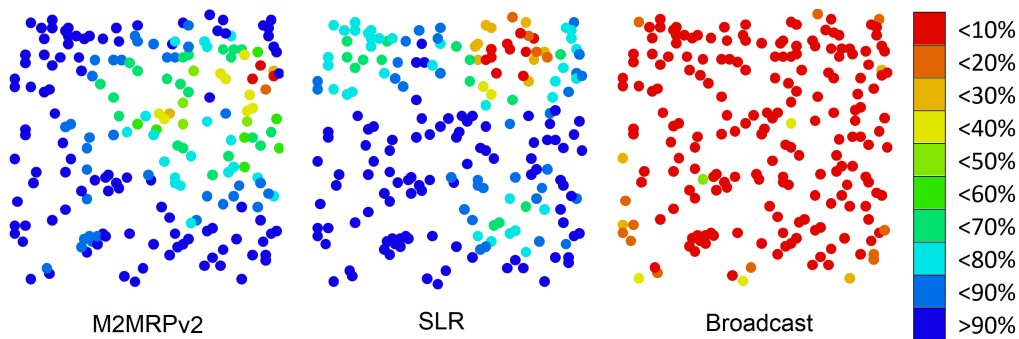


Figure 7.11: Batteries level after 4 routing cycles with three routing protocols: Broadcast, SLR, and M2MRPv2 protocols. Tests are made over a square topology nanonetwork with 200 nodes and an average traffic load of 0.2 packets per data cycle.

much better than the broadcast method. Indeed, M2MRPv2 adapts the data flow circulation to the state of charge of the nanonodes in each area, which allows overloaded nodes to recharge their batteries.

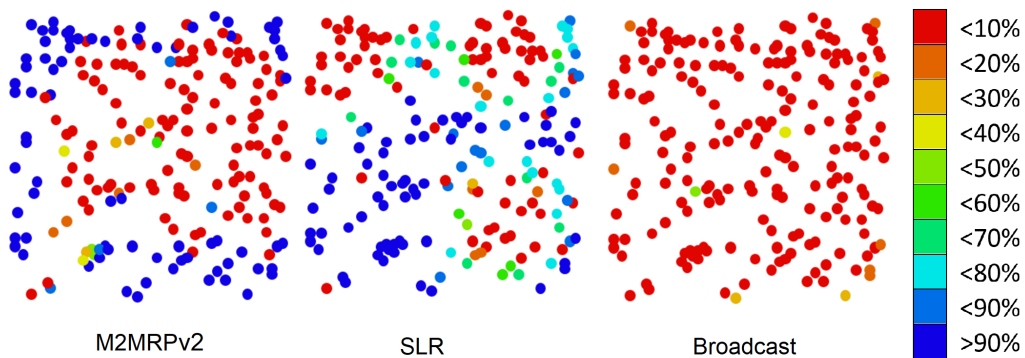


Figure 7.12: Batteries level after 100 routing cycles with three routing protocols: Broadcast, SLR, and M2MRPv2 protocols. Tests are made over a square topology nanonetwork with 200 nodes and an average traffic load of 0.2 packets per data cycle.

7.7/ Conclusion

The routing in ultra-dense unstable nanonetwork is a novel problem. The classical approaches based on point-to-point relaying schemes are not relevant due to the nanonodes' uncertainty. On the other hand, the high density of the network and the nanonode constraints make some multirelay-to-multirelay approaches, such as OLSR, unusable.

In this chapter, we presented a new and efficient Multipoint-to-Multipoint Routing Protocol (M2MRP) for ultra-dense volatile nanonetworks. This protocol provides a powerful and scalable distributed procedure to dynamically and continuously compute each node's best transmission and reception directions.

M2MRP protocol presents a natural way to express how the energy availability, congestion, radio quality, and communication reliability should be taken into account for determining data routing paths over the network.

We compared two well-known multirelay-to-multirelay routing protocols with our new approach called M2MRPv2. The comparisons are made over scenarios representing different topological and traffic profiles. From these results, we deduce that M2MRPv2 protocol significantly improves the reliability of the system under energy-limited nanonodes.

The work addresses, more particularly, the Terahertz nanonetwork. But the M2MRPv2 protocol is clearly well adapted to any ultra-dense networks, including dense sensor nanonetwork, IoT networks, and D2D 5G networks.

The optimization of the discharging/recharging cycles represents one of the important issues to address. Depending on the batteries' characteristics, it could be preferable to completely discharge the battery before recharging it or, inversely, prevent the battery from being significantly discharged. Indeed, the way the battery is used impacts the service life duration of the batteries (number of discharging/recharging cycles).



General conclusion

General conclusion

This thesis work focuses on nanocommunication protocols for dense wireless nanonetworks under hardware capacity restrictions of nanodevices and severe constraints imposed by the communication medium exposed to electromagnetic signals radiated in Terahertz band frequency. These nanonetworks are composed of nanodevices such as nanosensors, nanorobots, etc., supposed to be able performing detection, recognition and actuations on predefined sub-millimeter size entities.

The proposed networking protocols address different layers of the protocol stack in particular: the network layer and its end-to-end routing mechanisms, the MAC sub-layer with different techniques for managing communication channels and transmission media, and the physical layer responsible of adapting transmissions to the communication medium via the modulation of the Terahertz radio signals and the management of throughput, errors and physical resources. All of these layers, working in close collaboration, help make Terahertz frequencies band a perfect environment for nanocommunication issues. The objective is to optimize a certain number of performance metrics leading the protocol to meet the operational conditions of the targeted application.

Satisfying all performance metrics with a single protocol is certainly a desirable goal. However, the complexity of achieving the objectives of such a protocol is going to generate an unacceptable cost that could put the mission of the nanonetwork in difficulty. This is why, in the current state of immaturity of nanotechnology, simplicity would seem to be a factor encouraging success and progress.

Indeed, the objective of simultaneously achieving several performance metrics in the same protocol must be carefully considered, because in addition to the complexity involved, some contradictory metrics may weaken the effect of the expected overall objective. As WNNs are application-dependent, the priority is given to a specific performance metric or just a few, at the expense of others, according to the nature of the application.

8.1/ Contributions

Our contribution throughout this thesis work consists of several proposals for Terahertz nanocommunication technology for dense wireless nanonetwork applications. These proposals address various problems raised in the different networking layers and attempt to provide adapted solutions to improve different performance metrics, as summarized below:

1. In dense nanonetworks, the need for an appropriate channel sharing scheme raises a

serious challenge for efficient concurrent channel access. For this, our proposal named Slot Division Multiple Access Time Spread On Of Keying (SDMA-TSOOK) improves the trade-off between the channel access balancing, the success rate, and the collision rate, regarding the other published methods.

First, we provided a review of channel access approaches based on femtosecond-long pulse modulation, particularly TS-OOK, RD-TSOOK, and SRH-TSOOK approaches. This study investigated the drawbacks of these approaches. Then we proposed SDMA-TSOOK to overcome these weaknesses. SDMA-TSOOK is inspired by Time Division Multiple Access technique (TDMA) and frequency hopping techniques. The transmitter and receiver agree on a sequence of time slot indexes corresponding to the times of pulse or silence transmission. This mechanism leads to highly mitigating the collisions and therefore the reduction of co-channel and selective interference, while guaranteeing the channel access fairness.

We evaluated the performance of SDMA-TSOOK, compared to the published approaches, in terms of channel access balancing, collision, and success rate. As a result, our proposal protocol ensured fairness between nanodevices and significantly reduced collisions while keeping the success rate. Finally, through the simulation, we succeed to determine the optimal slots interval that improves the SDMA-TSOOK performance.

2. In the second proposition, we have suggested a novel distributed protocol for optimizing the physical topology of none-uniform, unstable, ultra-dense Terahertz nanonetworks. The objective of this optimization is to reduce the amount of interference due to the concentration of numerous nodes transmitting in all directions at random instants. The logical topology we proposed fixes, for each node, the moments during which it can send data in a given direction to given selected destination nodes. Each node ignores messages sent by nodes that do not belong to the predefined subset of neighbors, which reduces the energy consumption.

Furthermore, the reduction of direct communication links between nodes does not impact data broadcasting coverage. Simulation showed that the diminution of the broadcasting speed is limited compared to the gain in terms of transmission redundancy and generated interferences.

Finally, the traffic control protocol exploits the Terahertz frequencies division into short, mid and long range adapted frequency window. The successors of a given node in a specific direction are in the same range of distance from the transmitter. Therefore, all the nodes covered in the same direction are served by the same frequency sub-band. The distance between nodes and their successors varies according to the transmission direction leading to a better use of the Terahertz band.

3. The third proposal attempts to establish efficient coordination of communications in uniform and under controlled WNN with very high nodes density in order to significantly reduce the collisions and energy consumption. To this end, we assume that nanonodes are equipped with directional antennas allowing steering signals for accurate nodes discovery. The nanonetwork is then organized into clusters leading to hierarchical bi-level communication architecture. The first level concerns communications inside clusters with the use of TDMA approach, while the second level is dedicated to inter cluster communications using a forwarding dominate nodes procedure and a distributed TDMA scheme. This multilevel approach allows regulating the high number of data, generated by the nanonetwork nodes, by scheduling the transmissions and optimizing the data routing.

The proposed approach takes into account the particularities of the Terahertz band. Every cluster head corresponds to a given frequency windows adapted to the distance between the cluster head and the member nodes. This way, the undesirable inter-cluster interference is also reduced.

4. The fourth proposition aims to provide a communication environment adapted to highly concurrent low data-rate applications where the elimination of collision risk is of crucial importance. To this end, we proposed a hierarchical access link protocol for WNN, with a high reliability, short latency, and low control traffic. In this case, the network area is subdivided into relatively equal areas (clusters). The intra-cluster and inter-cluster communications are scheduled in such manner to prevent collisions. Based on simulation results, this proposal ensures the nanonetwork connectivity, a low control packets exchange, and a good delivery success rate. Furthermore, this proposed scheme exhibited more efficiency in dense nanonetwork.
5. In the last proposal, a new and efficient Multipoint-to-Multipoint Routing Protocol (M2MRP) for ultra-dense volatile nanonetworks is proposed. This protocol provides a powerful and scalable distributed procedure to dynamically and continuously compute the best transmission and reception directions of each node. As a result, M2MRP protocol carries out a natural way to express how the energy availability, congestion, radio quality and communication reliability are taken into account for determining data routing paths over the network.

We compared two well-known multirelay-to-multirelay routing protocols with our new approach. The comparisons are made over scenarios representing different topological and traffic profiles. From these results, we deduced that M2MRPv2 protocol improved significantly the reliability of the system under energy-limited nanonodes.

The work addresses more particularly the Terahertz nanonetwork, but M2MRP protocol is clearly well adapted to any ultra-dense networks including dense sensor nanonetwork, IoT networks, and D2D 5G networks.

8.2/ Future works

Terahertz nanonetworks represent a new research field that remains unexplored. Some problems remain posed and others have been given special attention leading to acceptable solutions that need to be constantly improved. In this context, we need to improve the proposed mechanisms inspired by the following potential research issues:

- **Nanomachine Mobility** Among the plethora of articles proposed for THz nanocommunications, very few addressed the issue of nanomachine mobility. However, the application fields requiring this mobility are important and numerous, in particular within fluid and air environment. Particularly the case for the important medical field (Mobility in body fluids) and the environmental field (Mobility in air, water, etc.). Thus, the subject of mobility needs to be integrated in the THz nanocommunication to be supported in the protocols while evaluating its influence on performance metrics such as: energy harvesting and consumption, transmission coverage, obstacles to transmission.
- **Nanomachine Dependability (Security, Robustness)** The security issue is almost nonexistent in Thz nanocommunication, probably, because the quality of service will be

taken into account when the operational aspects of nanomachines should be well delimited. Many application areas of nanonetworks are quite critical and, therefore, any unforeseen changes in the functionality of nanomachines could have enormous consequences. It is therefore necessary to further explore the safety issues related to nanocommunications, with the aim of proposing safety aspect in Thz protocol with care of fundamental functionalities. This is also the case for robustness, which has so far received little attention. Then, how can we ensure that the information transmitted by nanomachines reaches its destination completely and correctly?

- **Verification and Theoretical analysis** For the time being, most of the work relating to nanonetworks remains in the theoretical field. As well, most nanocommunication protocols reinforce their algorithms or processes with analytical studies or simulations. Formal verification of their fundamental properties remains nonexistent. As a result, the theoretical analysis of nanocommunication protocols and their formal verification are lacking. Therefore, it would be very useful to have theoretically proven and guaranteed properties of algorithms and processes in nanonetworks.

Bibliography

- [1] Aulin, T., Rydbeck, N., and Sundberg, C.-E. **Continuous phase modulation-part ii: Partial response signaling**. *IEEE Transactions on Communications* 29, 3 (1981), 210–225.
- [2] Bjorklund, G. C., Levenson, M., Lenth, W., and Ortiz, C. **Frequency modulation (fm) spectroscopy**. *Applied Physics B* 32, 3 (1983), 145–152.
- [3] Laurent, P. **Exact and approximate construction of digital phase modulations by superposition of amplitude modulated pulses (amp)**. *IEEE transactions on communications* 34, 2 (1986), 150–160.
- [4] Garcia-Lunes-Aceves, J. J. **Loop-free routing using diffusing computations**. *IEEE/ACM transactions on networking* 1, 1 (1993), 130–141.
- [5] Basagni, S. I. C. V. R. S. B. A. **A distance routing effect algorithm for mobility (dream)**. In *International Conference on Mobile Computing and Networking Proceedings of the 4th annual ACM/IEEE international conference on Mobile computing and networking* (1998), New York: ACM Press, p. 76–84.
- [6] Chiao, J.-C., Fu, Y., Chio, I. M., DeLisio, M., and Lin, L.-Y. **Mems reconfigurable vee antenna**. In *1999 IEEE MTT-S International Microwave Symposium Digest (Cat. No. 99CH36282)* (1999), vol. 4, IEEE, pp. 1515–1518.
- [7] Perkins, C. E., and Royer, E. M. **Ad-hoc on-demand distance vector routing**. In *Proceedings WMCSA'99. Second IEEE Workshop on Mobile Computing Systems and Applications* (1999), IEEE, pp. 90–100.
- [8] Kondylis, G. D., Krishnamurthy, S. V., Dao, S. K., and Pottie, G. J. **Multicasting sustained cbr and vbr traffic in wireless ad-hoc networks**. In *2000 IEEE International Conference on Communications. ICC 2000. Global Convergence Through Communications. Conference Record* (2000), vol. 1, IEEE, pp. 543–549.
- [9] Ramachandran, L., Kapoor, M., Sarkar, A., and Aggarwal, A. **Clustering algorithms for wireless ad hoc networks**. In *Proceedings of the 4th international workshop on Discrete algorithms and methods for mobile computing and communications* (2000), pp. 54–63.
- [10] Johnson, D. B., Maltz, D. A., Broch, J., and others. **Dsr: The dynamic source routing protocol for multi-hop wireless ad hoc networks**. In *Ad hoc networking* (2001), vol. 5, Addison Wesley, pp. 139–172.
- [11] Judy, J. W. **Microelectromechanical systems (mems): fabrication, design and applications**. *Smart materials and Structures* 10, 6 (2001), 1115.

- [12] Bettstetter, C. **On the minimum node degree and connectivity of a wireless multihop network.** In *Proceedings of the 3rd ACM international symposium on Mobile ad hoc networking & computing* (2002), pp. 80–91.
- [13] Radhakrishnan, S., Racherla, G., Sekharan, C. N., Rao, N. S., and Batsell, S. G. **Protocol for dynamic ad-hoc networks using distributed spanning trees.** *Wireless Networks* 9, 6 (2003), 673–686.
- [14] Chen, C.-J., Haik, Y., and Chatterjee, J. **Development of nanotechnology for biomedical applications.** In *Conference, Emerging Information Technology 2005*. (2005), IEEE, pp. 4–pp.
- [15] Freitas, R. A. **Nanotechnology, nanomedicine and nanosurgery.** *International Journal of Surgery* 4, 3 (2005), 243–246.
- [16] Freitasjr, R. **What is nanomedicine? nanomedicine: nanotechnology.** *Biol. Med* 1 (2005), 2.
- [17] Plesse, T., Adjih, C., Minet, P., Laouiti, A., Plakoo, A., Badel, M., Muhlethaler, P., Jacquet, P., and Lecomte, J. **Olsr performance measurement in a military mobile ad hoc network.** *Ad Hoc Networks* 3, 5 (2005), 575–588.
- [18] Tessier, D., Radu, I., and Filteau, M. **Antimicrobial fabrics coated with nano-sized silver salt crystals.** In *NSTI Nanotech* (2005), vol. 1, pp. 762–764.
- [19] Babakhani, A., Guan, X., Komijani, A., Natarajan, A., and Hajimiri, A. **A 77-ghz phased-array transceiver with on-chip antennas in silicon: Receiver and antennas.** *IEEE Journal of Solid-State Circuits* 41, 12 (2006), 2795–2806.
- [20] Freitas, R. A. **Pharmacytes: An ideal vehicle for targeted drug delivery.** *Journal of Nanoscience and Nanotechnology* 6, 9-10 (2006), 2769–2775.
- [21] Han, B., and Jia, W. **Clustering wireless ad hoc networks with weakly connected dominating set.** *Journal of Parallel and Distributed Computing* 67, 6 (2007), 727–737.
- [22] Rodolakis, G., Adjih, C., Laouiti, A., and Boudjit, S. **Quality-of-service multicast overlay spanning tree algorithms for wireless ad hoc networks.** In *Asian Internet Engineering Conference* (2007), Springer, pp. 226–241.
- [23] Rodolakis, G., Naimi, A. M., and Laouiti, A. **Multicast overlay spanning tree protocol for ad hoc networks.** In *International Conference on Wired/Wireless Internet Communications* (2007), Springer, pp. 290–301.
- [24] Akyildiz, I. F., Brunetti, F., and Blázquez, C. **Nanonetworks: A new communication paradigm.** *Computer Networks* 52, 12 (2008), 2260–2279.
- [25] Wang, Z. L. **Towards self-powered nanosystems: from nanogenerators to nanopiezotronics.** *Advanced Functional Materials* 18, 22 (2008), 3553–3567.
- [26] Beeby, S. P., and O'Donnell, T. **Electromagnetic energy harvesting.** In *Energy Harvesting Technologies*. Springer, 2009, pp. 129–161.
- [27] Demirkol, I., Ersoy, C., and Onur, E. **Wake-up receivers for wireless sensor networks: benefits and challenges.** *IEEE wireless Communications* 16, 4 (2009), 88–96.

- [28] Akyildiz, I. F., and Jornet, J. M. **Electromagnetic wireless nanosensor networks.** *Nano Communication Networks* 1, 1 (2010), 3–19.
- [29] Gupta, N., and Gupta, R. **Routing protocols in mobile ad-hoc networks: an overview.** In *INTERACT-2010* (2010), IEEE, pp. 173–177.
- [30] Islam, M. S., and Vj, L. **Nanoscale materials and devices for future communication networks.** *IEEE Communications Magazine* 48, 6 (2010), 112–120.
- [31] Jornet, J. M., and Akyildiz, I. F. **Graphene-based nano-antennas for electromagnetic nanocommunications in the terahertz band.** In *Antennas and Propagation (EuCAP), 2010 Proceedings of the Fourth European Conference on* (2010), IEEE, pp. 1–5.
- [32] Pierobon, M., and Akyildiz, I. F. **A physical end-to-end model for molecular communication in nanonetworks.** *IEEE Journal on Selected Areas in Communications* 28, 4 (2010), 602–611.
- [33] Xu, S., Qin, Y., Xu, C., Wei, Y., Yang, R., and Wang, Z. L. **Self-powered nanowire devices.** *Nature nanotechnology* 5, 5 (2010), 366–373.
- [34] Akyildiz, I. F., Jornet, J. M., and Pierobon, M. **Nanonetworks: A new frontier in communications.** *Communications of the ACM* 54, 11 (2011), 84–89.
- [35] Jornet, J. M., and Akyildiz, I. F. **Channel modeling and capacity analysis for electromagnetic wireless nanonetworks in the terahertz band.** *IEEE Transactions on Wireless Communications* 10, 10 (2011), 3211–3221.
- [36] Jornet, J. M., and Akyildiz, I. F. **Low-weight channel coding for interference mitigation in electromagnetic nanonetworks in the terahertz band.** In *2011 IEEE international conference on communications (ICC)* (2011), IEEE, pp. 1–6.
- [37] Narra, H., Cheng, Y., Cetinkaya, E. K., Rohrer, J. P., and Sterbenz, J. P. **Destination-sequenced distance vector (dsv) routing protocol implementation in ns-3.** In *Proceedings of the 4th International ICST Conference on Simulation Tools and Techniques* (2011), pp. 439–446.
- [38] Adinya, O. J., and Daoliang, L. **Transceiver energy consumption models for the design of low power wireless sensor networks.** In *2012 IEEE Student Conference on Research and Development (SCORED)* (2012), IEEE, pp. 193–197.
- [39] Atakan, B., Akan, O. B., and Balasubramaniam, S. **Body area nanonetworks with molecular communications in nanomedicine.** *IEEE Communications Magazine* 50, 1 (2012), 28–34.
- [40] Boisseau, S., Despesse, G., and Seddik, B. A. **Electrostatic conversion for vibration energy harvesting.** *Small-Scale Energy Harvesting* (2012), 1–39.
- [41] Guin, A. **Programmable matter-claytronics.** In *presented at the 58th international instrumentation symposium, San Diego, California* (2012), pp. 4–8.
- [42] Jornet, J. M., Pujol, J. C., and Pareta, J. S. **Phlame: A physical layer aware mac protocol for electromagnetic nanonetworks in the terahertz band.** *Nano Communication Networks* 3, 1 (2012), 74–81.

- [43] Kürner, T. **Towards future thz communications systems.** *Terahertz science and technology* 5, 1 (2012), 11–17.
- [44] Liu, X. **A survey on clustering routing protocols in wireless sensor networks.** *sensors* 12, 8 (2012), 11113–11153.
- [45] Nakano, T., Moore, M. J., Wei, F., Vasilakos, A. V., and Shuai, J. **Molecular communication and networking: Opportunities and challenges.** *IEEE transactions on nanobioscience* 11, 2 (2012), 135–148.
- [46] Senouci, M. R., Mellouk, A., Senouci, H., and Aissani, A. **Performance evaluation of network lifetime spatial-temporal distribution for wsn routing protocols.** *Journal of Network and Computer Applications* 35, 4 (2012), 1317–1328.
- [47] Srikanth, V., Chaluvadi, S., and others. **Energy efficient, scalable and reliable mac protocol for electromagnetic communication among nano devices.** *International Journal of Distributed and Parallel Systems* 3, 1 (2012), 249.
- [48] Upadhyay, V., and Agarwal, S. **Application of wireless nano sensor networks for wild lives.** *International Journal of Distributed and Parallel systems* 3, 4 (2012), 173.
- [49] Alabady, S. A., and Salleh, M. **Overview of wireless mesh networks.** *Journal of Communications* 8, 9 (2013), 134–144.
- [50] Chi, K., Zhu, Y.-h., Jiang, X., and Tian, X. **Optimal coding for transmission energy minimization in wireless nanosensor networks.** *Nano Communication Networks* 4, 3 (2013), 120–130.
- [51] Feuillet-Palma, C., Todorov, Y., Vasanelli, A., and Sirtori, C. **Strong near field enhancement in thz nano-antenna arrays.** *Scientific reports* 3, 1 (2013), 1–8.
- [52] Kocaoglu, M., and Akan, O. B. **Minimum energy channel codes for nanoscale wireless communications.** *IEEE Transactions on Wireless Communications* 12, 4 (2013), 1492–1500.
- [53] Llatser, I., Cabellos-Aparicio, A., Pierobon, M., and Alarcón, E. **Detection techniques for diffusion-based molecular communication.** *IEEE Journal on Selected Areas in Communications* 31, 12 (2013), 726–734.
- [54] Orsini, C., Gregori, E., Lenzini, L., and Krioukov, D. **Evolution of the internet k -dense structure.** *IEEE/ACM Transactions on Networking* 22, 6 (2013), 1769–1780.
- [55] Piro, G., Grieco, L. A., Boggia, G., and Camarda, P. **Nano-sim: simulating electromagnetic-based nanonetworks in the network simulator 3.** In *Proc. of the 6th Intl. ICST Conf. on Simulation Tools and Techniques* (2013), ICST, pp. 203–210.
- [56] Rikhtegar, N., and Keshtgary, M. **A brief survey on molecular and electromagnetic communications in nano-networks.** *International Journal of Computer Applications* 79, 3 (2013).
- [57] Salous, S. **Radio propagation measurement and channel modelling.** John Wiley & Sons, 2013.

- [58] Wang, P., Jornet, J. M., Malik, M. A., Akkari, N., and Akyildiz, I. F. **Energy and spectrum-aware mac protocol for perpetual wireless nanosensor networks in the terahertz band.** *Ad Hoc Networks* 11, 8 (2013), 2541–2555.
- [59] Aijaz, A., and Aghvami, A.-H. **Error performance of diffusion-based molecular communication using pulse-based modulation.** *IEEE transactions on nanobioscience* 14, 1 (2014), 146–151.
- [60] Akyildiz, I. F., Jornet, J. M., and Han, C. **Terahertz band: Next frontier for wireless communications.** *Physical Communication* 12 (2014), 16–32.
- [61] Bhatt, U. R., Nema, N., and Upadhyay, R. **Enhanced dsr: An efficient routing protocol for manet.** In *2014 International Conference on Issues and Challenges in Intelligent Computing Techniques (ICICT)* (2014), IEEE, pp. 215–219.
- [62] Boillot, N., Dhoutaut, D., and Bourgeois, J. **Using nano-wireless communications in micro-robots applications.** *International Conference on Nanoscale Computing and Communication* 1 (05 2014).
- [63] Dehankar, J. N., Patil, P., and Agarwal, G. **Survey on energy consumption in wireless sensor network.** *International Journal of Engineering Research Technology (IJERT)* 2, 1 (2014), 1–4. <https://www.ijert.org/research/survey-on-energy-consumption-in-wireless-sensor-network-IJERTV2IS1071.pdf>
- [64] Deng, R., Yang, F., Xu, S., and Pirinoli, P. **Terahertz reflectarray antennas: An overview of the state-of-the-art technology.** In *2014 International Conference on Electromagnetics in Advanced Applications (ICEAA)* (2014), IEEE, pp. 667–670.
- [65] Han, C., and Akyildiz, I. F. **Distance-aware multi-carrier (damc) modulation in terahertz band communication.** In *Communications (ICC), 2014 IEEE International Conference on* (2014), IEEE, pp. 5461–5467.
- [66] Jornet, J. M., and Akyildiz, I. F. **Femtosecond-long pulse-based modulation for terahertz band communication in nanonetworks.** *IEEE Transactions on Communications* 62, 5 (2014), 1742–1754.
- [67] Mohrehkesh, S., and Weigle, M. C. **Optimizing energy consumption in terahertz band nanonetworks.** *IEEE Journal on Selected Areas in Communications* 32, 12 (2014), 2432–2441.
- [68] Neupane, S. R. **Routing in resource constrained sensor nanonetworks.** Master's thesis, 2014.
- [69] Pierobon, M., Jornet, J. M., Akkari, N., Almasri, S., and Akyildiz, I. F. **A routing framework for energy harvesting wireless nanosensor networks in the terahertz band.** *Wireless networks* 20, 5 (2014), 1169–1183.
- [70] Zarepour, E., Hassan, M., Chou, C. T., and Adesina, A. A. **Frequency hopping strategies for improving terahertz sensor network performance over composition varying channels.** In *Proceeding of IEEE International Symposium on a World of Wireless, Mobile and Multimedia Networks 2014* (2014), IEEE, pp. 1–9.
- [71] D'Oro, S., Galluccio, L., Morabito, G., and Palazzo, S. **A timing channel-based mac protocol for energy-efficient nanonetworks.** *Nano Communication Networks* 6, 2 (2015), 39–50.

- [72] Lin, C., and Li, G. Y. **Adaptive beamforming with resource allocation for distance-aware multi-user indoor terahertz communications.** *IEEE Transactions on Communications* 63, 8 (2015), 2985–2995.
- [73] Mohrehkesh, S., Weigle, M. C., and Das, S. K. **Drih-mac: A distributed receiver-initiated harvesting-aware mac for nanonetworks.** *IEEE Transactions on Molecular, Biological and Multi-Scale Communications* 1, 1 (2015), 97–110.
- [74] Sgora, A., Vergados, D. J., and Vergados, D. D. **A survey of tdma scheduling schemes in wireless multihop networks.** *ACM Computing Surveys (CSUR)* 47, 3 (2015), 53.
- [75] Tsioliariidou, A., Liaskos, C., Ioannidis, S., and Pitsillides, A. **Corona: A coordinate and routing system for nanonetworks.** In *Proceedings of the second annual international conference on nanoscale computing and communication* (2015), vol. 18, pp. 1–6.
- [76] Abdallah, A. E. **Smart partial flooding routing algorithms for 3d ad hoc networks.** *Procedia Computer Science* 94 (2016), 264–271.
- [77] Acar, H., Alptekin, G. I., Gelas, J.-P., and Ghodous, P. **Beyond cpu: Considering memory power consumption of software.** In *2016 5th International Conference on Smart Cities and Green ICT Systems (SMARTGREENS)* (2016), IEEE, pp. 1–8.
- [78] Akkari, N., Wang, P., Jornet, J. M., Fadel, E., Elrefaei, L., Malik, M. G. A., Almasri, S., and Akyildiz, I. F. **Distributed timely throughput optimal scheduling for the internet of nano-things.** *IEEE Internet of Things Journal* 3, 6 (2016), 1202–1212.
- [79] Alsheikh, R., Akkari, N., and Fadel, E. **Mac protocols for wireless nano-sensor networks: Performance analysis and design guidelines.** In *2016 Sixth International Conference on Digital Information Processing and Communications (ICDIPC)* (2016), IEEE, pp. 129–134.
- [80] Desai, S. B., Madhupathy, S. R., Sachid, A. B., Llinas, J. P., Wang, Q., Ahn, G. H., Pitner, G., Kim, M. J., Bokor, J., Hu, C., and others. **Mos2 transistors with 1-nanometer gate lengths.** *Science* 354, 6308 (2016), 99–102.
- [81] Farsad, N., Yilmaz, H. B., Eckford, A., Chae, C.-B., and Guo, W. **A comprehensive survey of recent advancements in molecular communication.** *IEEE Communications Surveys & Tutorials* 18, 3 (2016), 1887–1919.
- [82] Jianling, C., Min, W., Cong, C., and Zhi, R. **High-throughput low-delay mac protocol for terahertz ultra-high data-rate wireless networks.** *The Journal of China Universities of Posts and Telecommunications* 23, 4 (2016), 17–24.
- [83] Liaskos, C., Tsioliariidou, A., Ioannidis, S., Kantartzis, N., and Pitsillides, A. **A deployable routing system for nanonetworks.** In *2016 IEEE International Conference on Communications (ICC)* (2016), IEEE, pp. 1–6.
- [84] Mabed, H., and Bourgeois, J. **Scalable distributed protocol for modular micro-robots network reorganization.** *IEEE Internet of Things Journal* 3, 6 (dec 2016), 1070 – 1083.
- [85] Moldovan, A., Kisseleff, S., Akyildiz, I. F., and Gerstacker, W. H. **Data rate maximization for terahertz communication systems using finite alphabets.** In *2016 IEEE International Conference on Communications (ICC)* (2016), IEEE, pp. 1–7.

- [86] Petrov, V., Pyattaev, A., Moltchanov, D., and Koucheryavy, Y. **Terahertz band communications: Applications, research challenges, and standardization activities.** In *2016 8th International Congress on Ultra Modern Telecommunications and Control Systems and Workshops (ICUMT)* (2016), IEEE, pp. 183–190.
- [87] Shrestha, A. P., Yoo, S.-J., Choi, H. J., and Kwak, K. S. **Enhanced rate division multiple access for electromagnetic nanonetworks.** *IEEE Sensors Journal* 16, 19 (2016), 7287–7296.
- [88] Tsioliariidou, A., Liaskos, C., Dedu, E., and Ioannidis, S. **Stateless linear-path routing for 3d nanonetworks.** In *Proceedings of the 3rd ACM International Conference on Nanoscale Computing and Communication* (2016), pp. 1–6.
- [89] Uchendu, I., and Kelly, J. R. **Survey of beam steering techniques available for millimeter wave applications.** *Progress In Electromagnetics Research* 68 (2016), 35–54.
- [90] Wu, X., and Sengupta, K. **Dynamic waveform shaping with picosecond time widths.** *IEEE Journal of Solid-State Circuits* 52, 2 (2016), 389–405.
- [91] Brunete, A., Ranganath, A., Segovia, S., de Frutos, J. P., Hernando, M., and Gambao, E. **Current trends in reconfigurable modular robots design.** *International Journal of Advanced Robotic Systems* 14, 3 (2017), 1729881417710457.
- [92] Correias-Serrano, D., and Gomez-Diaz, J. S. **Graphene-based antennas for terahertz systems: A review.** *arXiv preprint arXiv:1704.00371* (2017).
- [93] Feng, J., and Zhao, X. **Performance analysis of oof-based fso systems in gamma-gamma turbulence with imprecise channel models.** *Optics Communications* 402 (2017), 340–348.
- [94] Mabed, H. **Enhanced spread in time on-off keying technique for dense terahertz nanonetworks.** In *2017 IEEE Symposium on Computers and Communications (ISCC)* (2017), IEEE, pp. 710–716.
- [95] Malwe, S. R., Taneja, N., and Biswas, G. **Enhancement of dsr and aodv protocols using link availability prediction.** *Wireless Personal Communications* 97, 3 (2017), 4451–4466.
- [96] Petrov, V., Moltchanov, D., Komar, M., Antonov, A., Kustarev, P., Rakheja, S., and Koucheryavy, Y. **Terahertz band intra-chip communications: Can wireless links scale modern x86 cpus?** *IEEE Access* 5 (2017), 6095–6109.
- [97] Rikhtegar, N., Keshtgari, M., and Ronaghi, Z. **Eewnsn: Energy efficient wireless nano sensor network mac protocol for communications in the terahertz band.** *Wireless Personal Communications* 97, 1 (2017), 521–537.
- [98] Visconti, P., Primiceri, P., Ferri, R., Pucciarelli, M., and Venere, E. **An overview on state-of-art energy harvesting techniques and choice criteria: a wsn node for goods transport and storage powered by a smart solar-based eh system.** *International Journal of Renewable Energy Research (IJRER)* 7, 3 (2017), 1281–1295. <https://www.ijrer.org/ijrer/index.php/ijrer/article/view/6052/pdf>.

- [99] Afsana, F., Asif-Ur-Rahman, M., Ahmed, M. R., Mahmud, M., and Kaiser, M. S. **An energy conserving routing scheme for wireless body sensor nanonetwork communication.** *IEEE Access* 6 (2018), 9186–9200.
- [100] Al-Turjman, F., and Kilic, K. I. **Lagoon: a simple energy-aware routing protocol for wireless nano-sensor networks.** *IET Wireless Sensor Systems* 9, 3 (2018), 110–118.
- [101] Dhoutaut, D., Arrabal, T., and Dedu, E. **Bit simulator, an electromagnetic nanonetworks simulator.** In *Proceedings of the 5th ACM International Conference on Nanoscale Computing and Communication* (2018), pp. 1–6.
- [102] Fontana Jr, R. E., and Decad, G. M. **Moore’s law realities for recording systems and memory storage components: Hdd, tape, nand, and optical.** *AIP Advances* 8, 5 (2018), 056506.
- [103] Goudarzi, F., Asgari, H., and Al-Raweshidy, H. S. **Traffic-aware vanet routing for city environments—a protocol based on ant colony optimization.** *IEEE Systems Journal* 13, 1 (2018), 571–581.
- [104] Lee, S. J., Choi, H., and Kim, S. **Slotted csma/ca based energy efficient mac protocol design in nanonetworks.** *International Journal of Wireless & Mobile Networks (IJWMN) Vol 10* (2018).
- [105] Singh, P., Kim, B.-W., and Jung, S.-Y. **Th-ppm with non-coherent detection for multiple access in electromagnetic wireless nanocommunications.** *Nano Communication Networks* 17 (2018), 1–13.
- [106] Vavouris, A. K., Dervisi, F. D., Papanikolaou, V. K., and Karagiannidis, G. K. **An energy efficient modulation scheme for body-centric nano-communications in the thz band.** In *2018 7th International Conference on Modern Circuits and Systems Technologies (MOCAST)* (2018), IEEE, pp. 1–4.
- [107] Yu, H., Ng, B., and Seah, W. **Multi-gateway polling for nanonetworks under dynamic iot backhaul bandwidth.** In *2018 IEEE International Conference on Sensing, Communication and Networking (SECON Workshops)* (2018), IEEE, pp. 1–4.
- [108] Cheng, J., Gao, Y., Zhang, N., and Yang, H. **An energy-efficient two-stage cooperative routing scheme in wireless multi-hop networks.** *Sensors* 19, 5 (2019), 1002.
- [109] Ghafoor, S., Boujnah, N., Rehmani, M. H., and Davy, A. **Mac protocols for terahertz communication: A comprehensive survey.** *arXiv preprint arXiv:1904.11441* (2019).
- [110] Hossain, Z., and Jornet, J. M. **Hierarchical bandwidth modulation for ultra-broadband terahertz communications.** In *ICC 2019-2019 IEEE International Conference on Communications (ICC)* (2019), IEEE, pp. 1–7.
- [111] Lemic, F., Abadal, S., Tavernier, W., Stroobant, P., Colle, D., Alarcón, E., Marquez-Barja, J., and Famaey, J. **Survey on terahertz nanocommunication and networking: A top-down perspective.** *arXiv preprint arXiv:1909.05703* (2019).
- [112] Saad, M., Bader, F., Palicot, J., Al Ghouwayel, A. C., and Hijazi, H. **Single carrier with index modulation for low power terabit systems.** In *2019 IEEE Wireless Communications and Networking Conference (WCNC)* (2019), IEEE, pp. 1–7.

- [113] Tasolamprou, A. C., Koulouklidis, A. D., Daskalaki, C., Mavidis, C. P., Kenanakis, G., Deligeorgis, G., Viskadourakis, Z., Kuzhir, P., Tzortzakis, S., Kafesaki, M., and others. **Experimental demonstration of ultrafast thz modulation in a graphene-based thin film absorber through negative photoinduced conductivity.** *ACS photonics* 6, 3 (2019), 720–727.
- [114] Tekbıyık, K., Ekti, A. R., Kurt, G. K., and Görçin, A. **Terahertz band communication systems: Challenges, novelties and standardization efforts.** *Physical Communication* 35 (2019), 100700.
- [115] Xia, Q., Hossain, Z., Medley, M. J., and Jornet, J. M. **A link-layer synchronization and medium access control protocol for terahertz-band communication networks.** *IEEE Transactions on Mobile Computing* (2019).
- [116] Yao, X.-W., Huang, W., and others. **Routing techniques in wireless nanonetworks: A survey.** *Nano Communication Networks* 21 (2019), 100250.
- [117] Yao, X.-W., Yao, Y., Qi, C.-F., Huang, W., and others. **Eecr: Energy-efficient cooperative routing for em-based nanonetworks.** In *International Conference on Cooperative Design, Visualization and Engineering* (2019), Springer, pp. 30–38.
- [118] Fu, X., Yang, F., Liu, C., Wu, X., and Cui, T. J. **Terahertz beam steering technologies: From phased arrays to field-programmable metasurfaces.** *Advanced Optical Materials* 8, 3 (2020), 1900628.
- [119] Lemic, F., Han, C., and Famaey, J. **Idling energy modeling and reduction in energy harvesting terahertz nanonetworks for controlling software-defined metamaterials.** *IEEE Journal on Emerging and Selected Topics in Circuits and Systems* 10, 1 (2020), 88–99.
- [120] Nasif, A. O., and Mahfuz, M. U. **Spatial nanomechanical communications based on state transitions.** *IEEE Transactions on NanoBioscience* (2020).
- [121] Singh, P., Kim, B. W., and Jung, S.-Y. **Ds-ook for terahertz band nanonetworks.** *National Academy Science Letters* (2020), 1–4.
- [122] Usman, M., Farooq, M., Wakeel, A., Nawaz, A., Cheema, S. A., ur Rehman, H., Ashraf, I., and Sanallah, M. **Nanotechnology in agriculture: Current status, challenges and future opportunities.** *Science of The Total Environment* (2020), 137778.
- [123] Varshney, G. **Reconfigurable graphene antenna for thz applications: a mode conversion approach.** *Nanotechnology* 31, 13 (2020), 135208.

List of Figures

2.1	An integrated nanosensor device [28].	13
3.1	Distributed vs. Hierarchical MAC protocols [survey]	23
3.2	A colorful graph. Each number reflects specific colour.	24
3.3	Multi-hop communication in EEWNSN-MAC [133].	25
3.4	Classification of WNNs routing protocols.	29
3.5	An example of RADAR routing [116].	30
3.6	Illustration of CORONA Coordinate/routing protocol [116].	31
3.7	Comparison of the routing behavior of CORONA (yellow area) and SLR (dark curve) for a given communication node pair in a high resolution area [88].	31
3.8	DEROUS-system routing cases. The sender (S) and receiver (R) locations can be interchanged [83].	32
3.9	The architecture of ECR [116].	33
3.10	In the initialization phase, nanonodes reach the required hop counts to the nanocontroller [117].	34
4.1	TS-OOK modulation: All nanodevices have the same symbol rate T_s	40
4.2	RD-TSOOK modulation: Each nanodevice has its symbol rate different from others.	42
4.3	SRH-TSOOK modulation: different symbol rate β is used at each frame.	43
4.4	SDMA-TSOOK: different time slot $Pslot$ is used at each frame for each node.	45
4.5	Different nanonetwork models in terms of distribution	46
4.6	Illustration of two data traffic generation methods	47
4.7	Different densities	48
4.8	Comparison of collisions number in different scenarios	50
4.9	Comparison of success rate in different scenarios	51
4.10	Scenarios & protocols appropriate for application types	52
4.11	SDMA-TSOOK performance under beta and slots sequence	53
5.1	Traffic regulation problem: from physical to logical topology	56

5.2	Example of TDMA synchronization: each edge (x,y) is indexed by the index of the transmission period on x (S_i) and the index of the reception period on y (S_j). Each period $S[tb - te]$ is designated by its beginning and end time (the time is given relatively to the concerned node). The colored arcs display the antenna orientation at the corresponding period.	58
5.3	At every period, the transmitting node selects its successors according to their distance from the node in order to optimize the used frequency window. The colored arcs represent the orientation and coverage of the node at a given period.	59
5.4	Traffic regulation for 3 scenarios: 200 nodes, 500 nodes and 1000 nodes. Tests are implemented using Microsoft Excel VBA.	62
6.1	Clustering and communication phases	66
6.2	Sequence diagram of clustering phase	68
6.3	Switching Antennas in ADVs step. At (c) step, the ordinary node receives the ADV message.	68
6.4	Flood diffusion (left) and optimized diffusion (right)	69
6.5	Distributed TDMA inter cluster scheduling	72
6.6	Clustering vs Flooding regarding number of messages generated. Tests are made with different network densities.	73
6.7	Optimal CH rate for covering the entire nanonetwork	74
6.8	The proposed protocol phases.	74
6.9	Positionning of the nanonodes with the lowest weight (in blue) among their direct neighbors.	75
6.10	Selected spines after the first step under different threshold values.	77
6.11	Spines selection phase.	77
6.12	Area division using two spines.	78
6.13	Nanonetwork topology after the clustering phase.	80
6.14	Time domain architecture of the Inter Cluster TDMA	80
6.15	Illustration of The Inter Cluster TDMA Algorithm.	81
6.16	Illustration of the FDN selection algorithm.	82
6.17	Impact of the used clustering approaches on the nanonetwork connectivity.	83
6.18	Comparison of cluster heads distribution between uniform based approach and random based approach	84
6.19	Percentage of isolated CHs obtained in each approach.	84
6.20	Required clustering messages at each round in each approach.	85
6.21	Generated control packets arriving at a specific round.	86
7.1	Wireless Body Area Network (WBAN) is deployed inside a bowel. The nanonetwork deployment follows the bowel shape and consequently forms a concave shape.	89

7.2	Comparison between direct line multipoint-to-multipoint approach (left) and M2MRP protocol (right). The surrounded node is a sink and the dark one is the source. The direct line approach fails to route the message until the sink node, whereas M2MRP approach succeeds.	90
7.3	An example of M2MRP(v2) data flows pattern describing the trajectory of data from any source node towards one of the three available sink nodes.	92
7.4	Routing cycle: every 100ms, the node recomputes its attractiveness vector (the transmission direction).	93
7.5	The computing of the attractiveness vector of the reference node in the center. For simplification, only cardinal directions are considered. The computation of $P(o, EAST)$ and $P(o, SOUTH)$ are given. $P(o, WEST)$ and $P(o, NORTH)$ are equal to zero. The East direction (the best direction) is selected as the attractiveness vector. The node located in the extreme West is ignored since it is out of coverage of the reference node.	94
7.6	Block Scheme of the multirelay to multirelay routing protocol including an ordinary nanonode o and a sink node s	95
7.7	Comparison between the computation of the attractiveness vector in M2MRP and M2MRPv2 methods. Reference node is in the center.	96
7.8	Two classes of nanonetwork topologies: square and tie bow. Black nodes represent sink nodes.	98
7.9	Comparison of broadcast, SLR, and M2MRPv2 routing protocols over two network topologies and under two traffic profiles. A comparison is given according to the success rate and the number of sent messages. The traffic load measures the average number of new packets generated each 0.1ms.	100
7.10	Comparison between Broadcast, SLR, and M2MRP protocols according to the number of received messages and relaying rate. Test parameters are the same as above and traffic load is of 0.2 packets per communication cycle per node.	101
7.11	Batteries level after 4 routing cycles with three routing protocols: Broadcast, SLR, and M2MRPv2 protocols. Tests are made over a square topology nanonetwork with 200 nodes and an average traffic load of 0.2 packets per data cycle.	102
7.12	Batteries level after 100 routing cycles with three routing protocols: Broadcast, SLR, and M2MRPv2 protocols. Tests are made over a square topology nanonetwork with 200 nodes and an average traffic load of 0.2 packets per data cycle.	102

List of Tables

3.1	Summary of modulation and channel access schemes.	21
3.2	Summary of link layer protocols	27
3.3	Summary of network layer protocol	35
4.1	Protocol performance comparison based on probabilistic analysis	44
6.1	Number of Clusters obtained using different spines.	77
6.2	PLR of Area Protocol and Random Protocol.	86
6.3	Synthesis of the features of the three studied de-densification approaches	87
7.1	Complexity comparison between routing techniques for ad hoc networks and nanonetworks.	97
7.2	Comparison between nanonetworks routing protocols.	97
7.3	Simulation parameters	99

